

**Modeling the personalized variations in liver disease due to α 1-antitrypsin deficiency
using induced pluripotent stem cell-derived hepatocyte-like cells**

by

Edgar N. Tafaleng

BS Molecular Biology and Biotechnology, University of the Philippines - Diliman, 2004

Submitted to the Graduate Faculty of
School of Medicine in partial fulfillment
of the requirements for the degree of
Doctor of Philosophy in Cellular and Molecular Pathology

University of Pittsburgh

2015

UNIVERSITY OF PITTSBURGH
SCHOOL OF MEDICINE

This dissertation was presented

by

Edgar N. Tafaleng

It was defended on

February 12, 2015

and approved by

Committee Chair: Donna Beer Stolz, PhD, Associate Professor, Department of Cell Biology

Andrew W. Duncan, PhD, Assistant Professor, Department of Pathology

David H. Perlmutter, MD, Vira I. Heinz Professor, Department of Pediatrics

Steven D. Shapiro, MD, Professor, Department of Medicine

Dissertation Advisor: Ira J. Fox, MD, Professor, Department of Surgery

Copyright © by Edgar N. Tafaleng

2015

**Modeling the personalized variations in liver disease due to α 1-antitrypsin deficiency
using induced pluripotent stem cell-derived hepatocyte-like cells**

Edgar Tafaleng, PhD

University of Pittsburgh, 2015

In the classical form of α 1-antitrypsin deficiency (ATD), aberrant intracellular accumulation of misfolded mutant α 1-antitrypsin Z (ATZ) in hepatocytes causes hepatic damage by a gain-of-function, “proteotoxic” mechanism. Whereas some ATD patients develop severe liver disease that necessitates liver transplantation, others with the same genetic defect completely escape this clinical phenotype. We investigated whether induced pluripotent stem cells (iPSCs) from ATD individuals with or without severe liver disease could model these personalized variations in hepatic disease phenotypes. Patient-specific iPSCs were generated from ATD patients and a control, and differentiated into hepatocyte-like cells (iHeps) having many characteristics of hepatocytes. Pulse-chase and endoglycosidase H analysis demonstrate that the iHeps recapitulate the abnormal accumulation and processing of the ATZ molecule, compared to the wild-type AT molecule. Measurements of the fate of intracellular ATZ show a marked delay in the rate of ATZ degradation in iHeps from severe liver disease patients, compared to those from no liver disease patients. Transmission electron microscopy showed dilated rough endoplasmic reticulum in iHeps from all individuals with ATD, not in controls, but globular inclusions that are partially covered with ribosomes were observed only in iHeps from individuals with severe liver disease. These results provide definitive validation that iHeps model the individual disease phenotypes of ATD patients with more rapid degradation of misfolded ATZ and lack of globular inclusions in cells from patients who have escaped liver disease. The results support the concept that

“proteostasis” mechanisms, such as intracellular degradation pathways, play a role in observed variations in clinical phenotype and show that iPSCs can potentially be used to facilitate predictions of disease susceptibility for more precise and timely application of therapeutic strategies.

TABLE OF CONTENTS

| | |
|--|--------------|
| LIST OF TABLES | X |
| LIST OF FIGURES | XI |
| LIST OF ABBREVIATIONS | XIII |
| ACKNOWLEDGEMENTS | XVI |
| PREFACE..... | XVIII |
| 1.0 INTRODUCTION..... | 1 |
| 1.1 ALPHA-1 ANTITRYPSIN | 1 |
| 1.2 CLASSICAL ALPHA-1 ANTITRYPSIN DEFICIENCY | 2 |
| 1.3 ALPHA-1 ANTITRYPSIN DEFICIENCY-MEDIATED LIVER DISEASE..... | 4 |
| 1.4 MODELS FOR ATD-MEDIATED LIVER DISEASE..... | 5 |
| 1.5 INDUCED PLURIPOTENT STEM CELLS | 8 |
| 1.6 GENERATION OF INDUCED PLURIPOTENT STEM CELLS | 10 |
| 1.7 DISEASE-SPECIFIC INDUCED PLURIPOTENT STEM CELLS | 13 |
| 1.8 DIFFERENTIATION OF IPSCS INTO HEPATOCYTES | 16 |
| 1.9 DISEASE MODELING USING IPSC-DERIVED HEPATOCYTE-LIKE CELLS | 19 |
| 1.10 SPECIFIC AIMS..... | 21 |

| | | |
|------------|---|-----------|
| 1.10.1 | Reprogramming of alpha-1 antitrypsin deficient patient-derived somatic cells into iPScs..... | 23 |
| 1.10.2 | Differentiation of alpha-1 antitrypsin deficient patient-derived iPScs into hepatocyte-like cells | 23 |
| 1.10.3 | Modeling the pathogenesis and variability of alpha-1 antitrypsin deficiency using patient-derived iPSc generated hepatocyte-like cells..... | 24 |
| 2.0 | REPROGRAMMING OF ALPHA-1 ANTITRYPSIN DEFICIENT PATIENT-DERIVED SOMATIC CELLS INTO IPSCS | 25 |
| 2.1 | INTRODUCTION | 25 |
| 2.2 | MATERIALS AND METHODS..... | 26 |
| 2.2.1 | Use of human- and animal-derived tissues | 26 |
| 2.2.2 | Hepatocyte isolation from liver explants..... | 26 |
| 2.2.3 | Cell culture..... | 28 |
| 2.2.4 | Generation of iPScs from somatic cells | 30 |
| 2.2.5 | RNA Extraction, cDNA synthesis and qPCR | 32 |
| 2.2.6 | Pluripotency-marker staining..... | 33 |
| 2.2.7 | Teratoma formation assay..... | 34 |
| 2.2.8 | Genomic DNA sequencing..... | 35 |
| 2.3 | RESULTS..... | 35 |
| 2.4 | DISCUSSION..... | 42 |
| 3.0 | DIFFERENTIATION OF ALPHA-1 ANTITRYPSIN DEFICIENT PATIENT-DERIVED IPSCS INTO HEPATOCYTE-LIKE CELLS | 45 |
| 3.1 | INTRODUCTION..... | 45 |

| | | |
|------------|--|-----------|
| 3.2 | MATERIALS AND METHODS..... | 47 |
| 3.2.1 | Differentiation of ATD iPScs into hepatocyte-like cells..... | 47 |
| 3.2.2 | RNA Extraction, cDNA synthesis and qPCR | 48 |
| 3.2.3 | Immunofluorescent staining..... | 49 |
| 3.2.4 | Sandwich ELISA | 50 |
| 3.2.5 | Transmission Electron Microscopy | 51 |
| 3.3 | RESULTS..... | 52 |
| 3.4 | DISCUSSION | 59 |
| 4.0 | MODELING THE PATHOGENESIS AND VARIABILITY OF ALPHA-1 ANTITRYPSIN DEFICIENCY USING PATIENT-DERIVED IPSC GENERATED HEPATOCYTE-LIKE CELLS..... | 62 |
| 4.1 | INTRODUCTION..... | 62 |
| 4.2 | MATERIALS AND METHODS..... | 63 |
| 4.2.1 | Use of human-derived tissues..... | 63 |
| 4.2.2 | Hepatocyte isolation from liver explants..... | 64 |
| 4.2.3 | Pulse chase analysis and Densitometry | 66 |
| 4.2.4 | Endoglycosidase H and PNGase F digestion | 67 |
| 4.2.5 | Immunofluorescent Staining..... | 67 |
| 4.2.6 | Transmission Electron Microscopy | 68 |
| 4.3 | RESULTS..... | 70 |
| 4.3.1 | iHeps from ATD patients recapitulate the accumulation and processing of the mutant ATZ molecule..... | 70 |

| | | |
|-------|--|----|
| 4.3.2 | iHeps from ATD patients with no liver disease more efficiently degrade misfolded ATZ..... | 74 |
| 4.3.3 | The mutant ATZ molecule accumulates in the rER as well as in non-rER compartments of ATD iHeps | 78 |
| 4.3.4 | No LD iHeps lack intracellular inclusions that are the cellular hallmark of the disease | 84 |
| 4.4 | DISCUSSION | 87 |
| 5.0 | CONCLUSION | 89 |
| 6.0 | FUTURE DIRECTIONS..... | 91 |
| 6.1 | REPROGRAMMING OF ATD PATIENT-DERIVED SOMATIC CELLS USING SENDAI VIRUS..... | 91 |
| 6.2 | DIFFERENTIATION AND TRANSPLANTATION OF ATD PATIENT-DERIVED IPSCS TO GENERATE MATURE HEPATOCYTES..... | 92 |
| 6.3 | ANALYSIS OF OTHER FORMS OF ATD-MEDIATED LIVER DISEASE | 94 |
| 6.4 | IDENTIFICATION OF MODIFIER GENES FOR ATD | 94 |
| 6.5 | DRUG TREATMENT OF ATD IHEPS..... | 95 |
| | BIBLIOGRAPHY | 96 |

LIST OF TABLES

| | |
|---|----|
| Table 1. Diseases modeled using induced pluripotent stem cell technology..... | 15 |
| Table 2. Taqman Gene Expression Assay IDs for the qPCR analysis for pluripotency factors... | 32 |
| Table 3. List of antibodies and dilutions used for the immunofluorescent staining for pluripotency factors | 34 |
| Table 4. Human induced pluripotent stem cell lines were generated from ATD patients with severe liver disease and those with lung disease but no liver disease, and wild type control | 36 |
| Table 5. Taqman Gene Expression Assay IDs for the qPCR analysis for pluripotency factors... | 48 |
| Table 6. List of antibodies and dilutions used for the immunofluorescent staining for hepatocyte-directed differentiation..... | 50 |
| Table 7. List of antibodies and dilutions used for sandwich ELISA | 51 |
| Table 8. List of antibodies and dilutions used for colocalization of AT with rER and golgi markers..... | 68 |

LIST OF FIGURES

| | |
|---|----|
| Figure 1. Induced pluripotent stem cells (iPSCs) were generated from ATD patients with severe liver disease (severe LD) and no overt liver disease (no LD)..... | 37 |
| Figure 2. Induced pluripotent stem cells (iPSCs) expressed pluripotency-associated markers..... | 40 |
| Figure 3. Induced pluripotent stem cells (iPSCs) generate teratomas when injected in immunodeficient NOD SCID mice..... | 41 |
| Figure 4. ATD iPSCs carry homozygous G11940→A PiZ alleles while wild type iPSCs were homozygous for the WT alleles | 42 |
| Figure 5. Changes in the morphology of iPSCs during differentiation to iHeps..... | 53 |
| Figure 6. Differentiation of iPSCs to iHeps results in changes in the expression of stage-specific markers..... | 55 |
| Figure 7. ATD iHeps express mature hepatocyte markers ALB and ASGPR1 but have continued expression of the immature hepatocyte marker AFP..... | 56 |
| Figure 8. ATD iHeps exhibit many characteristics of primary human hepatocytes..... | 58 |
| Figure 9. ATD iHeps recapitulate the accumulation and secretion of ATZ observed in ATD primary human hepatocytes | 71 |
| Figure 10. iHeps and primary hepatocytes secrete lower levels of AT in the extracellular fraction compared to HeLa inducible cell lines transduced to express wild type AT (HTO/M) or ATZ (HTO/Z) | 72 |

| | |
|---|----|
| Figure 11. The ATZ polypeptide accumulates as a partially glycosylated intermediate in iHeps and primary hepatocytes from patients with ATD..... | 74 |
| Figure 12. The rate of degradation of intracellular ATZ correlates with liver disease severity in ATD iHeps..... | 76 |
| Figure 13. The disappearance of intracellular ATZ in no LD iHeps does not lead to increased secretion in the extracellular compartment..... | 77 |
| Figure 14. ATZ in severe LD iHeps accumulates in rER and in compartments that are devoid of calnexin, calreticulin, or GM130..... | 79 |
| Figure 15. Severe LD iHeps and severe LD liver tissue sections exhibit dilated rER and dilated globular inclusions that are partially covered with ribosomes..... | 81 |
| Figure 16. Electron micrographs of severe LD iHeps (A-F) showing the presence of autophagosomes (black arrows) and autophagolysosomes (red arrows)..... | 82 |
| Figure 17. Mitochondrial dilation is evident in severe LD iHeps..... | 83 |
| Figure 18. Golgi fragmentation is evident in severe LD iHeps..... | 84 |
| Figure 19. Severe LD iHeps and no LD iHeps exhibit dilated rER but only severe LD iHeps exhibit globular inclusions..... | 86 |

LIST OF ABBREVIATIONS

| | |
|--------|--|
| AFP | Alpha-fetoprotein |
| ALB | Albumin |
| AP | Alkaline phosphatase |
| ASGPR1 | Asialoglycoprotein receptor 1 |
| AT | Alpha-1 antitrypsin |
| ATD | Alpha-1 antitrypsin deficiency |
| ATZ | Alpha-1 antitrypsin type Z |
| BAP31 | B-cell receptor-associated protein 31 |
| BiP | Immunoglobulin heavy chain-binding protein |
| BMP4 | Bone morphogenetic protein 4 |
| Cas9 | CRISPR-associated nuclease 9 |
| CBZ | Carbamazepine |
| cDNA | Complementary deoxyribonucleic acid |
| COPD | Chronic obstructive pulmonary disorder |
| CRISPR | Clustered regularly interspaced short palindromic repeat |
| CXCR4 | Chemokine (C-X-C Motif) receptor 4 |
| DE | Definitive endoderm |
| DNMT3B | DNA (Cytosine-5-)-Methyltransferase 3 Beta |
| EB | Embryoid body |
| EBNA-1 | Epstein-Barr nuclear antigen 1 |
| EC | Extracellular |

| | |
|--------|--|
| ELISA | Enzyme-linked immunosorbent assay |
| ER | Endoplasmic reticulum |
| ERAD | Endoplasmic reticulum-associated degradation |
| F7 | Coagulation factor VII |
| FGF2 | Fibroblast growth factor 2 |
| FOXA2 | Forkhead box A2 |
| GM130 | Golgi matrix protein GM130 |
| hESc | Human embryonic stem cells |
| HGF | Hepatocyte growth factor |
| HI | Hepatic induction |
| HM | Hepatic maturation |
| HNF1A | Hepatocyte nuclear factor 1Alpha |
| HNF4 | Hepatocyte nuclear factor 4 |
| HNF4A | Hepatocyte nuclear factor 4 Alpha |
| HS | Hepatic specification |
| IC | Intracellular |
| IEF | Isoelectric focusing |
| iHeps | iPSc-derived hepatocyte-like cells |
| IL-6 | Interleukin 6 |
| iPSc | Induced pluripotent stem cells |
| KLF4 | Kruppel-like factor 4 |
| LB | Liver bud |
| LD | Liver disease |
| LIN28 | Lin-28 Homolog A |
| mESc | Mouse embryonic stem cells |
| mRNA | Messenger ribonucleic acid |
| NFkB | Nuclear factor of Kappa light polypeptide gene enhancer in B-Cells |
| OCT3/4 | Octamer-binding transcription factor 3/4 |

| | |
|----------|---|
| oriP | Origin of plasmid replication of the Epstein-Barr virus |
| OSM | Oncostatin M |
| PAS | Periodic acid-Schiff |
| PCR | Polymerase chain reaction |
| PiMM | Protease inhibitor type M (normal/wild type) |
| PiZ | Protease inhibitor type Z allele |
| PiZZ | Protease inhibitor type Z homozygous mutation |
| qPCR | Quantitative polymerase chain reaction |
| rER | Rough endoplasmic reticulum |
| REX1 | Reduced expression 1 |
| RNAi | Ribonucleic acid interference |
| SDS-PAGE | Sodium dodecyl sulfate-polyacrylamide gel electrophoresis |
| SERPIN | Serine protease inhibitor |
| SERPINA1 | Serine protease inhibitor A1 |
| shRNA | Short hairpin ribonucleic acid |
| siRNA | Small interfering ribonucleic acid |
| SOX17 | SRY (sex determining region Y)-Box 17 |
| SOX2 | SRY (sex determining region Y)-Box 2 |
| SSEA1 | Stage-specific embryonic antigen 1 |
| SSEA4 | Stage-specific embryonic antigen 4 |
| TALEN | Transcription activator-like effector nuclease |
| TERT | Telomerase reverse transcriptase |
| TRA160 | Tumor rejection antigen 160 |
| TRA181 | Tumor rejection antigen 181 |
| UPR | Unfolded protein response |
| ZFN | Zinc finger nuclease |

ACKNOWLEDGEMENTS

I am deeply indebted to my adviser Dr. Ira J. Fox for his fundamental role in my doctoral work. You had provided me with every bit of guidance, encouragement, and expertise that I needed over the years. You have given me the freedom to make my own mistakes and learn from them, while at the same time continuing to offer valuable feedback and advice. In addition to our academic collaboration, I greatly value the close personal rapport that we have forged over the years.

I would like to extend my heartfelt gratitude to the members of my eminent and encouraging thesis committee: Drs. Donna B. Stolz, Andrew W. Duncan, David H. Perlmutter, and Steven D. Shapiro. You have always helped focus my project towards productive and exciting directions. Without your guidance, I would not have been able to finish this work. I would like to acknowledge Dr. David H. Perlmutter and Dr. Donna B. Stolz for our fruitful collaboration. This work would not have been realized without your substantial contribution.

I wish to thank members of the Fox, Perlmutter, and the Stolz laboratory who helped me finish this work. I would like to especially thank Dr. Bing Han, Dr. Souvik Chakraborty, Pamela Hale, Christine Dippold, Mark Ross, Ming Sun, Jonathan Franks, Kevin McHugh, Jenna Brooks, Dr. Masaki Nagaya, and Dr. Victoria Kelly who have been invaluable sources of advice,

technical and scientific feedback, and support over the years. I would like to express my sincere gratitude to Dr. Alex Soto-Gutiérrez for his help, advice, and encouragement.

I am deeply thankful to my family – my dad, my brothers Eric and Ferds, my sisters Chris and Cats, and my dog Stuart – and my friends – K-Ann, Sophia, Qian (Katie), Kristia, Madhav, Vincent, Matt, Gigi, Patricia, Mike, Jo-Erika, Kellsye, Junriz, Jocey, Josh, Carlos, Kevin, Oliver, Carol, Clare, Philip and Rudy – for the love, support, and sacrifices. Without you, graduate school would have been impossible.

I dedicate this work to the memory of my beloved mother. It is your shining example that I try to emulate in all that I do. Thank you for everything.

PREFACE

Chapters 2, 3, and 4 of this dissertation contain data from a peer-reviewed published manuscript on which I am first author:

Tafaleng, E.N., Chakraborty, S., Han, B., Hale, P., Wu, W., Soto-Gutierrez, A., Feghali-Bostwick, C.A., Wilson, A.A., Kotton, D.N., Nagaya, M., Strom, S.C., Roy-Chowdhury, J., Stolz, D.B., Perlmutter, D.H., Fox, I.J. Induced pluripotent stem cells model personalized variations in liver disease due to α 1-antitrypsin deficiency. *Hepatology (Baltimore, Md.)* **62**, 147-157 (2015).

1.0 INTRODUCTION

1.1 ALPHA-1 ANTITRYPSIN

Alpha-1 antitrypsin (AT) is a secreted glycoprotein consisting of 394 amino acids and 3 asparagine-linked carbohydrate chains¹⁻³. AT is one of the most abundant glycoproteins in the serum, with circulating levels of about 100-300 mg/dl⁴. It is a liver-derived acute phase protein whose plasma concentration increases up to four-fold in response to inflammation and/or injury⁵.⁶ AT is a serine protease inhibitor (SERPIN) that can inhibit a wide variety of proteases *in vitro* including trypsin, chymotrypsin, cathepsin G, plasmin, thrombin, tissue kallikrein, coagulation factor Xa, and plasminogen⁷⁻⁹. However, its main biological role is to inhibit neutrophil elastase, a potent protease that can cleave extracellular matrix proteins, coagulation and complement proteins and *E. coli* cell wall components^{3, 8, 10, 11}. Neutrophil elastase is released in response to infection or irritants to degrade bacteria and damaged cells but once the insult is resolved, AT is mobilized to neutralize neutrophil elastase activity and prevent damage to healthy lung tissues¹²⁻¹⁴.

AT is encoded by the serine protease inhibitor clade A 1 gene (SERPINA1), previously designated as the protease inhibitor 1 gene (PI1)^{15, 16}. The 13,947-base gene is located on chromosome 14q32.1 and is comprised of 3 non-coding (I_A, I_B and I_C) and four coding exons (II, III, IV and V). Carbohydrate attachment occurs on two asparagine residues encoded by exon II

and one encoded by exon III while the active site is encoded by exon V¹⁷⁻¹⁹. The gene is predominantly expressed in hepatocytes and, to a lesser extent, in extrahepatic cells including blood monocytes, tissue macrophages, intestinal epithelial cells, respiratory epithelial cells, renal tubular epithelial cells, non-parietal cells of the gastric mucosa, and pancreatic islet cells^{18, 20-22}. The regulation of basal and induced AT expression is cell-type dependent^{18, 22-26} and in hepatocytes is regulated by three cis-acting elements 5' of the gene and is predominantly driven by the synergistic effects of the hepatocyte nuclear factors HNF1A and HNF4 and modulated by IL-6 during the acute phase reaction^{17, 23, 27-31}.

1.2 CLASSICAL ALPHA-1 ANTITRYPSIN DEFICIENCY

Studies have reported at least 75 variant alleles in the SERPINA1 gene^{8, 19}. However, the overwhelming majority of patients with liver disease are affected by the classical form of alpha-1 antitrypsin deficiency (ATD) resulting from the protease inhibitor type Z mutation (PiZZ)^{8, 16, 19}. This mutation is caused by a homozygous single G11940A nucleotide point mutation in the coding region of the SERPINA1 gene³²⁻³⁴. The mutation results in a Glu342Lys amino acid substitution that generates an abnormally folded mutant AT protein (ATZ). The ATZ protein has an increased tendency to polymerize and form aggregates³⁵. The ATZ mutant protein also has an impaired ability to traverse the secretory pathway with only 10-15% of newly synthesized proteins released from hepatocytes. Because serum AT levels are only 10% of normal (13-36.4 mg/dl), there is an apparent “deficiency” in the circulating protease inhibitor activity. The small amount of ATZ mutant protein that is released into circulation is functionally active in inhibiting neutrophil elastase but has a reduced capacity compared to wild type AT³⁶⁻⁴⁰.

ATD is an inborn error of metabolism that was first described in 1963 by Laurell and Eriksson^{4, 41}. It is an autosomal genetic condition characterized by low levels of AT in the serum and lung^{1, 8, 19, 41-44}. The prevalence of ATD varies in different populations but the disorder affects approximately 1 in every 2000-3000 live births in most populations⁴⁵⁻⁴⁹. Although ATD was originally discovered as a cause of pulmonary emphysema^{4, 41, 50}, it is now known that ATD can also lead to hepatic failure as well as hepatocellular carcinoma^{15, 51}.

The pathogenesis of emphysema or chronic obstructive pulmonary disease (COPD) mediated by ATD is not fully understood although three mechanisms have been proposed. Earlier studies have suggested that lung disease is due to a loss-of-function mechanism resulting from the deficiency in the circulating protease inhibitor activity. The inadequate serum levels of AT leads to diminished ability to inhibit neutrophil elastase from degrading the connective tissue components of the extracellular matrix in the lung⁵²⁻⁵⁶. Other studies have suggested that lung disease is a result of the decreased ability of ATZ to inhibit neutrophil elastase leading to uninhibited neutrophil elastase activity^{40, 57}. More recently, however, several groups have proposed that lung disease occurs because the pro-inflammatory effects of ATZ polymers exacerbate tissue damage that occurs in the lungs. This hypothesis is based on studies reporting that ATZ polymers are chemotactic to neutrophils *in vivo*^{58, 59}, co-localize with neutrophils in the alveoli of ATD patients, and can induce inflammation in cell and mouse models of the disease⁶⁰. It is possible that all three of these mechanisms, in addition to environmental factors such as cigarette smoke, act together to bring about lung disease in ATD patients.

The mechanism of ATD-mediated carcinogenesis is, likewise, not fully understood. Studies of liver specimens from ATD patients and ATD mouse models revealed distinct subpopulations of globule-containing and globule-devoid hepatocytes. Analysis of these two

subpopulations revealed that there is increased autophagy, activated NFκB, impaired proliferation, and increased levels of apoptosis in globule-containing cells suggesting that these cells are injured^{61, 62}. Analyses of cell proliferation using BrdU incorporation have also shown that globule-devoid hepatocytes have a proliferative advantage over globule-containing hepatocytes⁶³. These studies provide evidence for the hypothesis that carcinogenesis occurs because injured globule-containing cells release proliferative signals that chronically stimulate globule-devoid cells to divide.

1.3 ALPHA-1 ANTITRYPSIN DEFICIENCY-MEDIATED LIVER DISEASE

ATD is the most common genetic cause for liver disease in children. Although other mutations in the protease inhibitor gene can result in liver disease, the majority of ATD-mediated liver disease is caused by the classical mutation of ATD^{8, 16, 19}. Hepatic failure due to ATD is a result of a gain of toxic function mechanism. Several studies have shown that the polymerization of ATZ within hepatocytes leads to hepatocyte damage and cirrhosis. However, the molecular mechanisms that occur between the onset of ATZ accumulation and hepatotoxicity have not been fully determined. Studies using animal and cell models of ATD and liver biopsies from ATD patients have implicated mitochondrial injury, mitochondrial autophagy, and caspase activation in the pathogenesis of ATD-mediated hepatic failure⁶¹⁻⁷⁴. However, the pathway/s that link ATZ accumulation to mitochondrial injury, mitochondrial autophagy, and caspase activation is still unknown. In addition, there is a wide variability in incidence, severity and age of onset of ATD-mediated liver disease¹⁵. While some affected PiZZ individuals develop life-threatening liver

disease, a considerable number never develop clinical symptoms and in some cases the liver disease is first recognizable at 50-65 years of age.

While ATD-related liver disease presents with similar clinical manifestations as other forms of liver diseases, it can be distinguished by low serum levels of AT protein, about 10-15% of normal levels⁷⁵. Clinical diagnosis for ATD begins with the determination of AT serum levels by rocket immunoelectrophoresis, radial immunodiffusion, or nephelometry. Diagnosis can be confirmed by isoelectric focusing (IEF) of serum AT and more recently by genotyping through PCR or gene sequencing⁷⁶. Histological analyses of liver biopsies from affected patients also show the presence of PAS+/diastase resistant globules in the ER of some but not all hepatocytes of affected patients. There is also compelling evidence of mitochondrial injury and heightened autophagic activity in liver biopsies from patients⁷⁵.

1.4 MODELS FOR ATD-MEDIATED LIVER DISEASE

The PiZ mouse is a well-characterized *in vivo* model of ATD that expresses the human PiZ gene variant⁷⁷. The model is able to recapitulate many of the characteristics of the human condition including the accumulation of ATZ mutant proteins within the rER of hepatocytes, the presence of PAS+/diastase resistant intrahepatocytic globules in liver tissues, and the development of liver necrosis/inflammation and hepatocellular carcinoma. The fact that this model recapitulates the abnormalities associated with ATD even though the endogenous mouse AT orthologs are expressed in the mouse supports the idea that the ATD is due to a gain-of-function rather than a loss-of-function mechanism.

Studies using the PiZ mouse have improved our understanding of the pathobiology of ATD. ATZ accumulation in the PiZ mouse hepatocytes results in caspase 3 and caspase 9 activation indicating that ATZ accumulation leads to ATD-associated hepatotoxicity^{63, 64}. ATZ accumulation in the PiZ mouse liver also leads to the constitutive activation of the autophagic response that could not be further activated in the presence of additional physiological stress such as fasting⁶⁵. This autophagic response has been subsequently shown to affect the mitochondria leading to mitochondrial autophagy and mitochondrial injury that can be ameliorated by the treatment with cyclosporine A, an inhibitor of mitochondrial permeability transition⁶⁴. Further activation of autophagy by carbamazepine (CBZ) treatment lowered the levels of ATZ protein, decreased the number of globule-containing hepatocytes and reduced hepatic fibrosis⁶⁶ demonstrating the importance of autophagy as a cellular mechanism for protection against ATZ accumulation. Finally, the accumulation of ATZ in the liver of male PiZ mice also leads to the hepatocyte hyperproliferation due to testosterone-induced ATZ mRNA upregulation. In addition, hepatocytes devoid of ATZ globules were shown to have a relative proliferative advantage over globule-containing cells⁶³. All in all, these studies using the PiZ mouse model have revealed how ATZ accumulation might lead to liver injury and hepatocellular carcinoma and how hepatocytes respond to ATZ mutant protein accumulation.

The Z mouse is another transgenic mouse model for AT in which liver-specific expression of ATZ is turned off by doxycycline treatment of animals⁶¹. Accumulation of ATZ in the Z mouse activates signaling pathways including caspase 12, and NFκB but does not result in the induction of BiP or in the cleavage of XBP1 mRNA. In addition, microarray analysis of the Z mouse liver did not show changes in expression of any of the known target genes of the UPR. These results indicate that the accumulation of mutant ATZ activates specific signaling pathways

that are different from those activated by other nonpolymerogenic AT mutant variants⁶¹. By crossing the Z mouse with the GFP-LC3 mouse, it was also determined that the expression of ATZ in liver is sufficient to induce autophagy, thus definitively confirming the results observed in the PiZ mouse⁶².

More recently, a *Caenorhabditis elegans* model for ATD has been developed by expressing the GFP-tagged ATZ gene under the intestinal-specific promoter of *nhx-2*⁶⁷. In this model, ATZ forms aggregates in the endoplasmic reticulum of intestinal cells. Studies employing genome-wide RNAi screens and genetic crosses using this model system have identified genetic modifiers affecting the accumulation of the alpha-1 antitrypsin Z mutant (ATZ)^{69, 70}. Moreover, results of genome-wide RNAi screens, genetic crosses, and pharmacological screens in this model for ATD identified autophagy and ER-associated degradation (ERAD) pathways as critical for the degradation of intracellular ATZ⁶⁷⁻⁷⁰.

Various cell lines and patient derived-fibroblasts engineered to express the ATZ mutant protein have also been used to study ATD. Similar to results in mouse models of ATD, ATZ accumulation in human fibroblasts also resulted in the increased autophagic response⁷¹. In addition, ATZ protein accumulation in human and mouse cell lines led to the activation of caspase 4, caspase 12, NFkB, and BAP31 but not the members of unfolded protein response pathway⁶¹. Furthermore, studies show that proteasomal degradation is crucial for the disposal of accumulated ATZ proteins in the ER of ATZ-expressing cell lines⁷² and ATZ-expressing fibroblasts⁷³. More recently, a study using *Atg5*-deficient mouse embryonic fibroblasts expressing ATZ, also showed that the absence of autophagy results in a reduced rate of ATZ degradation, and increased formation of cytoplasmic ATZ inclusions⁶². Using ATZ-expressing dermal fibroblasts from PiZZ patients with liver disease (susceptible hosts) and those without

liver disease (protected hosts), a study demonstrated that there was a lag in the degradation of ATZ mutant proteins in susceptible compared to protected hosts⁷⁴. This suggests that genetic factors that influence the degradation of ATZ mutant proteins may confer susceptibility to liver disease. These studies reveal the cellular processes activated by ATZ accumulation and the factors that could predispose ATD patients to liver disease.

1.5 INDUCED PLURIPOTENT STEM CELLS

Human embryonic stem cells (hESCs) hold great promise for biomedical and clinical research because they have the ability to self-renew indefinitely and the capacity to differentiate into all somatic cell types in the body^{78, 79}. hESCs can thus potentially be an unlimited source of cells for disease modeling, drug discovery studies and the treatment of diseases and injuries^{78, 79}. However, the use of hESCs for research has been impeded because of ethical concerns related to the destruction of human embryos⁸⁰. Thus, considerable effort has been expended into developing or discovering cells that have equivalent capabilities as hESCs but that do not involve the destruction of human embryos.

Landmark studies in 2007 demonstrated the conversion of somatic cells into cells that closely resemble hESCs^{81, 82}. These cells, termed induced pluripotent stem cells (iPSs), are able to self-renew indefinitely and can differentiate into all somatic cell types^{81, 82}. Since iPSs are generated without destroying human embryos, it circumvents the ethical concerns that have limited the use of hESCs. iPSs are cells that have been reprogrammed to a pluripotent state by forced expression of exogenous genes and factors that are required for maintaining the defining characteristics of embryonic stem cells⁸¹⁻⁸³. iPSs were first generated from mouse cells in 2006

by Takahashi and Yamanaka when they successfully reprogrammed mouse fibroblasts through retroviral transduction with four transcription factors, octamer-binding transcription factor 3/4 (*Oct3/4*), SRY-box 2 (*Sox2*), *c-Myc*, and Kruppel-like factor 4 (*Klf4*)⁸³. Like mouse embryonic stem cells (mESCs), the mouse iPSCs expressed alkaline phosphatase (AP), the mESC-specific surface marker stage-specific embryonic antigen 1 (SSEA1), and Nanog. They were also able to differentiate into all three germ layers *in vitro*, and form teratomas when subcutaneously injected into immunodeficient mice.

Shortly after, in 2007, two groups demonstrated the reprogramming of human embryonic, neonatal and adult fibroblasts into iPSCs using retroviral⁸¹- or lentiviral⁸²- mediated approaches. In these studies, human iPSCs were isolated based on the distinct human hESC colony morphology. Like hESCs, human iPSCs were positive for alkaline phosphatase (AP), OCT3/4, NANOG, and the cell surface markers stage-specific embryonic antigen 3 (SSEA3), stage-specific embryonic antigen 4 (SSEA 4), tumor-related antigen 160 (TRA160) and tumor-related antigen 181 (TRA181). The human iPSCs also have the ability to differentiate into all three germ layers *in vitro* and generate mature teratomas when injected into immunodeficient mice. Using genome-wide microarray analysis, it was determined that the expression pattern of human iPSCs is more similar to hESCs than to fibroblasts and that a majority of hESC-specific genes are reactivated following reprogramming. One group achieved successful reprogramming using the human orthologs of the same four factors that were used for mouse fibroblasts⁸³ with ~0.02% efficiency 30 days post transduction⁸¹. The other group used a different combination of four factors that replaced *c-MYC* and *KLF4* with *NANOG* and a RNA binding protein *LIN28* with 0.01-0.05% efficiency 20 days post transduction⁸². The identification of novel combinations of pluripotency factors indicates that reprogramming could be achieved through several different

transcription factor networks although *OCT3/4* and *SOX2* appear to be essential for this process^{81, 82, 84}. However, whether the iPSCs generated through distinct combinations of factors are identical remains to be determined.

1.6 GENERATION OF INDUCED PLURIPOTENT STEM CELLS

Like hESCs, iPSCs can self-renew indefinitely and are able to differentiate into cell lineages from all three germ layers^{81, 82}. Unlike hESCs, the use of iPSCs is not ethically controversial. In addition, iPSCs have the unique advantage of being donor-specific and therefore, have generated interest in the field of regenerative medicine and personalized drug testing. There are however, some caveats with the use of iPSCs. Initial methods for the generation of iPSCs involved the introduction of potential oncogenes delivered using either retrovirus or lentivirus^{81, 82}. This method has been particularly problematic because there are possible indirect negative effects because the insertion of exogenous genes in the host cell genome is random. This has been shown to occur in a viral-mediated gene therapy trial where transgene insertion could elevate the expression of nearby endogenous oncogenic factors that could lead to leukemia⁸⁵. Moreover, because viral gene integration is permanent and irreversible^{81, 82} there is always a risk for tumorigenesis due to possible reactivation and overexpression of oncogenic transgenes after silencing^{83, 86}. In addition, the low reprogramming efficiency (0.01-0.05%) associated with initial reprogramming methods is a major hurdle for the generation of iPSCs. In order to circumvent these problems, several groups aimed to develop novel reprogramming methods that involve either transient expression of pluripotency factors or using chemical modulators to efficiently generate clinically useful iPSCs.

To avoid the potential problems that are associated with first generation reprogramming techniques, one group developed a lentiviral vector carrying a single stem cell cassette (STEMCCA) that contains the four Yamanaka factors (*OCT3/4*, *SOX2*, *KLF4*, and *c-MYC*)⁸⁷. The vector was engineered to carry all the reprogramming factors and contain self-cleaving peptide signals in between each of the reprogramming factors as well as loxP sites at either end of the transgene. The technique has several advantages over earlier reprogramming techniques. Unlike retroviruses, lentiviruses can infect both non-proliferating and proliferating cells and has thus become the preferred vehicle for delivering reprogramming factors in somatic cells. In addition, the reprogramming efficiency achieved using a single cassette was superior compared to using four or more vectors. Finally, concern about lentiviral transgene incorporation into the host cell genome was addressed by the addition of loxP sites. After successful reprogramming of host cells, the integrated viral sequence could be excised by the overexpression of Cre-recombinase using either plasmids or adenoviruses. After Cre-mediated excision of transgene sequences it was shown that the iPSCs retained their pluripotency and their ability to differentiate. This method has now been widely used to generate iPSCs with reprogramming efficiencies of 0.1–1.5%. However, this technique still leaves undesirable alterations to the host genome because loxP sites are not removed by Cre-mediated excision.

Episomal plasmids have also been used for the transient expression of reprogramming factors allowing for the generation of integration-free iPSCs. For this method, plasmids containing the OriP/EBNA-1 (Epstein-Barr nuclear antigen-1) backbone are used because they can stably express reprogramming factors for a longer period of time allowing for reprogramming to occur. In one study, nucleofection of human foreskin fibroblasts with three oriP/EBNA-1 plasmids containing the reprogramming factors *OCT3/4*, *SOX2*, *NANOG*, *KLF4*, *c-*

MYC, and *LIN28* and SV40 large T antigen led to 0.0003-0.0006% reprogramming efficiency after 20 days⁸⁸. However, it is likely that the episomal vector integrated into the host genome as only one-third of the subclones from two of the original iPSc lines lost the episomal plasmid. The same group subsequently reported that the efficiency of episomal plasmid-mediated reprogramming is cell type dependent by showing that blood mononuclear cells (BM) can be reprogrammed more efficiently than fibroblasts (0.0352-0.2095% vs 0.0003-0.0356%). Moreover, the addition of the small molecule thiazovivin led to an increase in reprogramming efficiency of cord blood cells by more than ten-fold⁸⁹. In contrast to the initial paper, reprogramming occurred within 12 days and all the iPScs lost the plasmid by passage 15. Another study described plasmid-mediated reprogramming using a different combination of reprogramming factors. In the study, the electroporation of human dermal fibroblasts and dental pulp cells with three oriP/EBNA-1 expression plasmids encoding *OCT3/4* and *P53* shRNA, *SOX2* and *KLF4*, *l-MYC* and *LIN28*, resulted in reprogramming a efficiency of 0.03%⁹⁰. In this study, five out of the seven iPSc clones tested negative for the EBNA-1 DNA after 11-20 passages. This suggests that the episomal vectors were spontaneously lost in majority of the iPScs. Overall, episomal plasmid-mediated reprogramming is an effective strategy for generating footprint-free iPScs although downstream analyses of iPScs have to be performed to identify the small number of iPSc clones with random plasmid integration.

The use of mRNA as a method for obtaining footprint-free iPScs has also been reported⁹¹. The transfection of human fibroblasts with modified mRNA expressing the Yamanaka factors resulted in 1.4% reprogramming efficiency within 20 days. Further optimization studies determined that the inclusion of *LIN28* to the Yamanaka factors, incubation of the cells at 5% CO₂, and the addition of valproic acid to the medium increased the efficiency

to 4.4%⁹¹. However, this method is expensive and labor intensive because cells have to be transfected with modified mRNA for 17 days. Moreover, mRNA-based reprogramming kits have so far only been validated in fibroblasts.

The use of reprogramming factors in the form of proteins can be an ideal approach to generate integration-free iPSCs. However, the production of large quantities of bioactive proteins able to pass through the plasma membrane has been technically difficult. One study was able to produce reprogramming proteins (OCT3/4, SOX2, KLF4, and c-MYC) each fused with a cell penetrating peptide (CPP) composed of nine arginine residues using an HEK 293 system⁹². Direct treatment of human newborn fibroblasts with supernatant containing the CPP-anchored reprogramming proteins for six cycles resulted in stable iPSCs from human newborn fibroblasts within 8 weeks at an efficiency of 0.001%. Although successful at generating iPSCs, this reprogramming strategy is slow and inefficient and has not been tested on non-fibroblast cells. This approach therefore needs to be optimized in order to become a viable reprogramming method.

1.7 DISEASE-SPECIFIC INDUCED PLURIPOTENT STEM CELLS

Because of significant research advances in recent years, the pathophysiological mechanisms underlying various chronic diseases and disorders have been elucidated and therapies for their treatment have subsequently been developed. However, for some diseases and disorders the underlying mechanisms remain elusive because of the lack of disease models reflecting human pathogenesis. The lack of appropriate human models for these diseases and disorders has hampered the development of novel treatments and therapies. Cell line and animal disease

models have been developed for some of these disorders but there has been much debate as to whether these can accurately reflect the mechanisms that actually occur in the human setting because of cell line-specific and species-specific differences.

The advent of iPSc technology and the development of techniques for *in vitro* differentiation of pluripotent stem cells toward several somatic cells have paved a way for a new source of human cells for disease modeling. Because iPSCs are donor-specific, reprogramming of cells from an individual affected by a genetic disease generates iPSCs that carry patient-specific genetic information. These disease-specific iPSCs offer a unique opportunity to produce unlimited numbers of cell types affected by each patient's disease. The differentiated cells could then be used for modeling diseases and developing novel drugs or therapies. Neurological disorders, cardiac diseases and metabolic disorders have now been extensively modeled using iPSc technology (Table 1).

Table 1. Diseases modeled using induced pluripotent stem cell technology

| Disorder | References |
|---|-------------------|
| Amyotrophic lateral sclerosis | 93 |
| Adenosine deaminase deficiency-related SCID | 94 |
| Shwachman-Bodian-Diamond syndrome | 94 |
| Gaucher disease type III | 94 |
| Duchenne muscular dystrophy | 94 |
| Becker muscular dystrophy | 94 |
| Parkinson disease | 94 |
| Huntington disease | 94 |
| Juvenile-onset, type 1 diabetes mellitus | 94 |
| Down syndrome (trisomy 21) | 94 |
| The carrier state of Lesch-Nyhan syndrome | 94 |
| Spinal muscular atrophy | 95 |
| Idiopathic Parkinson's disease | 96 |
| ATD | 97 |
| Glycogen storage disease type 1a | 97 |
| Crigler-Najjar syndrome | 97 |
| Familial hypercholesterolemia | 97, 98 |
| Hereditary tyrosinemia type 1 | 97 |
| Wilson's disease | 99 |
| Familial transthyretin amyloidosis | 100 |
| Arrhythmogenic right ventricular cardiomyopathy | 101 |
| Long QT syndrome type 3 | 102 |

Aside from modeling various pathologies, iPSc technology could also be used to determine the link between mutations and their corresponding phenotype. The use of isogenic iPSc lines, which carry the same genetic information except for the gene of interest, allowed researchers to adequately determine changes in phenotype due to changes in a single gene. Genomic editing methods using Zinc Finger Nucleases (ZFN)¹⁰³ and piggyBac technology^{104, 105}, Clustered Regularly Interspaced Short Palindromic Repeat (CRISPR)/CRISPR-associated nuclease 9 (Cas9) system¹⁰⁶ or Transcription Activator-Like Effector Nucleases (TALENs)¹⁰⁷ have already been used to generate isogenic iPScs/hESCs. Indeed, recent studies have shown that the correction of disease-causing single mutations in iPScs results in the abrogation of disease

phenotypes indicating that these mutations are necessary for generating disease phenotypes¹⁰⁸⁻¹¹². One study also demonstrated that the targeted knock-in of the G2019S mutation in the Leucine-rich repeat kinase 2 (LRRK2) gene is sufficient to impart a Parkinson's disease phenotype on normal human embryonic stem cells (hESCs)¹¹³.

While disease-specific iPSc have provided an exciting tool to recapitulate known defects and uncover new mechanisms underlying human disease, there are still some limitations with using this technology for modeling and drug discovery. There is a need to ensure equivalence in the degree of maturation between the cells in order to achieve realistic comparisons between pathologic adult cells and disease-specific iPSc-derived cells. One study has shown that the gene expression profile of hESC-derived neurons were more similar to fetal neurons rather than adult ones¹¹⁴. Another study showed that the expression profile of cardiac-specific myosin heavy and light chains, cardiac troponin, ion channels, and actin related genes in iPSc-derived cardiomyocytes more closely resembled fetal cardiomyocytes than adult cardiomyocytes¹¹⁵. Finally, several groups have shown the persistent expression of the fetal hepatocyte marker alpha-fetoprotein by iPSc-derived hepatocytes which implies an immature phenotype^{97, 116, 117}. Modeling genetic diseases using iPSc technology is limited by the degree of maturation of differentiated cells. Modeling late-onset diseases would therefore be difficult unless new techniques are developed to improve the maturation of iPSc-derived cells.

1.8 DIFFERENTIATION OF IPSCS INTO HEPATOCYTES

Human hepatocytes are important for use in both therapeutic and experimental applications. The clinical transplantation of hepatocytes for the correction of certain metabolic liver disorders has

been an appealing prospect because the liver is amenable to the introduction of exogenous hepatocytes¹¹⁸⁻¹²³. There has also been a great deal of interest with the use of hepatocytes for disease modeling and drug discovery because hepatocytes are sites of drug metabolism and detoxification, are affected by several metabolic diseases, and are targeted by many pathogens that cause severe liver disease¹²⁴. However, the supply of primary human hepatocytes suitable for these applications cannot currently meet the demand, due to limited donor availability and inconsistent quality. Hepatocytes rapidly dedifferentiate and lose most of their liver specific gene expression and metabolic activity when grown *in vitro*^{125, 126}. In addition, cryopreservation of primary hepatocytes leads to reduced viability and metabolic function after thawing^{87, 127-136}. These constraints have therefore prompted a search for alternative sources of hepatocytes for both clinical and research purposes.

Numerous studies have described the differentiation of hESCs into cells that display several hepatocyte characteristics¹³⁷⁻¹⁴⁴. Although the protocols differ in the initial stage of differentiation, with some starting with a monolayer of cells while others with a three-dimensional cell aggregate called embryoid body (EB), all of them aim to recapitulate the developmental cues that occur during hepatogenesis, a process that involves a well-coordinated interaction between the definitive endoderm (DE), cardiac mesoderm and septum transversum mesenchyme. The methods generally follow a series of steps that involve definitive endoderm induction, hepatic induction and hepatic maturation¹⁴²⁻¹⁴⁸. This involves treating the cells with growth factors that are involved in each of the steps during development *in vivo*, such as mimicking Nodal expression by Activin A to induce definitive endoderm, treating with various fibroblast growth factors (FGF) and bone morphogenetic proteins (BMPs) to recapitulate secretion by the cardiac mesoderm and septum transversum mesenchyme, and hepatocyte growth

factor (HGF) to induce proliferation and maturation of hepatic progenitors¹⁴⁹⁻¹⁵². One study employed a 3-step protocol involving definitive endoderm induction, hepatic induction and hepatocyte maturation to generate hepatocyte-like cells that upon subsequent selection for asialoglycoprotein receptor 1 (ASGPR1) positive cells led to a population of hepatocytes similar to primary human hepatocytes in culture¹⁴². These cells expressed hepatic genes and did not express genes associated with other developmental lineages. The cells secrete ALB, AT, urea, and functional coagulation factor VII (F7) and in addition, the cells exhibit inducible and functional cytochrome p450 (CYP) activity. More importantly, the cells are able to engraft and repopulate in rodent livers.

The successful production of hESc-derived hepatocytes provided the foundation for producing patient-specific hepatocytes from iPSCs. The generation of iPSC-derived hepatocytes from patients is particularly exciting because it would provide disease-specific hepatocytes for disease modeling and drug testing. Additionally, it would provide autologous hepatocytes that can be genetically corrected and transplanted back into the patient. Several studies have reported the differentiation of iPSCs into hepatocyte-like cells. The first study reported the differentiation of iPSCs into hepatocyte-like cells following a 4-step protocol involving DE induction, hepatic specification, hepatoblast expansion, and hepatic maturation¹¹⁷. The expression of hepatic markers and liver-related functions of the iPSC-derived hepatic cells were similar to that of the hepatocytes except for alpha-fetoprotein (AFP) and cytokeratin 19 (CK19). The differentiated cells also exhibited liver cell functions including ALB secretion, glycogen synthesis, urea production and inducible CYP activity although the levels are significantly less than human hepatocyte activity. Another study described a 4-step approach involving DE induction at ambient O₂ levels, hepatic specification at 4% O₂ levels, hepatic induction at 4% O₂ levels, and

hepatic maturation at ambient O₂ levels¹¹⁶. The differentiated cells possessed a hepatocyte mRNA fingerprint that is similar to hESc-derived hepatocyte-like cells. The differentiated cells also performed several hepatic functions including the accumulation of glycogen and lipids, metabolism of indocyanine green, uptake of low-density lipoprotein, and synthesis of urea although the functionality of the cells were not compared to primary human hepatocytes. More importantly, the iPSc-derived hepatocytes exhibited short-term engraftment when transplanted in mouse liver. Subsequently, another group reported successful differentiation of liver disease-specific iPScs into hepatocyte-like cells using a 3-step method⁹⁷. Electron microscopy of differentiated cells showed the presence of glycogen deposits and apical microvilli as well as prominent nuclei, Golgi bodies and endoplasmic reticulum. The resulting cells are also able to store glycogen and LDL, secrete ALB, and metabolize drugs via the CYP pathway although the functionality of the cells were not compared to primary human hepatocytes. These studies provide proof that iPScs can be efficiently differentiated into hepatocyte-like cells *in vitro*.

1.9 DISEASE MODELING USING IPSC-DERIVED HEPATOCYTE-LIKE CELLS

The ability to conduct mechanistic studies on live human hepatocytes would facilitate the discovery of mechanisms underlying liver diseases and the development of novel treatments or therapies. However, liver tissues are not readily available especially those that are from patients affected by relatively rare liver diseases. In addition, although well-developed protocols are available for hepatocyte isolation from liver tissues, the isolation of hepatocytes from cirrhotic liver tissues is challenging. Moreover, hepatocytes isolated from liver tissues can only provide information about the latter stages of the disease. Various cell lines and inbred animals have

therefore been utilized as models to study liver diseases. Although considerable insights into human liver disease pathology have been revealed using these model systems, these systems lack the significant genetic diversity of humans and for some diseases only display an approximate resemblance to the human disease.

The generation of hepatocyte-like cells (iHeps) from disease-specific human iPSCs provides a unique platform for understanding liver disease biology and identifying and testing novel treatments. In the past five years, several studies have reported the use of disease-specific iHeps from patients with metabolic liver diseases to model the diseases *in vitro*. iHeps generated from patients with ATD showed the accumulation of AT polymers in ATD iHeps but not in control iHeps. The localization of AT polymers in the ER of the cells was also confirmed by subcellular fractionation and endoglycosidase H digestion⁹⁷. iHeps generated from a patient with familial hypercholesterolemia (FH) displayed the absence of the low-density lipoprotein receptor (LDLR). The FH iHeps also exhibited the known functional abnormality characteristic of LDLR deficiency that was evident by an impaired ability to incorporate LDL⁹⁷. In another study, iHeps from a FH patient with mutations in the LDLR gene that leads to homozygous loss of LDLR function (but not expression) exhibited inefficient uptake of LDL-cholesterol (LDL-C) and increased secretion of lipidated apolipoprotein B-100. More importantly, the study showed that upon treatment with the hepatoselective lipid-lowering drug lovastatin, FH iHeps have an increased ability for LDL uptake⁹⁸. iHeps generated from a patient with glycogen storage disease type 1a (GSD1a) exhibited elevated accumulation of intracellular lipid and glycogen, as well as excessive production of lactic acid⁹⁷. iHeps from a patient with Wilson's disease (WD) exhibited abnormal cytoplasmic localization of the mutated Cu²⁺ Transporting ATPase Beta (ATP7B) protein and significantly reduced copper-export activity. In addition, the study showed that the

functional defect of the WD iHeps could be rescued *in vitro* by transduction with a lentiviral vector that expresses codon optimized-ATP7B or treatment with the chaperone drug curcumin⁹⁹. iHeps have also been used to model familial transthyretin amyloidosis (ATTR), a multisystem disorder caused by mutations in the transthyretin (TTR) gene¹⁰⁰. In this protein-folding disorder, the mutant TTR protein that is produced by hepatocytes aggregates and forms fibrils in the heart and peripheral nervous system. In the study, iHeps, cardiomyocytes and neurons were generated from ATTR patient-specific iPSCs. iPSC-derived cardiomyocytes and neurons displayed oxidative stress, increased cell death, and upregulation of ATTR disease-associated genes when exposed to mutant TTR produced by the patient-matched iHeps, recapitulating the reported observations in both *in vivo* and *in vitro* model systems. Treatment of mutant TTR-exposed cardiomyocytes and neurons with small molecule TTR stabilizers ameliorated this pathology *in vitro*. All in all, these studies demonstrate not only the ability of iHeps to recapitulate the complex pathophysiology of several metabolic liver diseases in culture, but also their capacity to be used as a system for developing novel therapies or therapeutics for liver disease.

1.10 SPECIFIC AIMS

Classical alpha-1 antitrypsin deficiency (ATD) is caused by the PIZZ mutation, a homozygous single nucleotide G11940A substitution in the protease inhibitor gene (PI) that produces a mutant alpha-1 antitrypsin (AT) protein variant called ATZ. Hepatic dysfunction caused by ATD results from the toxic effects of ATZ accumulation within the endoplasmic reticulum (ER) of hepatocytes, the major site of AT synthesis. While some ATD patients develop severe liver

disease that necessitates liver transplantation, others with the same genetic defect completely escape this clinical phenotype¹⁵.

The limited number of patient-derived live human hepatocytes from ATD patients presents a major obstacle for understanding this observed variability in liver disease phenotype. While liver tissue from patients can be used for analyses, these samples can only reveal aspects of the disease at its culmination^{64, 153}. Studies using cellular and animal model systems have provided invaluable insights into the pathobiology of the disease^{62, 64, 66, 68, 71, 72, 74, 154-156}. However, except for patient-derived fibroblasts⁷⁴, these model systems lack the genetic diversity of humans that seems to be at least partly responsible for the observed variation in liver disease phenotype⁷⁴. Human induced pluripotent stem cells (iPSCs) have the potential to provide an unlimited source of hepatocytes for experimental analysis. We propose to generate ATD iPSC-derived hepatocyte-like cells as a model for understanding the variability associated with ATD-mediated liver disease. We believe that this would be a model that more faithfully recapitulates the human clinical condition and that can be used to validate the findings derived from other model systems.

The goal of this study is to (1) generate iPSCs from somatic cells of ATD patients with and without liver disease, (2) differentiate ATD iPSCs into iPSC-derived hepatocyte-like cells, and (3) determine the extent to which iHeps from ATD patients can model ATD. We hypothesize that iHeps from ATD patients can, not only model the primary genetic defect, but also the modifiers that define the patient-specific variations in severity of disease.

1.10.1 Reprogramming of alpha-1 antitrypsin deficient patient-derived somatic cells into iPSCs

We generated iPSCs from primary hepatocytes or fibroblasts obtained from a normal control and ATD patients with varying degrees of liver disease using either viPS™ lentiviral gene transfer kit, non-integrating episomal plasmids, or a single excisable lentivirus cassette. The pluripotency of iPSC lines were confirmed by qPCR for the expression of pluripotency makers *OCT3/4*, *NANOG*, *REX1 (ZFP42)*, *TERT*, *TRA160 (PODXL)*, and *DNMT3B*, immunofluorescent staining for the pluripotency markers *OCT3/4*, *NANOG*, *SOX2*, *TRA160*, and *SSEA4*, teratoma formation assay in NOD/SCID mice. Finally, genomic DNA sequencing was performed to confirm the genotype of the generated iPSC lines.

1.10.2 Differentiation of alpha-1 antitrypsin deficient patient-derived iPSCs into hepatocyte-like cells

We differentiated ATD and wild type iPSCs into iHeps using a variation of the 4-step protocol described by Si-Tayeb¹¹⁶. At the end of each step of the differentiation, changes in mRNA expression of stage specific markers (*NANOG*, *OCT3/4*, *CXCR4*, *FOXA2*, and *HNF4A*) were monitored by qPCR to ensure hepatocyte-directed differentiation. At the end of the differentiation, immunofluorescent staining was done to determine the percentage of iHeps expressing mature hepatocyte markers (*ALB* and *ASGPR1*) and those expressing immature hepatocyte markers (*ALB* and *AFP*). The iHeps were further characterized by examining their

ultrastructure using transmission electron microscopy (TEM). Finally, the ability of iHeps to functionally secrete ALB and AT was assayed by ELISA.

1.10.3 Modeling the pathogenesis and variability of alpha-1 antitrypsin deficiency using patient-derived iPSc generated hepatocyte-like cells

We first tested the ability of ATD iHeps to model the known biochemical abnormalities associated with the misfolded ATZ molecule. The kinetics of ATZ processing and secretion in ATD iHeps was assayed using pulse-chase radiolabeling and PNGase F/Endo H deglycosylation assays. We then examined the extent to which ATD iHeps can model the morphological and ultrastructural characteristics of the disease using immunofluorescence staining for AT and rER/Golgi markers and TEM. Finally, we determined whether there are differences in the kinetics of intracellular ATZ degradation and ultrastructural features of severe LD and no LD iHeps using pulse-chase labeling and TEM.

2.0 REPROGRAMMING OF ALPHA-1 ANTITRYPSIN DEFICIENT PATIENT- DERIVED SOMATIC CELLS INTO IPSCS

2.1 INTRODUCTION

Relatively little is known about why some people with the classical form of alpha-1 antitrypsin deficiency (ATD) develop life-threatening liver disease, necessitating liver transplantation, while others with the exact same genetic defect completely escape this clinical phenotype¹⁵. The inability to analyze patient-derived live human hepatocytes from ATD patients in any significant numbers presents a major obstacle in understanding the biology of ATD-mediated liver disease and for the development of novel drugs and therapies. While liver tissue from patients can be used for analyses, these samples can only reveal aspects of the disease at its culmination^{64, 153}. Studies using cellular and animal models have provided invaluable insights into the pathobiology of the disease^{62, 64, 66, 68, 71, 72, 74, 154-156}. However, except for patient-derived fibroblasts⁷⁴, these model systems lack the genetic diversity of humans that seems to be at least partly responsible for the observed variation in liver disease phenotype⁷⁴. While liver tissue from patients can be used for analyses, these samples can only reveal aspects of the disease at its culmination^{64, 153}.

Induced pluripotent stem cells (iPSCs) generated from ATD patients have the potential to provide an unlimited source of hepatocytes for analysis^{97, 157-159}. Here, we generated of multiple human iPSc lines using lentiviral, episomal plasmid constructs or excisable lentiviral stem cell

cassettes carrying reprogramming factors from primary human cells of a normal control and ATD patients with varying severity of liver disease following exposure to either. ATD iPSCs can be used to produce theoretically unlimited numbers of ATD hepatocytes which can then be used to recapitulate pathologic tissue formation *in vitro* or *in vivo*, thereby providing a model which can represent the variability in liver disease phenotype.

2.2 MATERIALS AND METHODS

2.2.1 Use of human- and animal-derived tissues

All human tissues were obtained with informed consent following guidelines approved by the Institutional Review Boards of the University of Pittsburgh, Boston University School of Medicine and Albert Einstein College of Medicine. All animal experiments were performed in accordance with the Institutional Animal Care and Use Committee of the University of Pittsburgh guidelines for human use of animals for research.

2.2.2 Hepatocyte isolation from liver explants

Primary hepatocytes from an ATD patient with severe liver disease were obtained from the explanted liver of an ATD patient who received a liver transplant. Hepatocytes were isolated by three-step collagenase perfusion as described previously^{160, 161}. Briefly, silicone catheters were

inserted into the major portal and/or hepatic vessels and the tissue was perfused with Hank's Balanced Salt Solution (HBSS) without calcium, magnesium or phenol red (Lonza Walkersville Inc., Walkersville, MD) to determine the vessel(s) that would provide the most uniform perfusion of the tissue. Purse string sutures were then tied around each vessel with its accompanying catheter to prevent the leakage of buffer around the catheter during the perfusion. Perfusion proceeded once all remaining major vessels on the cut surfaces were closed with sutures around catheters or with surgical grade super glue. The liver tissue was placed in a sterile plastic bag and connected to a peristaltic pump with flow rate between 35 to 240 ml/min. The bag containing the tissue was placed in a circulating water bath at 37°C and the tissue was perfused with HBSS supplemented with 0.5 mM ethylene glycol tetraacetic acid (EGTA) (Sigma-Aldrich Corp., St. Louis, MO) without recirculation. Chelation of calcium by EGTA aids in the dissolution of intercellular junctions between hepatocytes and in the washing of hematopoietic cells. A second, non-recirculating perfusion with HBSS without EGTA was performed to flush residual EGTA from the tissue since calcium is essential for collagenase enzyme activity. During the second perfusion step, Clzyme™ collagenase MA (VitaCyte, LLC, Indianapolis, IN) was reconstituted and sterile-filtered according to manufacturer's recommendations. Just prior to the third perfusion step, 100 mg Clzyme™ collagenase MA and 24 mg Clzyme™ BP Protease (VitaCyte, LLC, Indianapolis, IN) were mixed with 1L of Eagle's Minimum Essential Medium (EMEM) (Lonza Walkersville Inc., Walkersville, MD). The tissue was then perfused with this EMEM-collagenase solution with recirculation as long as needed to complete the digestion. The duration of perfusion with the EMEM-collagenase solution was determined by continuously monitoring tissue integrity. Perfusion was stopped when the liver tissue beneath the capsule surface was visibly digested and separated from the capsule. The

tissue was then transferred to a sterile plastic beaker that contained ice-cold EMEM and was gently cut with sterile scissors to release hepatocytes. The cell suspension was filtered through a sterile gauze-covered funnel to remove cellular debris and clumps of undigested tissue. Hepatocytes were enriched by three consecutive centrifugation steps each at 80xg for 6 min at 4°C. After three washes in EMEM, hepatocytes were suspended in cold Hepatocyte Maintenance Medium™ (HMM) (Lonza Walkersville Inc., Walkersville, MD). Cell viability expressed as percentage of viable cells over the total cell number was assessed by trypan blue exclusion. For determining plating efficiency and for reprogramming, 1×10^6 cells were plated onto collagen-coated 6-well plates and cultured for 2 hours in HMM™ with SingleQuots of 1×10^{-7} M dexamethasone, 1×10^{-7} M insulin, and 50 ug/mL gentamicin/amphotericin-B (Lonza Walkersville Inc., Walkersville, MD) and supplemented with 5% fetal bovine serum (FBS) (Atlanta Biologicals, Inc., Lawrenceville, GA) to facilitate cell attachment. The media was then switched to HMM™ with SingleQuots of 1×10^{-7} M dexamethasone, 1×10^{-7} M insulin, and 50 ug/mL gentamicin/amphotericin-B (Lonza Walkersville Inc., Walkersville, MD) with no FBS and cultured overnight. Plating efficiency expressed as the percentage of cells that attached over the total number of plated cells was determined by counting the number of attached cells after detachment. Only cells with a viability of >80% and a plating efficiency of >70% were used for reprogramming.

2.2.3 Cell culture

Primary human fibroblasts were cultured in fibroblast medium containing Dulbecco's Modified Eagle Medium (DMEM) (Life Technologies, Carlsbad, CA) supplemented with 10% defined

fetal bovine serum (dFBS) (HyClone Laboratories, Logan, Utah), 1X L-glutamine (Life Technologies, Carlsbad, CA), 1X Minimum Essential Medium Non-Essential Amino Acids (MEM NEAA) (Life Technologies, Carlsbad, CA), and 1X penicillin-streptomycin (Life Technologies, Carlsbad, CA). Isolated primary human hepatocytes were cultured in HMM™ with SingleQuots of 1×10^{-7} M dexamethasone, 1×10^{-7} M insulin, and 50 ug/mL gentamicin/amphotericin-B.

iPSCs and hESCs were grown on culture plates or dishes coated with hESC-qualified matrigel (BD Biosciences, San Jose, CA) and maintained in mTeSR1™ (STEMCELL Technologies Inc., Vancouver, BC, Canada) with media changes done everyday until the cells are ~80% confluent and ready for passage. iPSCs were passaged according to standard feeder-free protocol. Briefly, cells were washed with Dulbecco's Modified Eagle Medium/Nutrient Mixture F-12 (DMEM/F12) (Life Technologies, Carlsbad, CA) and incubated with 1 mL of 1 mg/mL dispase (Life Technologies, Carlsbad, CA) at 37°C for 5-12 minutes until the colony edges start to detach. Cells were washed three times with DMEM/F12 and were given fresh mTeSR1™. Colonies were manually scratched using sterile 5 mL glass pipettes and were transferred into 15 mL conical tubes. Colonies were broken into smaller pieces by gentle aspiration using 5 mL glass pipettes. Detached colonies were centrifuged at 300 rpm for 5 minutes at room temperature. Colonies were then resuspended in mTeSR1™ and transferred onto hESC-qualified matrigel-coated culture plates or dishes. The splitting ratio depends on the iPSC line and on the confluence prior to passaging but is generally 1:6 to allow a week before the next passage.

2.2.4 Generation of iPSCs from somatic cells

Reprogramming of hepatocytes and fibroblasts was done using three different techniques. For all reprogramming techniques, colonies that had similar morphology and growth characteristics to H1 hESCs were selected for expansion between 20-30 days after reprogramming. Colonies were visualized using an inverted microscope inside a laminar flow hood. Selected colonies were gently scratched off of the bottom of the culture plate using a glass aspirating pipette with a smooth end and manually transferred using a 20 uL pipette onto freshly-prepared hESC-qualified matrigel-coated 24-well plates. Colonies were allowed to attach for 2 days and incubated in mTeSR1™ with media changes done every 2 days.

Lentiviral-mediated reprogramming was initiated using the viPS™ lentiviral gene transfer kit (Thermo Fisher Scientific, Waltham, MA) following the manufacturer's instructions to ectopically express *OCT3/4*, *NANOG*, *SOX2*, *LIN28*, *KLF4*, and *c-MYC*. Primary fibroblasts or freshly-isolated hepatocytes were seeded onto 1 well of a hESC-qualified matrigel (BD Biosciences, San Jose, CA)-coated 6-well plate at 1×10^5 cells/well in either fibroblast media or HMM™ and allowed to attach overnight. The following day, after washing the cells with Dulbecco's Phosphate-Buffered Saline (DPBS) (Life Technologies, Carlsbad, CA), the cells were incubated in 1 mL of transduction media consisting of the cell type's respective culture medium without serum and supplemented with 6 µg/ml polybrene (EMD Millipore, Billerica, MA) and each of the six lentiviruses (Thermo Fisher Scientific, Waltham, MA) at a multiplicity of infection (MOI) of 10. After 24 hours, the cells were washed 3X with DPBS and the cells were cultured in their respective media for 3 days. The culture medium was switched to mTeSR1™ starting on day 4 with media changes done every 2 days. Colonies started to appear within 15 days with new colonies appearing until day 35.

Plasmid-mediated reprogramming was done according to a previously described protocol⁹⁰ with some modifications. Primary fibroblasts were grown until the cells reach the log phase. Cells were trypsinized, washed twice with DPBS, and counted. For each nucleofection, 1×10^6 cells were resuspended in 100 μ L of the Amaxa™ normal human dermal fibroblast (NHDF) Nucleofector™ kit (Lonza Walkersville Inc., Walkersville, MD) containing 3 μ g of each of the four expression plasmids encoding *OCT3/4* and *P53* shRNA, *SOX2* and *KLF4*, *l-MYC* and *LIN28*, and *eGFP*. Cells were nucleofected using program U-23 on an Amaxa™ Nucleofector™ II (Lonza Walkersville Inc., Walkersville, MD). Nucleofected fibroblasts were plated on hESc-qualified matrigel-coated plates, cultured in mTeSR1™ medium for a week under ambient oxygen conditions, and then transferred into reduced oxygen conditions (4% O₂/5% CO₂). Colonies started to appear within 20 days with new colonies appearing until day 30.

Reprogramming of fibroblasts using the excisable lentivirus cassette containing human *OCT4*, *KLF4*, *SOX2*, and *c-MYC* has been described¹⁶². Briefly, 1×10^5 human fibroblasts were seeded onto a gelatin-coated 35-mm plastic tissue culture dish and cultured in fibroblast medium. The next day polybrene (5 μ g/ml) was added to the media, and the cells were infected with hSTEMCCA-loxP lentivirus at a multiplicity of infection of 10. The day after, the media was changed to serum-free iPSc media, and on day 6 the entire well was trypsinized and passaged at a 1:16 ratio by plating onto two 10-cm gelatin-coated culture dishes that were preseeded with mitomycin C-inactivated mouse embryonic fibroblasts (MEFs). iPSc colonies were mechanically isolated 30 days postinfection based on morphology and expanded on MEF feeders in iPSc media. The transfection of selected iPSc colonies for the excision of viral sequences was

performed using the HelaMONSTER® transfection reagent (Mirus Bio LLC, Madison, WI) according to manufacturer's instructions.

2.2.5 RNA Extraction, cDNA synthesis and qPCR

Total RNA was isolated according to manufacturers' instructions using the RNeasy Mini Kit (Qiagen, Germantown, MD). cDNA was synthesized according to manufacturers' instructions using SuperScript III First-Strand Synthesis System and oligo dT primers (Life Technologies, Carlsbad, CA). qPCR was performed according to manufacturers' instructions using the Taqman Fast Advanced Master Mix (Life Technologies, Carlsbad, CA) on a StepOnePlus Real-Time PCR System (Life Technologies, Carlsbad, CA) following the Fast Mode cycling conditions for Taqman Gene Expression Assays. H1 hESc cDNA was used as the positive cellular control. Primary hepatocyte cDNA was used as the negative cellular control. Nucelase-free water was used as the negative assay control. Coagulation factor VII (F7) was used as a non-pluripotent marker control. Values are shown as mean \pm s.d. Taqman Gene Expression Assay IDs are listed in Table 2.

Table 2. Taqman Gene Expression Assay IDs for the qPCR analysis for pluripotency factors

| Target Gene | Gene Expression Assay ID | Dye | Quencher |
|---|--------------------------|-----|----------|
| <i>PPIA</i> (<i>Cyclophilin A</i>) – Internal Control | Hs99999904_m1 | FAM | NFQ |
| <i>OCT3/4</i> (<i>POU5F1</i>) | Hs03005111_g1 | FAM | NFQ |
| <i>NANOG</i> | Hs02387400_g1 | FAM | NFQ |
| <i>REX1</i> (<i>ZFP42</i>) | Hs01938187_s1 | FAM | NFQ |
| <i>TERT</i> | Hs00972656_m1 | FAM | NFQ |
| <i>TRA160</i> (<i>PODXL</i>) | Hs01574644_m1 | FAM | NFQ |
| <i>DNMT3B</i> | Hs00171876_m1 | FAM | NFQ |
| <i>F7</i> | Hs01551992_m1 | FAM | NFQ |

2.2.6 Pluripotency-marker staining

Antibodies and their corresponding dilutions are listed in Table 3. For nuclear staining, cells were washed with phosphate buffered saline (PBS) (Life Technologies, Carlsbad, CA) and fixed in 100% pre-chilled ethanol at -20°C overnight. After three PBS washes, cells were washed with wash buffer containing 0.1% bovine serum albumin (BSA) (Sigma-Aldrich Corp., St. Louis, MO), and 0.1% TWEEN 20® (Sigma-Aldrich Corp., St. Louis, MO) in PBS. Samples were then blocked and permeabilized in blocking buffer containing 10% normal donkey or goat serum (Santa Cruz Biotechnology, Dallas TX), 1% BSA, 0.1% TWEEN 20®, and 0.1% Triton X-100 (Sigma-Aldrich Corp., St. Louis, MO) in PBS for 1 hour at room temperature. Cells were then stained with primary or conjugated antibodies in blocking buffer at 4°C overnight. After three washes with wash buffer, cells were stained with secondary antibodies for 1 hour in the dark at room temperature. After three washes with wash buffer, and three washes with PBS, cells were then incubated for 1 minute in 1 ug/mL Hoechst 33342 in PBS (Life Technologies, Carlsbad, CA), followed by three PBS washes before visualization. Cells were imaged on an IX71 inverted epifluorescent microscope (Olympus, Central Valley, PA).

For membrane staining, cells were washed with PBS and fixed in 4% paraformaldehyde for 15 minutes at room temperature. After three cold PBS washes, cells were blocked in blocking buffer containing 3% BSA and 5% donkey serum in PBS for 2 hours at room temperature. Cells were then stained with conjugated antibodies in blocking buffer at 4°C overnight. After three washes with PBS, cells were then incubated for 1 minute in 1 ug/mL Hoechst 33342 in PBS, followed by three PBS washes before visualization. Cells were imaged on an IX71 inverted epifluorescent microscope.

Alkaline phosphatase staining of cells was performed using the Vector® Blue Alkaline Phosphatase Substrate (Vector Laboratories, Inc., Burlingame, CA) according to manufacturer's recommendations. Cells were imaged on an IX71 inverted epifluorescent microscope using light microscopy settings.

Table 3. List of antibodies and dilutions used for the immunofluorescent staining for pluripotency factors

| Antibody | Manufacturer | Host | Catalogue No. | Dilutions |
|---------------------------------|--|--------|---------------|-----------|
| anti-NANOG | Cell Signaling Technology, Beverly, MA | mouse | 4893S | 1:2000 |
| anti-OCT3/4 | Santa Cruz Biotech, Santa Cruz, CA | rabbit | sc-9081 | 1:250 |
| anti-SOX2 | Millipore, Bedford, MA | rabbit | AB5603 | 1:300 |
| anti-SSEA4-Alexa Fluor 555 | BD Biosciences, San Jose, CA | mouse | 560218 | 1:100 |
| anti-TRA-1-60-Alexa Fluor 488 | BD Biosciences, San Jose, CA | mouse | 560173 | 1:100 |
| anti-rabbit IgG-Alexa Fluor 488 | Life Technologies, Carlsbad, CA | goat | A11008 | 1:250 |
| anti-mouse IgG-Alexa Fluor 546 | Life Technologies, Carlsbad, CA | goat | A11030 | 1:250 |

2.2.7 Teratoma formation assay

For each iPS cell line, a confluent well of cells was passaged according to standard protocols. Briefly, cells were washed with DMEM/F12 and treated with 1 mL of 1 mg/mL dispase for 5-12 minutes at 37°C. Cells were washed three times with DMEM/F12 and were manually scratched using sterile 5 mL glass pipettes. Detached colonies were centrifuged at 300 rpm for 5 minutes at 4°C. Colonies were then resuspended in chilled hESc-qualified matrigel and kept at 4°C. Colonies were subcutaneously injected into anesthetized nonobese diabetic/severe combined immunodeficiency (NOD/SCID) mice (Charles River, Malvern, PA). After 1-3 months, depending on tumor size, mice were anesthetized and sacrificed prior to tumor extraction. Fixed tissue samples were submitted to the Children's Hospital of UPMC Histology Core Laboratory for embedding, sectioning and hematoxylin and eosin (H&E) staining.

2.2.8 Genomic DNA sequencing

Genomic DNA was obtained using the DNeasy® Blood & Tissue kit (Qiagen, Germantown, MD). To ensure specificity, sequencing was performed using a nested PCR assay using AccuPrime™ Pfx DNA Polymerase (Life Technologies, Carlsbad, CA). First, 558bp of exon 5 of the *SERPINA1* containing the mutation site was amplified using amplifying primers (F: AAGATGGACAGAGGGGAGCC, R: CAGCACTGTTACCTGGAGCC). The amplicon was then sequenced using a sequencing primer (CAGCCAAAGCCTTGAGGAGG) that is downstream of the forward amplifying primer. Amplicons were submitted to the University of Pittsburgh Genomics and Proteomics Core Laboratories for sequencing.

2.3 RESULTS

iPSc lines were generated from 3 no liver disease (no LD) and 2 severe liver disease (severe LD) ATD PiZZ patients and a wild type control using lentiviral, plasmid-based, or excisable lentiviral stem cell cassette reprogramming (Table 4). Here, severe LD ATD iPScs are defined as cells generated from ATD patients less than 10 years of age who required liver transplantation and no LD ATD iPScs are defined as cells generated from ATD patients with lung disease but with no clinically overt symptoms of liver disease.

Table 4. Human induced pluripotent stem cell lines were generated from ATD patients with severe liver disease and those with lung disease but no liver disease, and wild type control

| Designation | iPS cell line | iPS cell source | Reprogramming Method | Pi Genotype |
|--------------------|---------------------------|--|--|--------------------|
| Severe LD1 | ATH1 | AT deficient human hepatocyte, Biopsy, Children’s Hospital of Pittsburgh of UPMC, 10-year old male that had a liver transplant | Lentivirus | ZZ |
| Severe LD2 | AAT2 | AT deficient dermal fibroblast, Biopsy, Einstein College of Medicine, 3 month old male with severe liver disease | Non-integrating plasmids | ZZ |
| No LD1a | AT10c15 | AT deficient lung fibroblast, Biopsy, UPMC Presbyterian, 42 year old female with COPD | Lentivirus | ZZ |
| No LD1b | AT10c16 | | | |
| No LD2 | 100-3-Cr-1 ¹⁶² | AT deficient dermal fibroblast, Biopsy, Boston University School of Medicine, 64 year old female with COPD | Single Excisable Lentiviral Stem Cell Cassette | ZZ |
| No LD3 | 103-3-Cr-1 ¹⁶² | AT deficient dermal fibroblast, Biopsy, Boston University School of Medicine, 47 year old female with COPD | Single Excisable Lentiviral Stem Cell Cassette | ZZ |
| Wild type | NFIF | Normal dermal fibroblast | Non-integrating plasmids | MM |

iPSCs were initially selected based on their morphologic resemblance to colonies of H1 hESCs. All iPSCs had high nuclear to cytoplasm ratio, well-defined cell membranes and distinct colony borders (Figure 1A). Colonies were then manually passaged several times to select for clones that could self-renew and maintain distinct colony borders (Figure 1B). The undifferentiated state of hESCs is characterized by alkaline phosphatase (AP) expression which indicates pluripotency and the potential for self-renewal¹⁶³. Although the expression of AP alone does not necessarily reflect a fully reprogrammed state, it is a relatively uncomplicated method for selecting clones for more stringent analysis. iPSC clones that showed high alkaline

phosphatase activity were therefore selected for subsequent expansion and pluripotency testing (Figure 1C).

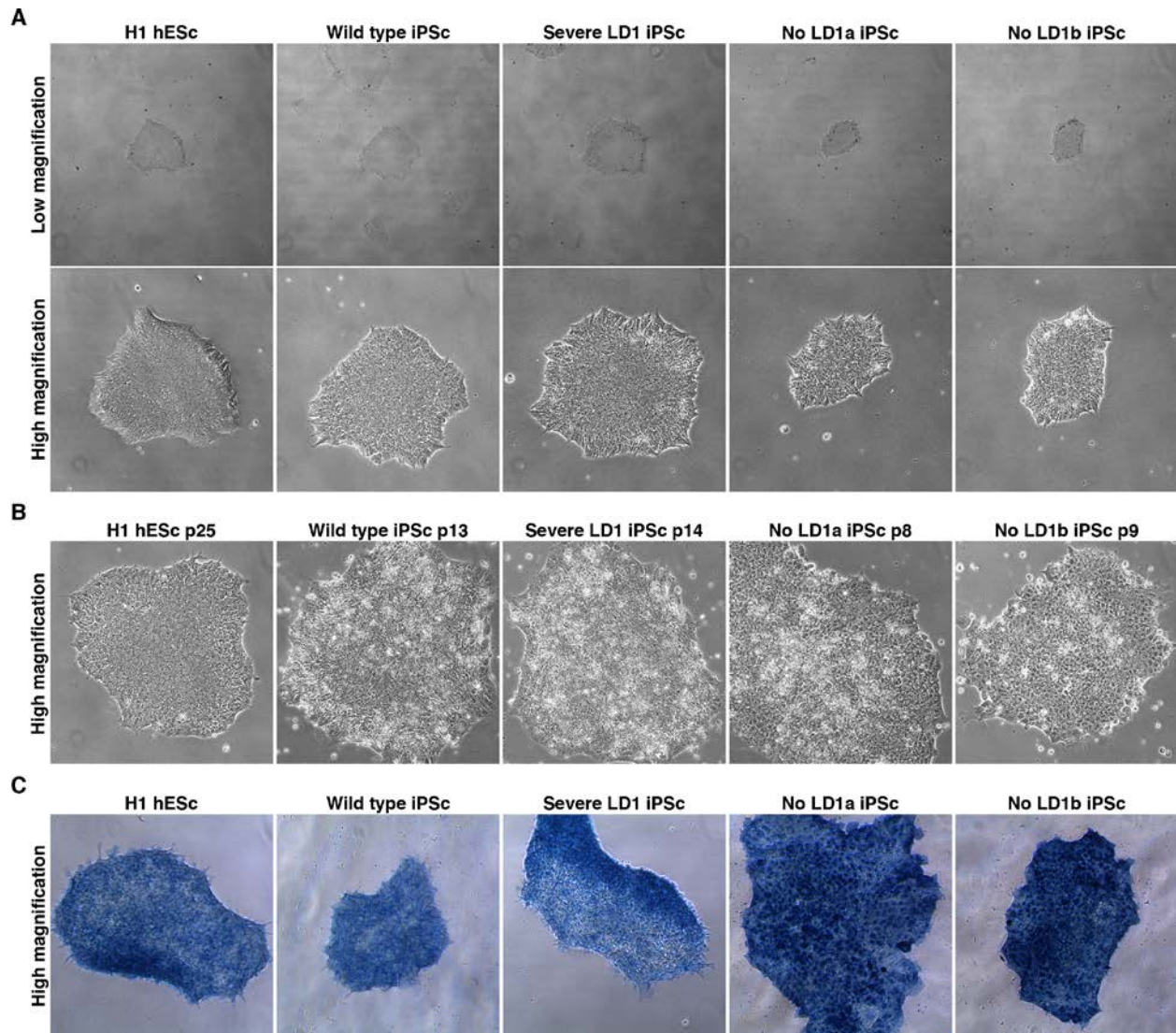


Figure 1. Induced pluripotent stem cells (iPScs) were generated from ATD patients with severe liver disease (severe LD) and no overt liver disease (no LD)

(A) Morphology of iPScs compared to H1 hEScs after initial colony selection. (B) Morphology of iPScs compared to H1 hEScs after several passages. (C) Alkaline phosphatase staining of wild type iPScs, severe LD iPScs and no LD iPScs compared to H1 hEScs. Low magnification (40X), High magnification (100X).

Reprogramming techniques that employ more than one vector (whether using viruses or plasmids) could result in the generation of reprogramming intermediates, cells expressing some but not all of the pluripotency factors required for full reprogramming^{81, 164}. Reprogramming intermediates could also arise from cells in which the copy number for each of the pluripotency factors are not optimized. It is therefore important to perform stringent assays to test for the pluripotency of selected colonies. Standard qPCR assays for testing the pluripotency of hESCs include the measurement or detection of the expression of classical markers including *OCT3/4*, *NANOG*, *SOX2*, *SSEA4*, and *TERT*. However, a recent study that made use of live cell imaging analysis determined that truly reprogrammed colonies express the pluripotency-associated markers Tumor Rejection Antigen 160 (TRA160), DNA (Cytosine-5-)-Methyltransferase 3 Beta (DNMT3B) and Zinc Finger Protein 42 (ZFP42)¹⁶⁴. The TRA160 antigen is a mucin-like antigen originally discovered on human embryonic carcinoma (EC) progenitor cells but has since been shown to be detected on the membrane of several other stem cells. The molecular identity of the TRA160 antigen was unknown until 2007 when a study determined that it is present on the glycosylated cell adhesion protein Podocalyxin (PODXL) in EC cells¹⁶⁵. DNMT3B is a DNA methyltransferase that is essential for epigenetic control early in human development. It functions for de novo methylation (as opposed to maintenance methylation) and is therefore essential for setting up DNA methylation patterns during genomic imprinting and X-chromosome inactivation¹⁶⁶. ZFP42, originally known as Reduced Expression 1 (REX1), is a zinc finger family transcription factor that is highly expressed in hESCs and is plays an important role in the maintenance of pluripotency as well as in the reprogramming of somatic cells to iPSCs^{167, 168}. We therefore analyzed the expression of all of these markers to confirm the pluripotency of the iPSC lines.

qPCR analysis revealed that the all iPSc lines expressed *OCT3/4*, *NANOG*, *REX1* (*ZFP42*), and *TERT* at levels that were similar to those in the H1 hESCs (Figure 2A). Surprisingly, the expression of *DNMT3B* and *TRA160* (*PODXL*) and was highly elevated in all iPSc lines by at least two-fold compared to H1 hESC (Figure 2A). A recent study determined that among the more than 40 *DNMT3B* mRNA splice variants, only the alternatively spliced mRNA transcripts that contain exon 10 are true markers of pluripotency¹⁶⁶. This new information prompted us to go back and check whether the qPCR primers we used for *DNMT3B* is specific for pluripotent-specific variants. Because the primers we used are specific for exons 6 to 8, the gene expression we obtained in our qPCR analysis is likely an overestimate of the actual level of pluripotent-specific *DNMT3B* mRNA. On the other hand, the highly glycosylated *PODXL* glycoprotein can be expressed in distinct forms in different cell types, a larger form that is modified with keratan sulfate glycosaminoglycan moieties, and a smaller form that is heavily glycosylated but contains no glycosaminoglycan groups. Only the larger form carries the pluripotency-defining *TRA160* epitope¹⁶⁵. Because the difference between the large and small form of *PODXL* is a result of post-translational modification, it is impossible to determine the level of pluripotent-specific *PODXL* by qPCR. We therefore confirmed the pluripotency of our iPSc lines by immunofluorescence analysis. Immunofluorescent staining for *NANOG*, *OCT3/4*, *SOX2*, *SSEA4* and *TRA160* in all iPSc lines revealed comparable expression to H1 hESCs thus confirming the pluripotency of the iPSCs (Figure 2B). Careful inspection of immunofluorescence images reveals that each cell in a hESC or iPSc colony has a variable level of pluripotency marker expression. However, this heterogeneity in the expression of pluripotency markers appears to be a normal occurrence as has been reported in both hESCs and iPSCs using fluorescence activated cell sorting (FACS) analysis¹⁶⁸ or single cell transcriptional profiling¹⁶⁹.

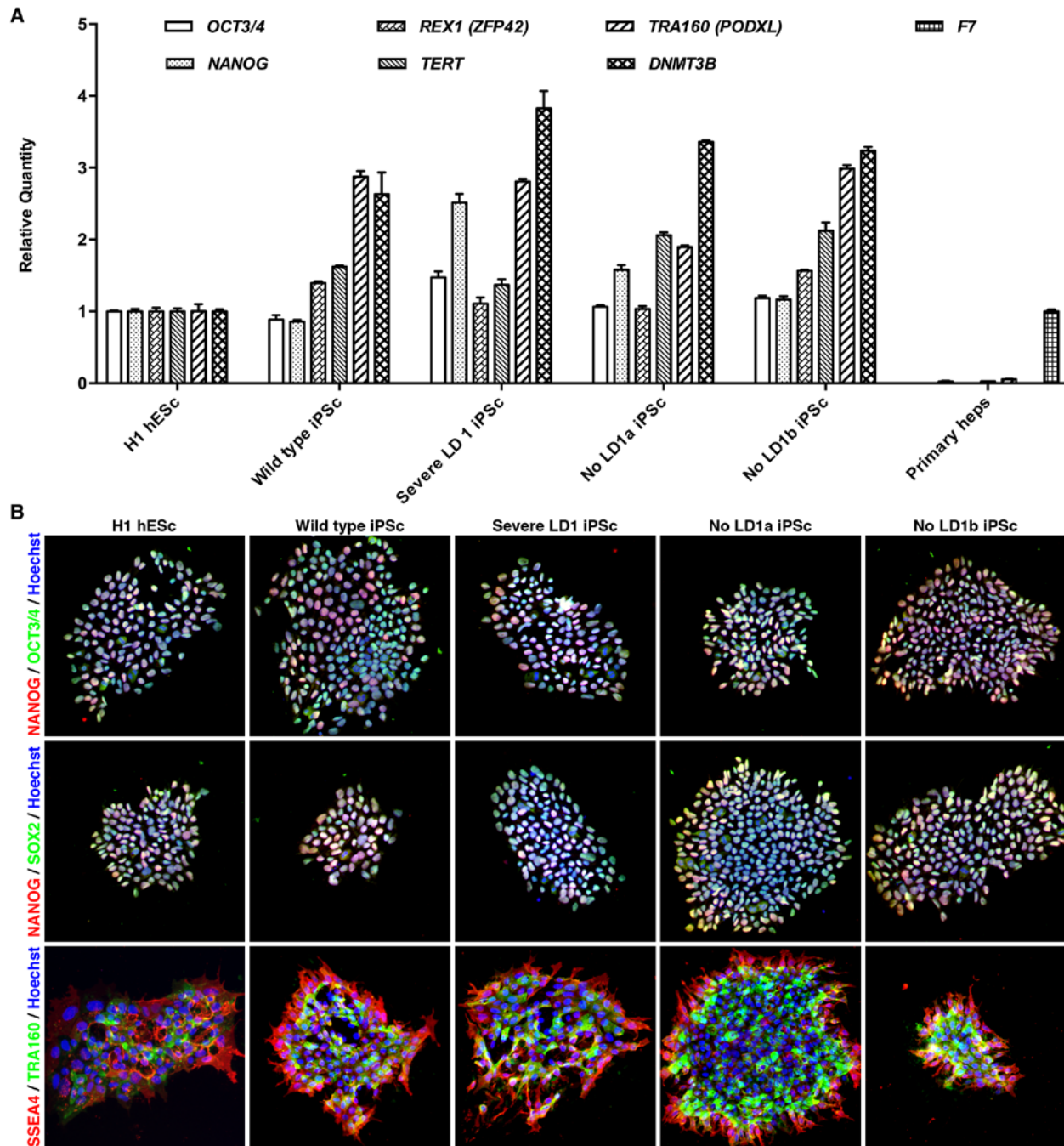


Figure 2. Induced pluripotent stem cells (iPScs) expressed pluripotency-associated markers

(A) qPCR for pluripotency-associated markers *OCT3/4*, *NANOG*, *REX1 (ZFP42)*, *TERT*, *TRA160 (PODXL)*, and *DNMT3B* in H1 hEScs and iPScs. *Coagulation Factor VII (F7)* was used as a non-pluripotent marker control while primary hepatocyte was used as a negative cellular control. (B) Immunofluorescent staining for pluripotency-associated markers *NANOG*, *OCT3/4*, *SOX2*, *SSEA4* and *TRA160* in H1 hEScs and iPScs (200X).

Although determining the expression of pluripotency-associated markers is a quick method for assessing pluripotency, the analysis of their ability to generate teratomas when injected subcutaneously into immunodeficient NOD/SCID mice is regarded as the gold standard for demonstrating the pluripotency of human iPSCs^{170, 171}. Two to three months after transplantation, all iPSC lines produced mature, cystic masses (Figure 3A). Upon histological analysis, the teratomas were shown to contain tissues derived from the embryonic germ layers endoderm, mesoderm and ectoderm, confirming the pluripotency of the iPSC lines (Figure 3B).

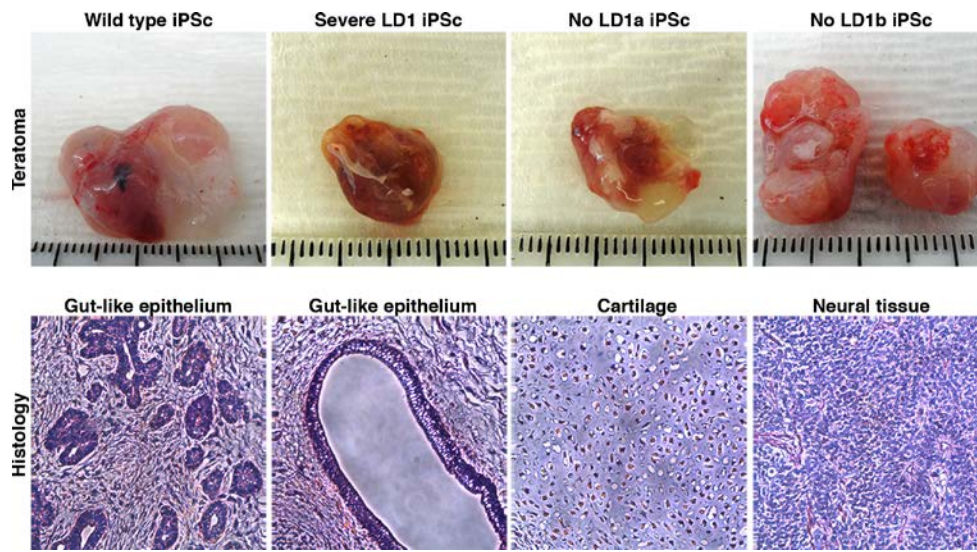


Figure 3. Induced pluripotent stem cells (iPSCs) generate teratomas when injected in immunodeficient NOD SCID mice

(A) Teratomas formed by wild type, severe LD and no LD iPSCs. (B) Selected slides showing areas of endodermal (gut-like epithelium), mesodermal (cartilage), and ectodermal (neural tissue) derivatives observed in severe LD1 iPSC-generated teratoma (200X).

Finally, to ensure that the generated iPSCs carried the Pi genotype of the parental cell lines, we performed genomic DNA sequencing. DNA sequencing confirmed that the wild type

iPSCs have the PiMM genotype (G11940, Glu342) while the ATD iPSCs carried the PiZZ genotype (G11940A, Glu342Lys) (Figure 4).

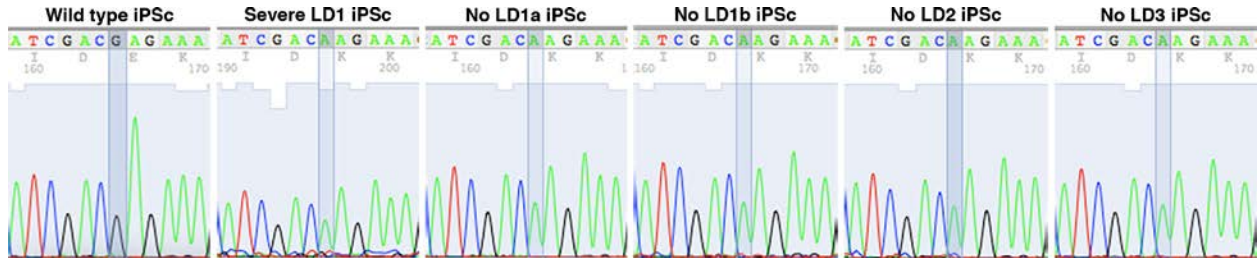


Figure 4. ATD iPSCs carry homozygous G11940→A PiZ alleles while wild type iPSCs were homozygous for the WT alleles

Genomic DNA sequencing of exon 10 of the protease inhibitor gene 1 (*SERPINA1*) in wild type, severe LD and no LD iPSCs. Wild type iPSCs have the PiMM genotype (G11940, Glu342) while severe LD and no LD iPSCs carry the PiZZ genotype (G11940A, Glu342Lys).

2.4 DISCUSSION

The generation of iPSCs from ATD patients has been reported in numerous studies^{97, 157-159}. However, to our knowledge, there have been no studies that generated iPSCs from ATD patients representing the observed variability in liver disease phenotypes. Here, we generated iPSCs from primary hepatocytes or fibroblasts of ATD patients with varying degrees of liver disease using either viPSTM lentiviral gene transfer kit, non-integrating episomal plasmids, or a single excisable lentivirus cassette. At the beginning of the study, only retroviral- and lentiviral-mediated reprogramming methods were available for the generation of iPSCs^{81, 82}. We decided to use lentiviruses for the initial reprogramming experiments because of two reasons. First, direct infection of human cells with retroviruses only results in 20% transduction⁸¹. Retroviral-

mediated reprogramming therefore required an extra initial lentiviral transduction step that introduced the mouse receptor for retroviruses (Slc7a1) to increase retroviral delivery of reprogramming factors to 60%⁸¹. Second, retroviruses are very inefficient at infecting slow-dividing or non-dividing cells such primary hepatocytes. Using lentiviral transduction, we successfully generated iPSCs from primary hepatocytes and fibroblasts at reprogramming efficiencies of 0.001-0.008%. In the years following the initial stages of the study, several groups developed new reprogramming techniques that generate iPSCs at higher efficiencies and with no integration of exogenous genetic sequences^{90, 162}. We, and our collaborators therefore generated iPSCs using either non-integrating episomal plasmids⁹⁰, or single excisable lentivirus cassette¹⁶². Using these techniques, reprogramming efficiencies were increased by more than ten-fold (0.03-0.1%). Despite the use of different cell sources and reprogramming method for generating iPSCs, minimal differences were detected when iPSCs were subjected to stringent pluripotency assays. The cell lines have similar morphology and growth properties compared to H1 hESCs, expressed the pluripotency-associated markers NANOG, OCT3/4, SOX2, SSEA4, TRA160, TERT, DNMT3B, and REX1 and were able to generate tumors when injected into immunodeficient mice.

In our attempts to generate iPSCs using the various available reprogramming protocols, we occasionally observed that some primary cells, particularly those that were derived from older patients or fibroblasts that were passaged multiple times, could not generate iPSCs even after several attempts. One common characteristic of these reprogramming-resistant cells is that they have very low proliferation rates *in vitro*. We therefore speculate that the inability of such cells to generate iPSCs is due to cellular senescence. Cellular senescence, characterized by an irreversible arrest in cell proliferation, has been strongly associated to physiological aging.

Studies have shown that several forms of cellular stress, including the activation of oncogenes, telomere shortening, DNA damage, oxidative stress, and mitochondrial dysfunction induce senescence. Because reprogramming is a stochastic process that is partially dependent on accelerated cell proliferation rate¹⁷², it is logical to think that slow-dividing cells would have a drastically lower probability to be reprogrammed to pluripotency.

Because the ATD iPSCs were generated from patients that represent the spectrum of disease severity, the cells can be used to produce various cell types which can then be used to study variability in ATD-mediated liver or lung pathologies. In the context of liver disease, the ATD iPSCs could be used to generate hepatocytes for analyzing genetic differences between hepatocytes from patients with liver disease and those without liver disease that could explain why only a subset of PiZZ individuals develop significant liver injury. Likewise, the ATD iPSCs could also be used to analyze genetic differences between lung epithelial cells, lung fibroblasts or macrophages that could explain variability in the severity of lung disease.

3.0 DIFFERENTIATION OF ALPHA-1 ANTITRYPSIN DEFICIENT PATIENT-DERIVED IPSCS INTO HEPATOCYTE-LIKE CELLS

3.1 INTRODUCTION

Although the retention of mutant alpha-1 antitrypsin Z protein (ATZ) within hepatocytes is a key step in the pathogenesis of alpha-1 antitrypsin deficiency (ATD), it does not explain why only a small subset of PiZZ individuals develops significant liver injury¹⁵. The ability to study patient-derived live human hepatocytes from ATD patients would be valuable in understanding the pathologic mechanisms of ATD because it could provide insights as to why variations in clinical phenotypes are observed between individuals sharing the same primary genetic mutation. However, because the disease is rare, primary hepatocytes from PiZZ patients are limited and are not readily available¹⁵. It is also difficult to recover hepatocytes from cirrhotic livers of ATD patients with severe liver disease. Moreover, long-term culture of primary hepatocytes has been difficult as hepatocytes lose their function and do not proliferate well *in vitro*^{125, 126}. In addition, cryopreservation of hepatocytes results in reduced viability and metabolic function after thawing^{87, 127-136}.

Induced pluripotent stem cells (iPSCs) could be used as an alternative source of hepatic cells to solve the paucity of liver cells for disease modeling. iPSCs can proliferate indefinitely *in vitro* while maintaining the ability to differentiate into several different cell types^{81, 82}, including

hepatocytes^{97, 116, 117}. Because iPSCs are patient-specific, they could be used to analyze patient-to-patient variability in clinical phenotypes. In recent years, several groups have reported the generation of disease specific iPSC-derived hepatocyte-like cells (iHeps) for modeling several liver diseases using various hepatocyte differentiation approaches^{97, 98, 100, 157-159}.

One study described the generation of iHeps from three patients with ATD and showed the accumulation of AT polymers in ATD cells but not in control cells⁹⁷. This demonstrates that iHeps from ATD patients can recapitulate some of the key pathological features of ATD *in vitro*. Moreover, the authors observed that the amount of ATZ polymers, while consistent among different iPSC lines from the same patient, varied between iPSC lines from different patients. Although not definitively analyzed in their study, the authors proposed that this variability in results between patient cells could correlate with severity of liver disease in patients.

Here, we report the differentiation of iPSCs from one wild type control and from five ATD patients into iHeps that exhibit many characteristics of primary human hepatocytes. Because the patient-specific ATD iHeps were derived from patients with or without severe liver disease, they could potentially be used to determine whether the biochemical and cellular characteristics of the iHeps correlate with liver disease severity in ATD patients.

3.2 MATERIALS AND METHODS

3.2.1 Differentiation of ATD iPSCs into hepatocyte-like cells

Directed differentiation of iPS cells into iHeps was performed *in vitro* using a variation of the 4-step protocol described by Si-Tayeb¹¹⁶. Briefly, iPS colonies were treated with accutase (STEMCELL Technologies Inc., Vancouver, BC, Canada) for 2-5 minutes to obtain single cells. mTESR1™ (STEMCELL Technologies Inc., Vancouver, BC, Canada) was added to the cells and centrifuged at 300 rpm for 5 minutes at room temperature. The cells were then transferred onto 6-well plates coated with growth factor reduced matrigel (BD Biosciences, San Jose, CA) at a density of $0.8-1 \times 10^6$ cells/well. Cells were allowed to attach by incubating at 4% O₂/5% CO₂ for 20-22 hours. Cells were then induced to differentiate into definitive endoderm cells by treatment with Roswell Park Memorial Institute (RPMI) 1640 medium (Life Technologies, Carlsbad, CA), 1X B27 without insulin (Life Technologies, Carlsbad, CA) and 0.5X NEAA (Life Technologies, Carlsbad, CA) containing 100 ng/mL activin A (R&D Systems, Minneapolis, MN), 10 ng/mL recombinant human bone morphogenetic protein 4 (rhBMP4) (R&D Systems, Minneapolis, MN) and 20 ng/mL recombinant human fibroblast growth factor 2 (rhFGF2) (BD Biosciences, San Jose, CA) for 2 days followed by treatment with RPMI 1640 medium, 1X B27 without insulin and 0.5X NEAA with 100 ng/mL activin A for 3 days at ambient O₂/5% CO₂. For hepatic specification, the cells were cultured in RPMI 1640 medium, 1X B27 with insulin (Life Technologies, Carlsbad, CA) and 0.5X NEAA containing 20 ng/mL rhBMP4 and 10 ng/mL rhFGF2 for 5 days at 4% O₂/5% CO₂. For hepatic induction, the cells were treated with RPMI 1640 medium, 1X B27 with insulin and 0.5X NEAA containing 20

ng/mL recombinant human hepatocyte growth factor (rhHGF) (R&D Systems, Minneapolis, MN) for 5 days at 4% O₂/5% CO₂. For hepatic maturation, the cells were cultured for 5 days in Hepatocyte Culture Medium™ Bullet Kit™ containing Hepatocyte Basal Medium™ with SingleQuots of ascorbic acid, fatty acid free bovine serum albumin, hydrocortisone, transferrin, insulin, gentamicin/amphotericin-B (minus epidermal growth factor) with 20 ng/mL recombinant human oncostatin M (rhOSM) (R&D Systems, Minneapolis, MN) at ambient O₂/5% CO₂.

3.2.2 RNA Extraction, cDNA synthesis and qPCR

Total RNA was isolated according to manufacturers' instructions using the RNeasy Mini Kit (Qiagen, Germantown, MD). cDNA was synthesized according to manufacturers' instructions using SuperScript III First-Strand Synthesis System and oligo dT primers (Life Technologies, Carlsbad, CA). qPCR was performed according to manufacturers' instructions using the Taqman Fast Advanced Master Mix (Life Technologies, Carlsbad, CA) on a StepOnePlus Real-Time PCR System (Life Technologies, Carlsbad, CA) following the Fast Mode cycling conditions for Taqman Gene Expression Assays. Values are shown as mean ± s.d. Taqman Gene Expression Assay IDs are listed in Table 5.

Table 5. Taqman Gene Expression Assay IDs for the qPCR analysis for pluripotency factors

| Target Gene | Gene Expression Assay ID | Dye | Quencher |
|---|--------------------------|-----|----------|
| <i>PPIA</i> (<i>Cyclophilin A</i>) – Internal Control | Hs99999904_m1 | FAM | NFQ |
| <i>NANOG</i> | Hs02387400_g1 | FAM | NFQ |
| <i>OCT3/4</i> (<i>POU5F1</i>) | Hs03005111_g1 | FAM | NFQ |
| <i>CXCR4</i> | Hs00607978_s1 | FAM | NFQ |
| <i>FOXA2</i> (<i>HNF3B</i>) | Hs00232764_m1 | FAM | NFQ |
| <i>HNF4A</i> | Hs00230853_m1 | FAM | NFQ |

3.2.3 Immunofluorescent staining

Antibodies and their corresponding dilutions are listed in Table 6. For cytoplasmic staining, cells were washed with phosphate buffered saline (PBS) (Life Technologies, Carlsbad, CA) and fixed in 4% paraformaldehyde for 15 minutes at room temperature. For nuclear staining, cells were washed with PBS and fixed in 100% pre-chilled ethanol at -20°C overnight. After three PBS washes, cells were washed with wash buffer containing 0.1% bovine serum albumin (BSA) (Sigma-Aldrich Corp., St. Louis, MO), and 0.1% TWEEN 20 (Sigma-Aldrich Corp., St. Louis, MO) in PBS. Samples were then blocked and permeabilized in blocking buffer containing 10% normal donkey or goat serum (Santa Cruz Biotechnology, Dallas TX), 1% BSA, 0.1% TWEEN 20, and 0.1% Triton X-100 (Sigma-Aldrich Corp., St. Louis, MO) in PBS for 1 hour at room temperature. Cells were then stained with primary or conjugated antibodies in blocking buffer at 4°C overnight. After three washes with wash buffer, cells were stained with secondary antibodies for 1 hour in the dark at room temperature. After three washes with wash buffer, and three washes with PBS, cells were then incubated for 1 minute in 1 ug/mL Hoechst 33342 (Life Technologies, Carlsbad, CA) in PBS, followed by three PBS washes before visualization. Cells were imaged on an IX71 inverted epifluorescent microscope (Olympus, Central Valley, PA). The percentage of cells that stained positive for the markers were determined using the Analyze Particle function of ImageJ software¹⁷³.

Table 6. List of antibodies and dilutions used for the immunofluorescent staining for hepatocyte-directed differentiation

| Antibody | Manufacturer | Host | Catalogue No. | Dilutions |
|---------------------------------|-------------------------------------|--------|---------------|-----------|
| anti-SOX17-Northern Lights 557 | R&D Systems, Minneapolis, MN | goat | NL1924R | 1:50 |
| anti-ALB | Bethyl Laboratories, Montgomery, TX | goat | A80-229A | 1:100 |
| anti-ASGR1 | Santa Cruz Biotech, Santa Cruz, CA | mouse | sc-52623 | 1:100 |
| anti-AFP | Life Technologies, Carlsbad, CA | rabbit | 18-0055 | 1:300 |
| anti-goat IgG-Alexa Fluor 488 | Life Technologies, Carlsbad, CA | donkey | A11055 | 1:250 |
| anti-mouse IgG-Alexa Fluor 594 | Life Technologies, Carlsbad, CA | donkey | A21203 | 1:250 |
| anti-rabbit IgG-Alexa Fluor 555 | Life Technologies, Carlsbad, CA | donkey | A31572 | 1:250 |

3.2.4 Sandwich ELISA

Antibodies and their corresponding dilutions are listed in Table 7. For ALB, ELISA was done using the Human Albumin ELISA Quantitation Set (Bethyl Laboratories, Montgomery, TX) according to manufacturer's protocol using Immulon™ 4HBX flat bottom microtiter plates (Thermo Fisher Scientific, Waltham, MA). The reaction was developed for 15 minutes with 100 uL/well TMB substrate solution (KPL, Gaithersburg, MD) and stopped with 100 uL/well 0.18 M H₂SO₄.

For AT, ELISA was carried out at room temperature and using 100 uL/well unless otherwise stated. Immulon™ 4HBX flat bottom microtiter plates were coated with coating antibody in 0.05M carbonate-bicarbonate buffer pH 9.6 for 1 hour. The wells were then washed five times with 200 uL ELISA wash solution (50 mM Tris, 0.14 M NaCl, 0.05% TWEEN 20, pH 8.0) and blocked with 200 uL blocking buffer (50 mM Tris, 0.14 M NaCl, 1% BSA, pH 8.0) overnight at 4°C. Human AT standard (Athens Research and Technology, Athens, GA) and unknown samples were diluted in sample/antibody diluent (50 mM Tris, 0.14 M NaCl, 0.05% TWEEN 20, 1% BSA pH 8.0) and incubated for 1 hour. After washing five times, wells were

incubated with primary antibody diluted in sample/antibody diluent for 1 hour. After washing five times, wells were incubated with secondary antibody diluted in sample/antibody diluent for 1 hour. The reaction was developed for 15 minutes with TMB substrate solution and stopped with 0.18 M H₂SO₄.

HRP activity was measured in a Thermo-max microplate reader (Molecular Devices, Sunnyvale, CA) at 450 nm. Values are presented as mean \pm s.d. with the significance calculated using one-way ANOVA followed by Bonferroni posttests for each pair of groups.

Table 7. List of antibodies and dilutions used for sandwich ELISA

| Antibody | Manufacturer | Host | Catalogue No. | Dilutions |
|-----------------------------|-------------------------------------|--------|---------------|-----------|
| anti-ALB (coating) | Bethyl Laboratories, Montgomery, TX | goat | A80-129A | 1:100 |
| anti-ALB-HRP (detection) | Bethyl Laboratories, Montgomery, TX | goat | A80-129P | 1:50000 |
| anti-AT (coating) | Bethyl Laboratories, Montgomery, TX | goat | A80-122A | 1:200 |
| anti-AT (primary) | Dako, Carpinteria, CA | rabbit | A0012 | 1:80000 |
| anti-rabbit-HRP (detection) | Dako, Carpinteria, CA | goat | P0448 | 1:5000 |

3.2.5 Transmission Electron Microscopy

iHeps were briefly washed with PBS, pH 7.4, fixed in situ with 2.5% glutaraldehyde in PBS for 1 hour at room temperature and washed three times with PBS. Samples were submitted to the University of Pittsburgh Center for Biologic Imaging for post-fixation with 1% osmium tetroxide and 1% potassium ferricyanide for 1 hour at room temperature. Samples were washed three times with PBS and dehydrated in a graded series of ethanol solution (30%, 50%, 70%, and 90% - 10 minutes each) and three 15-minute changes in fresh 100% ethanol. Infiltration was done with three 1-hour changes of epon. The last change of epon was removed and beam capsules filled with resin were inverted over relevant areas of the monolayers. The resin was allowed to

polymerize overnight at 37°C and then for 48 hours at 60°C. Beam capsules and underlying cells were detached from the bottom of the petri dish and sectioned. Image acquisition was done using either the JEM-1011 or the JEM-1400Plus transmission electron microscopes (Jeol, Peabody, MA) at 80kV fitted with a side mount AMT 2k digital camera (Advanced Microscopy Techniques, Danvers, MA).

3.3 RESULTS

ATD and wild type iPSCs were differentiated into iHeps *in vitro* following a variation of the 4-step protocol described by Si-Tayeb¹¹⁶ (Figure 5A) because of a presumed need to obtain a homogenous population of cells with hepatocyte characteristics for further analysis. Changes in the morphology of the cells were observed as the cells progressed through the different stages of the differentiation protocol (Figure 5B). During the single cell passage step, cells were initially homogeneously distributed throughout the plate but eventually migrate and come together to form small colonies or a network of cells (Figure 5B, first column). After the definitive endoderm step, about 50% of the cells die due to exposure to activin A, an outcome that has been reported in previous studies^{97, 116, 117}. The surviving cells spread out and change morphology appearing larger and flatter compared to iPSCs (Figure 5B, second column). In the hepatic specification step, the cells proliferate almost reaching confluency by the end of the stage. Small lipid droplets can be observed in the cytoplasm of some cells (Figure 5B, third column). In the hepatocyte induction stage, the cells proliferate slowly but begin to take the morphology of human hepatocytes, having a distinct polygonal shape with large cytoplasm and a well-defined plasma membrane (Figure 5B, fourth column). Most of the cells after this stage will exhibit lipid

droplets with some exhibiting double nuclei. In the hepatocyte maturation stage, the morphology of the cells does not change much compared to the previous stage. The cells continue to proliferate leading to overcrowding in some areas in the well (Figure 5B, last column).

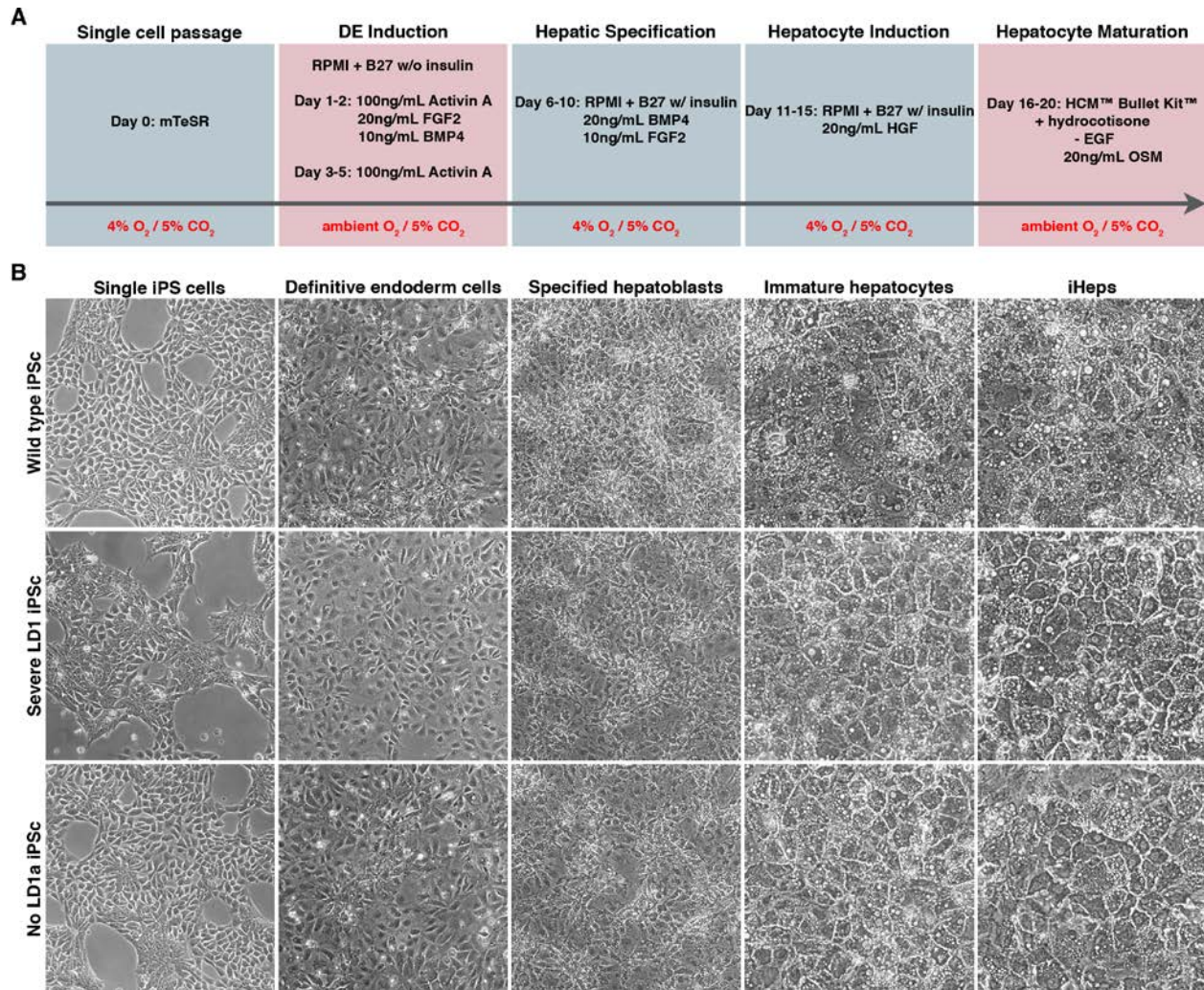


Figure 5. Changes in the morphology of iPScs during differentiation to iHeps

(A) Schematic diagram outlining the protocol used to differentiate iPScs into iHeps from single cell passage, to definitive endoderm (DE) induction, hepatic specification, hepatocyte induction and hepatocyte maturation. The media composition for each stage is shown in black text while the culture conditions are shown in red text. (B) Morphology of wild type, severe LD1 and no LD1a iPScs as they progressed from being single iPScs (100X) to definitive endoderm cells (100X), hepatoblasts (100X), immature hepatocytes (200X), and iHeps (200X).

To ensure hepatocyte-directed differentiation, changes in mRNA and protein expression of stage specific markers were monitored at the end of each step of the differentiation (Figure 6). The expression of the pluripotency factors *OCT3/4* and *NANOG* was monitored in order to determine if any pluripotent cells exist after the differentiation. This was important because transplantation of differentiated cells could result in tumorigenesis if pluripotent cells are present in the transplanted cells. As expected, the expression of the pluripotency factors gradually decreased as the differentiation progressed (Figure 6A, upper panels).

The expression of definitive endoderm markers Chemokine (C-X-C Motif) Receptor 4 (*CXCR4*), Forkhead Box A2 (*FOXA2*) and Sex Determining Region Y box 17 (*SOX17*) was also monitored to determine the efficiency of definitive endoderm induction. The expression of *CXCR4* was upregulated after the definitive endoderm stage and abruptly disappeared in the succeeding stages. *FOXA2* expression was induced after the definitive endoderm stage and abruptly increased in the hepatic specification stage (Figure 6A, lower panels). This trend was expected since *FOXA2* is not only essential for the formation of foregut DE cells, but is also necessary for further hepatic specification and liver bud differentiation during the development of the liver^{174, 175}. However, *FOXA2* expression unexpectedly declined towards the end of the differentiation. Immunofluorescent staining analysis showed that greater than 75% of cells after DE induction are *SOX17*-immunoreactive. This observed efficiency of DE induction is similar to what has been observed in other hepatocyte differentiation protocols of pluripotent stem cells^{116, 117, 176}.

Hepatocyte Nuclear Factor 4 alpha (*HNF4A*) is essential for establishing the network of hepatic transcription factors that regulates hepatogenesis¹⁷⁷. The expression of *HNF4A* was

therefore monitored as a marker for hepatocyte specification and maturation. After the hepatic specification stage, *HNF4A* was induced almost ten-fold to levels that were similar to that in primary human hepatocytes (Figure 6A, lower panels). However, *HNF4A* levels unexpectedly decreased towards the end of the differentiation (Figure 6A, lower panels).

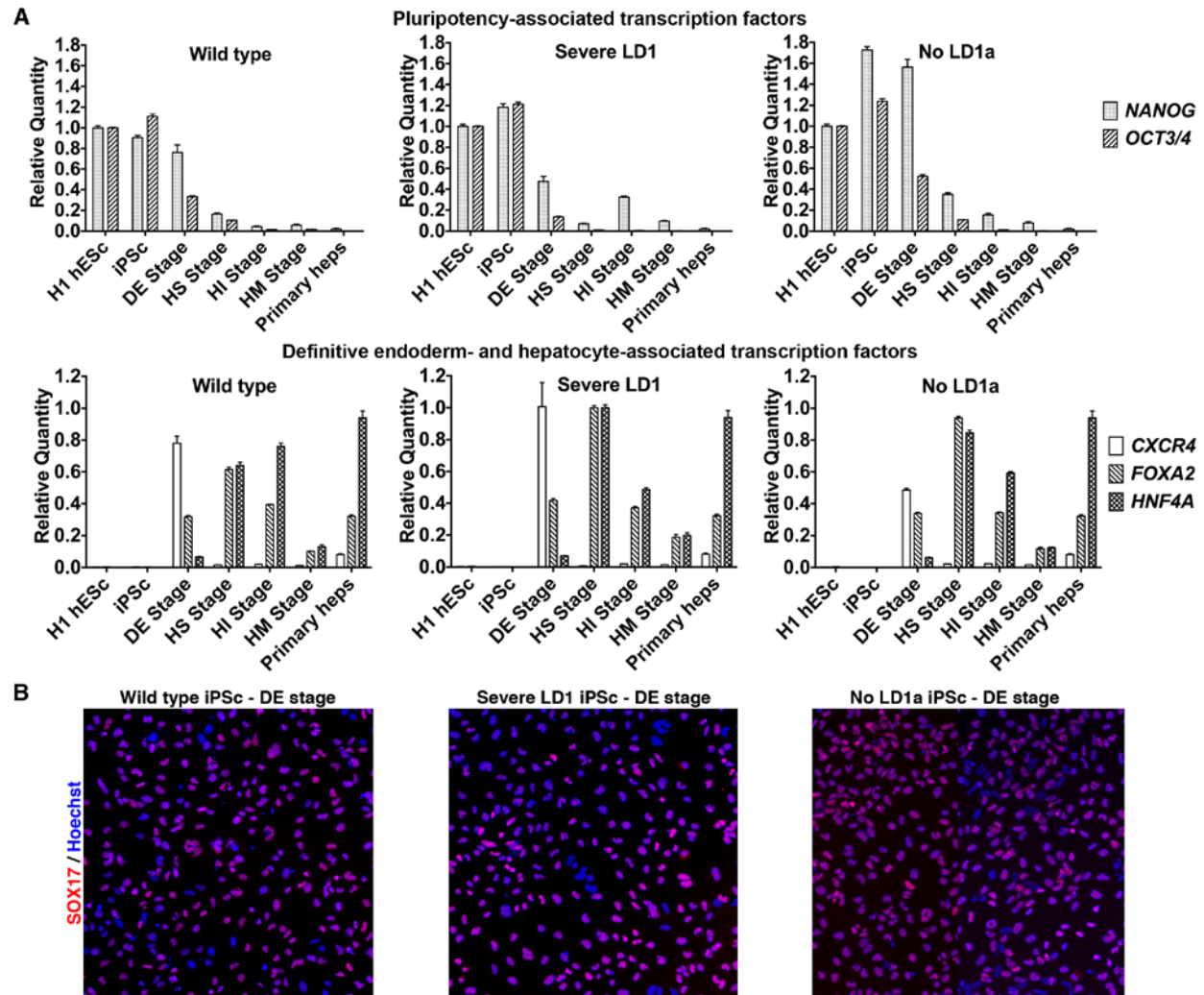


Figure 6. Differentiation of iPScs to iHeps results in changes in the expression of stage-specific markers

(A) qPCR showing the downregulation of pluripotency-associated transcription factor *NANOG* and *OCT3/4* (*POU5F1*), expression of the definitive endoderm markers *CXCR4* and *FOXA2*, and expression of the hepatocyte transcription factor *HNF4A* in iPSc cells during the differentiation. Data shown as mean \pm s.d. (n=3). DE: definitive endoderm, HS: hepatic specification, HI: hepatocyte induction, HM: hepatocyte maturation. (B) Immunofluorescent staining of iPSc cells after the DE stage for the definitive endoderm marker SOX17 (100X).

At the end of the differentiation protocol, immunofluorescent staining was performed to determine the expression of hepatocyte markers ALB and ASGPR1, and the immature hepatocyte marker AFP. Quantification of stained images revealed that upon completion of hepatic maturation only 50-60% of iHeps expressed ALB (Figure 7). This efficiency of hepatocyte differentiation was lower than that observed for differentiation of iPSCs reported previously¹¹⁶. About 30-40% of iHeps were positive for both ALB and ASGPR1 (Figure 7). However, 20-30% of the iHeps co-expressed ALB and AFP (Figure 7). This finding, together with the qPCR results showing the unexpected decrease in the expression of *FOXA2* and *HNF4A* towards the end of the differentiation, suggests that the iHeps did not have a fully mature hepatocyte phenotype.

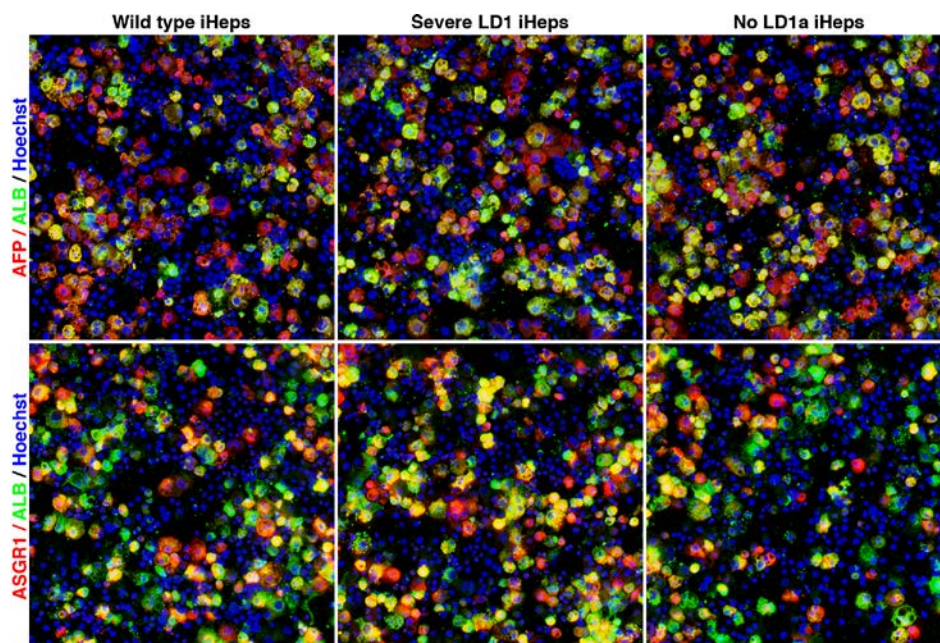


Figure 7. ATD iHeps express mature hepatocyte markers ALB and ASGPR1 but have continued expression of the immature hepatocyte marker AFP

Immunofluorescent staining of iHeps for mature hepatocyte markers ALB and ASGR1 and immature hepatocyte marker AFP (100X).

iHeps exhibited several ultrastructural features observed in primary human hepatocytes. The cells exhibited double nuclei, lipid droplets, glycogen rosettes and well-developed bile canaliculi with apical microvilli, desmosomes, and tight junctions as detected by transmission electron microscopy (Figure 8A). As a measure of function, the secretion of ALB and AT over a period of 24 hours was measured by ELISA (Figure 8B). iHeps were able to secrete ALB at levels that were ~40-50% of the amount secreted by primary human hepatocytes. Although the amount of ALB secreted by wild type and ATD iHeps were not significantly different, the levels of AT secreted by ATD iHeps were significantly lower compared to that secreted by wild type iHeps. This result was expected as the mutant ATZ molecule has a decreased ability to traverse the secretory pathway³⁶ leading to reduced plasma AT levels in ATD patients^{4, 8, 19}.

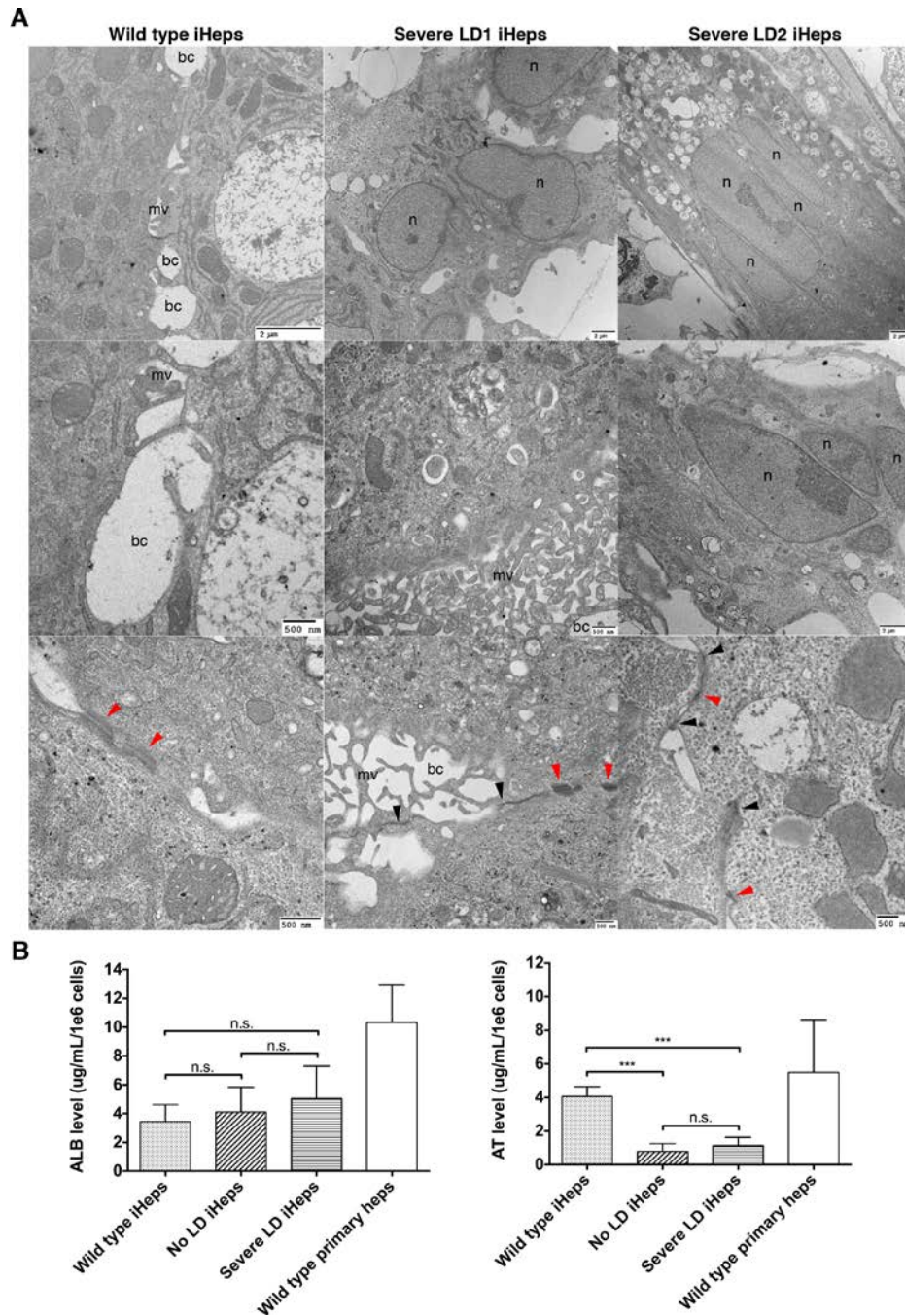


Figure 8. ATD iHeps exhibit many characteristics of primary human hepatocytes

(A) Electron micrograph of iHeps showing double nuclei (n) and bile canaliculi (bc) with apical microvilli (mv), tight junctions (black arrowheads) and desmosomes (red arrowheads). (B) ELISA measuring the amount of ALB and AT secreted by the wild type iHeps (n=3), no LD iHeps (n=2), severe LD iHeps (n=4), and severe LD primary hepatocytes (n=2) over a period of 24 hours shown as mean \pm s.d. *** p <0.001 (one-way ANOVA followed by Bonferroni posttests for each pair of samples).

3.4 DISCUSSION

In this study, we generated iHeps from ATD patients with and without severe liver disease with the ultimate goal of obtaining cells that could be analyzed to determine whether the biochemical and cellular features of the iHeps correlate with liver disease phenotype of ATD patients. The ATD and wild-type iHeps exhibited many of the characteristics of 1° human hepatocytes, but did not have a fully mature phenotype, as shown by the decrease in the expression of *FOXA2* and *HNF4A* and the residual expression of the immature hepatocyte marker AFP. Nevertheless, the iHeps had endogenous production and secretion of AT, a cellular function that is essential for modeling the pathogenesis of ATD.

We initially had concerns that the use of different cell sources and reprogramming methods for generating iPSCs might lead to variability in the differentiation potential of the differentiated cells. However, we found that the degree of hepatocyte differentiation was equivalent across all iPSC lines irrespective of these factors based on the fact that the levels of secreted ALB as well as the percentage of ALB/ASGPR1 and ALB/AFP marker expression were similar across all iPSC lines.

On some occasions, hepatocyte differentiation experiments failed to generate cells having the characteristics of primary hepatocytes. We found that in the majority of these failed differentiations, the percentage of SOX17+ cells was less than 75% after the definitive endoderm induction step. We therefore used SOX17 staining after the first step as a predictive tool to determine success of differentiation such that if we found less than 75% SOX17+ cells after the first step, the differentiation was discontinued.

Based on our experience, there are several factors that are critical for the proper differentiation of iPSCs into iHeps. It is essential to start with a well-maintained culture of iPSCs

that have minimal spontaneously differentiated cells. Spontaneously differentiated cells in the starting culture respond differently to the growth factors in each stage of the differentiation and would generate cells that are a non-hepatocytic. In addition, these cells secrete their own growth factors that will alter the level and combination of growth factors in culture which can ultimately affect the differentiation of the cells surrounding it. The confluence and the tightness of the cells after single cell passage seems to have a huge impact on the differentiation specifically on the critical first step. It is important to start the first step of differentiation when the confluence is about 50-60% and when the cells have not yet formed tight colonies typically before 20 hours post passage (Figure 5B). We believe that this allows the growth factors to efficiently stimulate the cells. It is also important to ensure that the growth factors maintain their maximal biological activity. In order to avoid loss of bioactivity, growth factors should be frozen properly in their recommended buffers and should not be subjected to multiple freeze-thaw cycles. Lot-to-lot variability in the bioactivity of growth factors can also affect differentiation. Although time-consuming, the best way to control for this is by performing side-by-side differentiations of the old and new batch of growth factor to determine comparable potency.

Several hepatocyte differentiation protocols, including the protocol used in this study, have generated iHeps that display many features of primary mature hepatocytes^{97, 116, 117, 178}. However, these iHeps have very high levels of AFP and exhibit underdeveloped mature hepatocyte function, such as inducible cytochrome P450 enzyme activity, indicating an immature phenotype. So far, only two protocols have been able to generate pluripotent stem cell-derived hepatocytes that exhibit mature hepatocyte function and that can engraft and expand after transplantation in rodent models of liver repopulation^{142, 179, 180}. In these studies, differentiation occurred in the presence of other non-hepatic cells such as endothelial cells and mesenchymal

stem cells. We believe that the presence of these “supporting” cell types could significantly improve hepatocyte differentiation *in vitro*.

4.0 MODELING THE PATHOGENESIS AND VARIABILITY OF ALPHA-1 ANTITRYPSIN DEFICIENCY USING PATIENT-DERIVED IPSC GENERATED HEPATOCYTE-LIKE CELLS

4.1 INTRODUCTION

The classical form of alpha-1 antitrypsin deficiency (ATD), homozygous for the PiZ allele, is a single gene defect that is associated with liver disease and chronic obstructive pulmonary disease. The protein affected, alpha-1 antitrypsin (AT), is a secretory glycoprotein predominantly synthesized in hepatocytes and primarily functions to inhibit neutrophil elastase and several related neutrophil proteases. In individuals with ATD, the point mutation renders this protein prone to misfolding such that it accumulates in early compartments of the secretory pathway resulting in decreased levels of the protein in extracellular fluids^{1, 21, 33, 181}. Lack of AT molecules to counteract neutrophil proteases is thought to be the primary mechanism for lung disease, a loss-of-function mechanism. In contrast, hepatic disease is caused by a gain-of-function mechanism attributable to the intracellular accumulation/“proteotoxicity” of mutant alpha-1 antitrypsin Z (ATZ) in hepatocytes¹⁸¹.

There is, however, a wide variability in incidence, severity and age of onset of ATD-mediated liver disease¹⁵. While some affected homozygotes develop life-threatening liver disease, a considerable number never develop clinical symptoms and in some cases the liver

disease is first recognizable at 50-65 years of age. These observations have led us to theorize that genetic and/or environmental modifiers play a critical role in determining susceptibility to liver disease and that putative modifiers⁷⁴ of pathways for intracellular ATZ degradation would be attractive targets for newly identified drug therapies⁶⁶⁻⁶⁸.

Groundbreaking studies demonstrating that somatic cells can be reprogrammed into induced pluripotent stem cells (iPSCs)^{81, 82, 88, 182} have created the opportunity to generate a variety of patient-specific somatic cell types including hepatocyte-like cells^{97, 116, 117, 142}. Recent studies have demonstrated that iPSC-derived hepatocyte-like cells (iHeps) derived from patients with metabolic liver diseases, including ATD, could be utilized for disease modeling^{97, 98, 100, 157-159}. Here, we expand on previous work to investigate whether patient-specific iHeps could be used to model personalized variations in the severity of liver disease among ATD patients and ultimately be used to identify patients at risk for severe disease and address the “modifier” theory.

4.2 MATERIALS AND METHODS

4.2.1 Use of human-derived tissues

All human liver tissues were obtained with informed consent following guidelines approved by the Institutional Review Board of the University of Pittsburgh.

4.2.2 Hepatocyte isolation from liver explants

Primary hepatocytes from ATD patients with severe liver disease were obtained from the explanted liver of an ATD patient who received a liver transplant. Primary hepatocytes from normal controls were obtained from liver resection specimens containing normal tissues. Hepatocytes were isolated by three-step collagenase perfusion as described previously^{160, 161}. Briefly, silicone catheters were inserted into the major portal and/or hepatic vessels and the tissue was perfused with Hank's Balanced Salt Solution (HBSS) without calcium, magnesium or phenol red (Lonza Walkersville Inc., Walkersville, MD) to determine the vessel(s) that would provide the most uniform perfusion of the tissue. Purse string sutures were then tied around each vessel with its accompanying catheter to prevent the leakage of buffer around the catheter during the perfusion. Perfusion proceeded once all remaining major vessels on the cut surfaces were closed with sutures around catheters or with surgical grade super glue. The liver tissue was placed in a sterile plastic bag and connected to a peristaltic pump with flow rate between 35 to 240 ml/min. The bag containing the tissue was placed in a circulating water bath at 37°C and the tissue was perfused with HBSS supplemented with 0.5 mM ethylene glycol tetraacetic acid (EGTA) (Sigma-Aldrich Corp., St. Louis, MO) without recirculation. Chelation of calcium by EGTA aids in the dissolution of intercellular junctions between hepatocytes and in the washing of hematopoietic cells. A second, non-recirculating perfusion with HBSS without EGTA was performed to flush residual EGTA from the tissue since calcium is essential for collagenase enzyme activity. During the second perfusion step, Clzyme™ collagenase MA (VitaCyte, LLC, Indianapolis, Indiana) was reconstituted and sterile-filtered according to manufacturer's recommendations. Just prior to the third perfusion step, 100 mg Clzyme™ collagenase MA and 24 mg Clzyme™ BP Protease (VitaCyte, LLC, Indianapolis, Indiana) were mixed with 1L of

Eagle's Minimum Essential Medium (EMEM) (Lonza Walkersville Inc., Walkersville, MD). The tissue was then perfused with this EMEM-collagenase solution with recirculation as long as needed to complete the digestion. The duration of perfusion with the EMEM-collagenase solution was determined by continuously monitoring tissue integrity. Perfusion was stopped when the liver tissue beneath the capsule surface was visibly digested and separated from the capsule. The tissue was then transferred to a sterile plastic beaker that contained ice-cold EMEM and was gently cut with sterile scissors to release hepatocytes. The cell suspension was filtered through a sterile gauze-covered funnel to remove cellular debris and clumps of undigested tissue. Hepatocytes were enriched by three consecutive centrifugation steps each at 80xg for 6 min at 4°C. After three washes in EMEM, hepatocytes were suspended in cold Hepatocyte Maintenance Medium™ (HMM) (Lonza Walkersville Inc., Walkersville, MD). Cell viability expressed as percentage of viable cells over the total cell number was assessed by trypan blue exclusion. For determining plating efficiency and for reprogramming, 1×10^6 cells were plated onto collagen-coated 6-well plates and cultured for 2 hours in HMM™ with SingleQuots of 1×10^{-7} M dexamethasone, 1×10^{-7} M insulin, and 50 ug/mL gentamicin/amphotericin-B (Lonza Walkersville Inc., Walkersville, MD) and supplemented with 5% fetal bovine serum (FBS) (Atlanta Biologicals, Inc., Lawrenceville, GA) to facilitate cell attachment. The media was then switched to HMM™ with SingleQuots of 1×10^{-7} M dexamethasone, 1×10^{-7} M insulin, and 50 ug/mL gentamicin/amphotericin-B (Lonza Walkersville Inc., Walkersville, MD) with no FBS and cultured overnight. Plating efficiency expressed as the percentage of cells that attached over the total number of plated cells was determined by counting the number of attached cells after detachment. Only cells with a viability of >80% and a plating efficiency of >70% were used for kinetic analysis.

4.2.3 Pulse chase analysis and Densitometry

Methods for biosynthetic labeling with ^{35}S methionine, immunoprecipitation, sodium dodecyl sulfate-polyacrylamide gel electrophoresis (SDS-PAGE), fluorography, and densitometric analysis have been described⁷⁴. Briefly, cells were washed three times with Hank's Balanced Salt Solution (HBSS) (Life Technologies, Carlsbad, CA) and pulse-labeled with DMEM minus methionine and cysteine (Life Technologies, Carlsbad, CA) containing 250 $\mu\text{Ci}/\text{mL}$ TRAN ^{35}S -LABELTM metabolic labeling reagent (MP Biomedicals, Solon, OH) for 1 hour. Cells were then washed three times with HBSS and incubated in DMEM with methionine and cysteine (Life Technologies, Carlsbad, CA) without labeling reagent for several different time intervals to constitute the chase. The intracellular and extracellular fractions were subjected to immunoprecipitation with anti-AT nephelometric serum (Diasorin, Stillwater, MN) and the immunoprecipitates were analyzed by SDS-PAGE and fluorography. All fluorograms were subjected to densitometric analysis using ImageJ software¹⁷³. The relative densitometric value at T_0 is set at 100% and the remainder of the data set expressed as % of this value. Values are presented as mean \pm s.d. with the significance calculated using two-way repeated measures ANOVA followed by Bonferroni posttests at each time point. Variations in rates of degradation and secretion within replicates and groups (wild type, severe LD, no LD) were within the range previously reported for pulse-chase analyses of this type^{21, 74}.

4.2.4 Endoglycosidase H and PNGase F digestion

Immunoprecipitates of pulse chase fractions were boiled in glycoprotein denaturing buffer containing 0.5% sodium dodecyl sulfate (SDS) and 0.04 M dithiothreitol (DTT) (New England Biolabs Inc., Ipswich, MA) for 10 mins. Samples were centrifuged at 13200 rpm for 10 mins. For endoglycosidase H (endo H), supernatants were added to a reaction containing 0.05 M sodium citrate pH 5.5 (G5 Reaction Buffer) (New England Biolabs Inc., Ipswich, MA), 1 mM phenylmethylsulfonyl fluoride (PMSF) (MP Biomedicals, Solon, OH), 10 uM pepstatin A (MP Biomedicals, Solon, OH), and 20 U/uL endo H (New England Biolabs Inc., Ipswich, MA) and incubated at 37°C for 1 hour. For PNGase F, supernatants were added to a reaction containing 0.05 M sodium phosphate pH 7.5 (G5 Reaction Buffer) (New England Biolabs Inc., Ipswich, MA), 1% NP-40 (New England Biolabs Inc., Ipswich, MA), 1 mM PMSF (MP Biomedicals, Solon, OH), 10 uM pepstatin A (MP Biomedicals, Solon, OH), and 10 U/uL PNGase F (New England Biolabs Inc., Ipswich, MA) and incubated at 37°C for 1 hour. Samples were analyzed by analyzed by SDS-PAGE/fluorography.

4.2.5 Immunofluorescent Staining

Antibodies and their corresponding dilutions are listed in Table 8. Cells were washed with phosphate buffered saline (PBS) (Life Technologies, Carlsbad, CA) and fixed in 4% paraformaldehyde for 15 minutes at room temperature. After three PBS washes, cells were washed with wash buffer containing 0.1% bovine serum albumin (BSA) (Sigma-Aldrich Corp., St. Louis, MO), and 0.1% TWEEN 20 (Sigma-Aldrich Corp., St. Louis, MO) in PBS. Samples

were then blocked and permeabilized in blocking buffer containing 10% normal donkey or goat serum (Santa Cruz Biotechnology, Dallas TX), 1% BSA, 0.1% TWEEN 20, and 0.1% Triton X-100 (Sigma-Aldrich Corp., St. Louis, MO) in PBS for 1 hour at room temperature. Cells were then stained with primary antibodies in blocking buffer at 4°C overnight. After three washes with wash buffer, cells were stained with secondary antibodies for 1 hour in the dark at room temperature. After three washes with wash buffer, and three washes with PBS, cells were then incubated for 1 minute in 1 ug/mL Hoechst 33342 (Life Technologies, Carlsbad, CA) in PBS, followed by three PBS washes before visualization. Cells were imaged on a Fluoview 1000 confocal microscope (Olympus, Central Valley, PA). Confocal stacks were rendered using MetaMorph Image analysis software (Molecular Dynamics, Piscataway, NJ). Surface reconstructions were performed using Imaris Image analysis software (Bitplane USA, South Windsor, CT).

Table 8. List of antibodies and dilutions used for colocalization of AT with rER and golgi markers

| Antibody | Manufacturer | Host | Catalogue No. | Dilutions |
|---------------------------------|---------------------------------------|--------|---------------|-----------|
| anti-AT | Bethyl Laboratories, Montgomery, TX | goat | A80-122A | 1:1000 |
| anti-Calnexin | Sigma-Aldrich Corp., St. Louis, MO | rabbit | HPA009433 | 1:100 |
| anti-Calreticulin | Thermo Fisher Scientific, Waltham, MA | rabbit | PA3-900 | 1:1000 |
| anti-GM130 | BD Biosciences, San Jose, CA | mouse | 610822 | 1:250 |
| anti-goat IgG-Alexa Fluor 488 | Life Technologies, Carlsbad, CA | donkey | A11055 | 1:250 |
| anti-rabbit IgG-Alexa Fluor 555 | Life Technologies, Carlsbad, CA | donkey | A31572 | 1:250 |
| anti-mouse IgG-Alexa Fluor 594 | Life Technologies, Carlsbad, CA | donkey | A21203 | 1:250 |

4.2.6 Transmission Electron Microscopy

For iHeps, cell monolayers were briefly washed with PBS, pH 7.4. Samples were fixed in situ with 2.5% glutaraldehyde in PBS for 1 hour at room temperature and washed three times with

PBS. Samples were submitted to the University of Pittsburgh Center for Biologic Imaging for post-fixation with 1% osmium tetroxide and 1% potassium ferricyanide for 1 hour at room temperature. Samples were washed three times with PBS and dehydrated in a graded series of ethanol solution (30%, 50%, 70%, and 90% - 10 minutes each) and three 15-minute changes in fresh 100% ethanol. Infiltration was done with three 1-hour changes of epon. The last change of epon was removed and beam capsules filled with resin were inverted over relevant areas of the monolayers. The resin was allowed to polymerize overnight at 37°C and then for 48 hours at 60°C. Beam capsules and underlying cells were detached from the bottom of the petri dish and sectioned. For tissue samples, tissues were cut into 1mm³ blocks and fixed with 2.5% glutaraldehyde in PBS, pH 7.4 overnight and processed as for the cell cultures, except that tissue samples were further dehydrated in two 10-minute changes of propylene oxide. Samples were infiltrated with a 1:1 mix of propylene oxide and epon overnight and infiltrated with pure epon overnight at 4°C. Infiltration was continued with three 1-hour changes of epon. Samples were embedded in pure epon for 24 hours at 37°C and cured for 48 hours at 60°C. Image acquisition was done using either the JEM-1011 or the JEM-1400Plus transmission electron microscopes (Jeol, Peabody, MA) at 80 kV fitted with a side mount AMT 2k digital camera (Advanced Microscopy Techniques, Danvers, MA). Morphometric analysis of electron micrographs to determine the percentage of cells that contained globular inclusions was done by counting individual cells in the no LD1a iHeps (n=98), no LD2 iHeps (n=103), no LD3 iHeps (n=128), severe LD1 iHeps (n=97), and severe LD2 iHeps (n=111). Values are presented as mean ± s.d.

4.3 RESULTS

4.3.1 iHeps from ATD patients recapitulate the accumulation and processing of the mutant ATZ molecule

We used pulse-chase radiolabeling to analyze the kinetics of ATZ processing and secretion in iHeps from severe LD patients as the most sophisticated and definitive strategy to determine whether these cells model the known cellular defect that characterizes ATD. In both wild type iHeps and primary hepatocyte controls, AT is synthesized as a 52-kDa polypeptide that quickly becomes converted to a 55-kDa polypeptide. AT disappears from the intracellular compartment between 1 and 2 hours, coincident with appearance of the 55-kDa polypeptide in the extracellular medium (Figure 9A). In iHeps from severe LD patients, the 52-kDa ATZ polypeptide very slowly disappears from the intracellular compartment over the entire 4 hours of the chase period with minimal conversion to the 55-kDa polypeptide. A lesser amount of the 55-kDa ATZ polypeptide is detected in the extracellular fluid and it begins to appear only at the 3.0-hour time point (Figure 9A). The fate of ATZ in iHeps from severe LD patients was identical to its fate in primary hepatocytes from severe LD patients (Figure 9A). The half-time for the disappearance of AT from the intracellular compartment for wild type iHeps and primary hepatocyte controls was 1.4 ± 0.1 hours as compared to 3.6 ± 0.4 hours for the iHeps and primary hepatocytes from severe LD patients (Figure 9B).

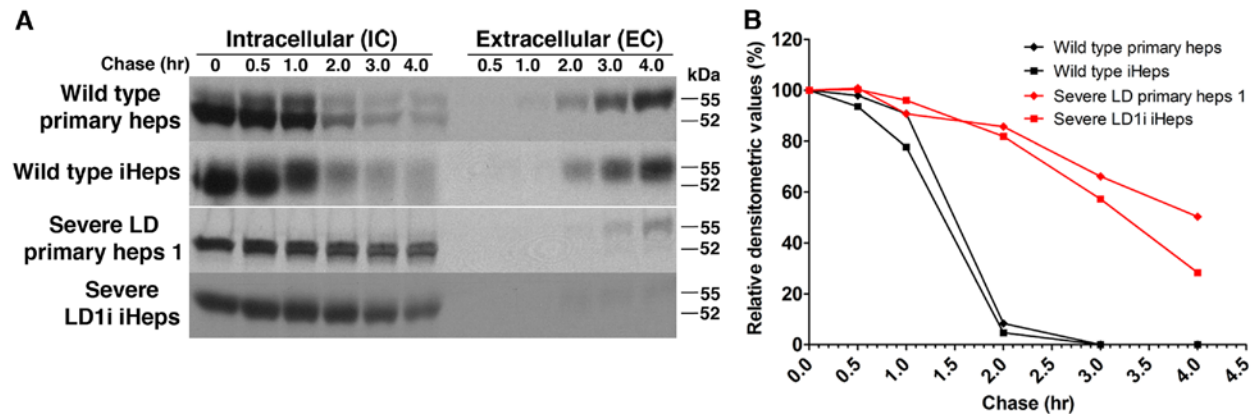


Figure 9. ATD iHeps recapitulate the accumulation and secretion of ATZ observed in ATD primary human hepatocytes

(A) Pulse-chase labeling showing intracellular accumulation of AT in severe LD cells but not in wild type cells. (B) Kinetics of the disappearance of AT in severe LD and wild type cells. Values are band densities of IC fractions in (A) relative to IC signal at time 0.

Furthermore, analysis of the percentage of AT in the extracellular fluid at 3.0 and 4.0 hours of the chase period relative to the amount of AT in the intracellular compartment at time 0 revealed that iHeps and primary hepatocytes from severe LD patients have markedly reduced AT secretion compared to wild type iHeps and primary hepatocyte controls (Figure 10). This was an important analysis because we found that the relative rate of secretion of AT from wild type iHeps and primary hepatocyte controls is lower than in model cell lines generated by gene transfer. These cells include the HeLa HTO/M cell line (Figure 10), human fibroblast cell lines⁷⁴, human hepatoma HepG2 and Hep3B cell lines, and human monocytes in primary culture²¹. This difference in rate of secretion of AT could therefore represent “leakiness” in the previous model cell lines or lack of full differentiated function in iHeps and primary hepatocytes in culture. Nevertheless, each of these cell systems are models and the important result is the clear difference in secretion between AT and the misfolded variant ATZ in each system. Thus, we conclude from the investigations thus far that iHeps from patients with severe LD accurately

model the intracellular accumulation and diminished secretion characteristic of the misfolded ATZ molecule^{21, 74}. Indeed, this is the first time that this type of sophisticated kinetic analysis with pulse-chase radiolabeling has been used to definitively and quantitatively show that iHeps faithfully model the basic defect of the classical form of ATD and to provide quantitative rate measurements for the fate of ATZ.

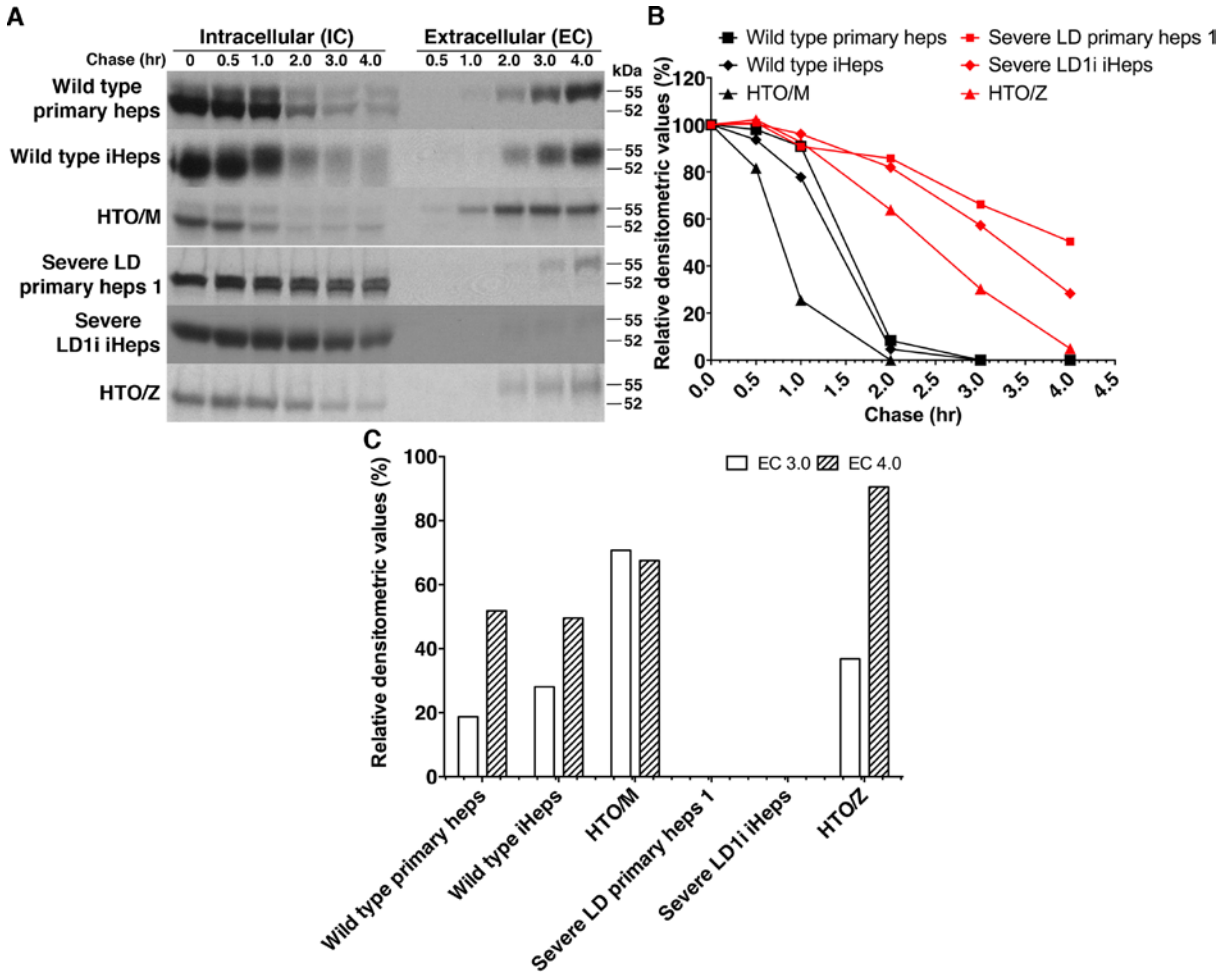


Figure 10. iHeps and primary hepatocytes secrete lower levels of AT in the extracellular fraction compared to HeLa inducible cell lines transduced to express wild type AT (HTO/M) or ATZ (HTO/Z)

(A) Pulse-chase labeling comparing the AT in IC and EC fractions in the indicated cells. (B) Kinetics of the disappearance of AT in indicated cells. Values are band densities of IC fractions in (A) relative to IC signal at time 0. (C) Band densities of the EC fractions in (A) at 3 hours (EC 3.0) and 4 hours (EC 4.0) relative to IC signal at time 0.

Next we used the peptide-N-glycosidase F (PNGase F) deglycosylation assay to determine whether the AT and ATZ polypeptides undergoes N-linked glycosylation in the ER of iHeps. In both wild type and severe LD cells, the 52-kDa and 55-kDa AT polypeptides are PNGase-sensitive (Figure 11A) signifying that the AT and ATZ polypeptides received the N-linked core glycan in the ER. We then performed the endoglycosidase H (endo H) deglycosylation assay to further characterize the fate of ATZ in the intracellular and extracellular compartment. In wild type iHeps and primary hepatocyte controls, the 52-kDa AT polypeptide is an endo H-sensitive partially glycosylated intermediate and the 55-kDa polypeptide that is detected intracellularly and extracellularly is endo H-resistant. In iHeps and primary hepatocytes from severe LD patients, the 52-kDa ATZ polypeptide that accumulates is endo H-sensitive whereas the very small amount of 55-kDa polypeptide that can be detected is endo H-resistant (Figure 11B). This indicates that the ATZ molecule that accumulates is a partially glycosylated intermediate and is predominantly localized to pre-Golgi compartments. This result is similar to what is observed in HeLa HTO/M and HTO/Z cell line models (Figure 11B).

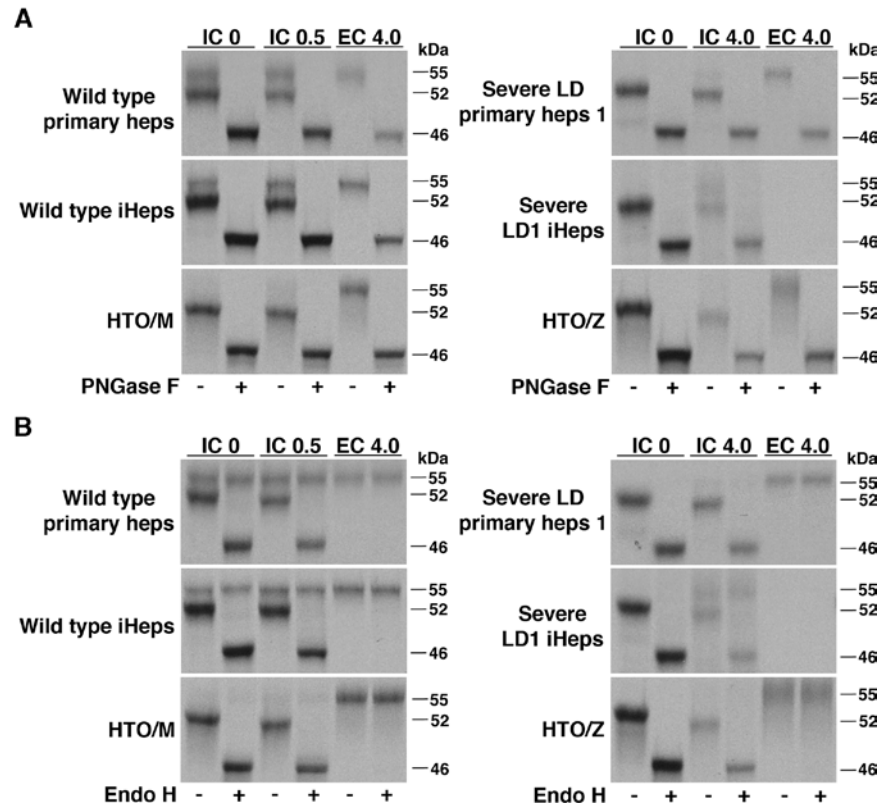


Figure 11. The ATZ polypeptide accumulates as a partially glycosylated intermediate in iHeps and primary hepatocytes from patients with ATD

Effect of PNGase F (A) and endo H (B) on AT in pulse-chase intracellular (IC) and extracellular (EC) fractions of indicated cells. (-) mock digestion, (+) enzyme digestion.

4.3.2 iHeps from ATD patients with no liver disease more efficiently degrade misfolded ATZ

Having established that ATD iHeps model the known biochemical abnormalities associated with the misfolded ATZ molecule^{72, 74, 183}, we next investigated whether there is a difference in the fate of ATZ in severe LD and no LD iHeps using pulse-chase labeling (Figure 12A). In severe LD iHeps, intracellular ATZ slowly disappeared with more than ~30% of radioactively labeled

ATZ remaining after 4 hours. In no LD iHeps however, intracellular ATZ disappears more rapidly, beginning at the 2- and 3-hour time points with minimal radioactively labeled ATZ remaining at 4 hours (Figure 12, A and B). Intracellular ATZ disappeared slower in severe LD iHeps ($p < 0.005$) with a half-time of 3.6 ± 0.1 hours compared to 2.2 ± 0.3 hours in no LD iHeps (Figure 12C). Quantitative accounting for all of the radiolabeled ATZ showed that the more rapid disappearance of ATZ from the intracellular compartment in the no LD iHeps could not be explained by increased secretion in the extracellular compartment (Figure 13) and is therefore entirely due to enhanced intracellular degradation. The validity of the modeling was apparent in several other ways. The kinetics of disappearance of ATZ was similar in iHeps from multiple iPSc clones from the same patient and in iHeps from unrelated PiZZ individuals that have the same liver disease phenotype (Figure 12, B and C). Thus, these results indicate that ATZ has a different fate in iHeps from ATD patients with liver disease with significantly slower intracellular degradation than in iHeps from ATD patients with no liver disease. Importantly, the kinetic measurements of ATZ degradation in iHeps reported here are further validated by the fact that similar rates of ATZ degradation were observed years ago in genetically engineered skin fibroblasts from ATD patients⁷⁴, a model system that lacked hepatocyte characteristics and proved unwieldy for long-term studies. The similarity in rates of degradation in these 2 different systems provides further evidence for the validity of the difference between severe LD and no LD patients and for the validity of the pulse-chase analytic method.

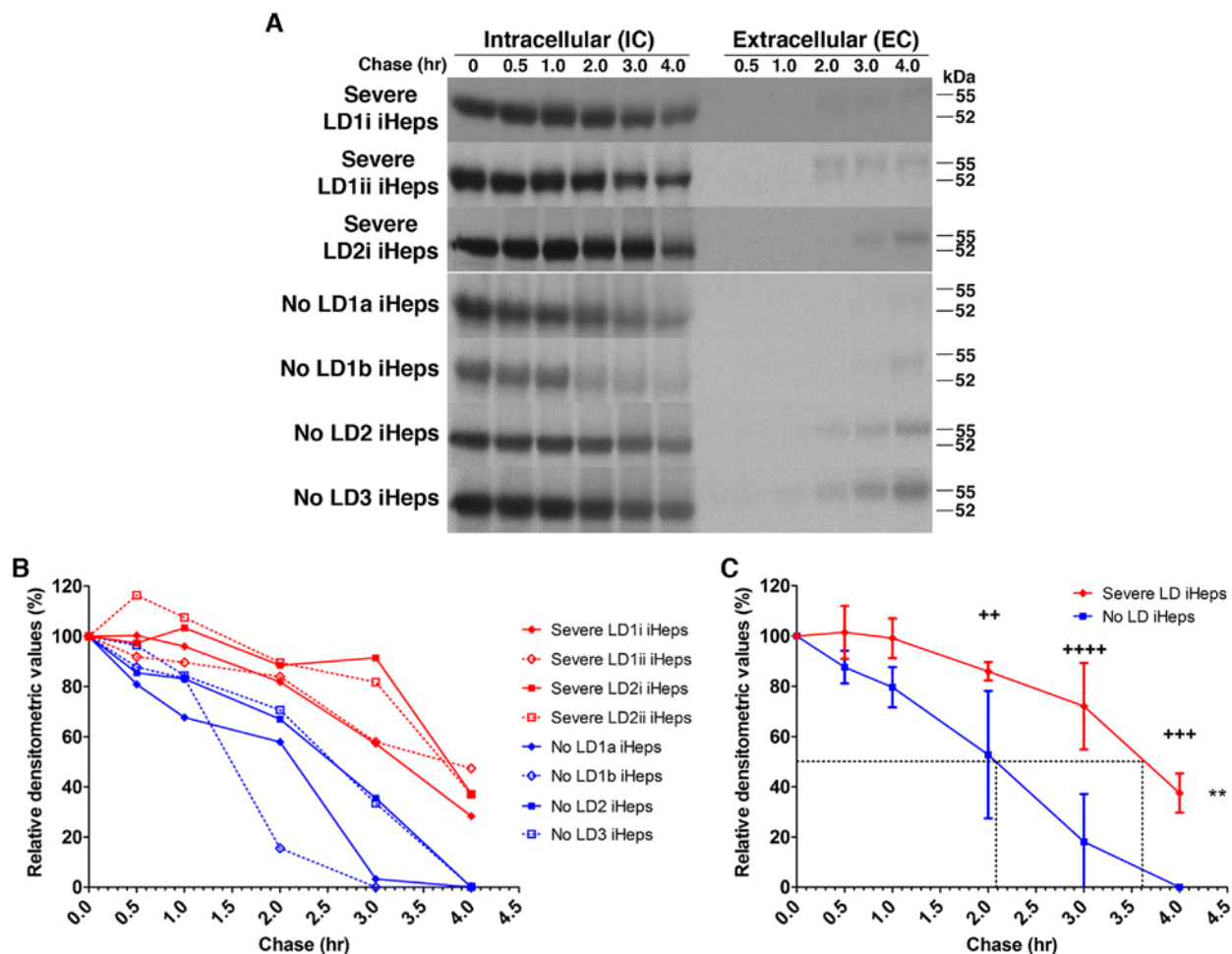


Figure 12. The rate of degradation of intracellular ATZ correlates with liver disease severity in ATD iHeps

(A) Pulse-chase labeling comparing the disappearance of intracellular AT in severe and no LD iHeps. Severe LD1i and LD1ii are replicates from the same iPS cell line. No LD1a and no LD1b are different iPS cell clones from the same patient. (B) Kinetics of the degradation of AT in severe and no LD iHeps. Values are band densities of IC fractions in (A) relative to IC signal at time 0. (C) Composite curves of (B) shown as mean \pm s.d. Dashed lines represent the half-time for disappearance of intracellular AT. ** $p < 0.005$ (two-way repeated measures ANOVA), ++ $p < 0.01$, +++ $p < 0.001$, ++++ $p < 0.0001$ (Bonferroni posttests at each time point). Although densitometric values for the no LD iHeps appear to reach zero, the absolute values are $< 1\%$ in B and C.

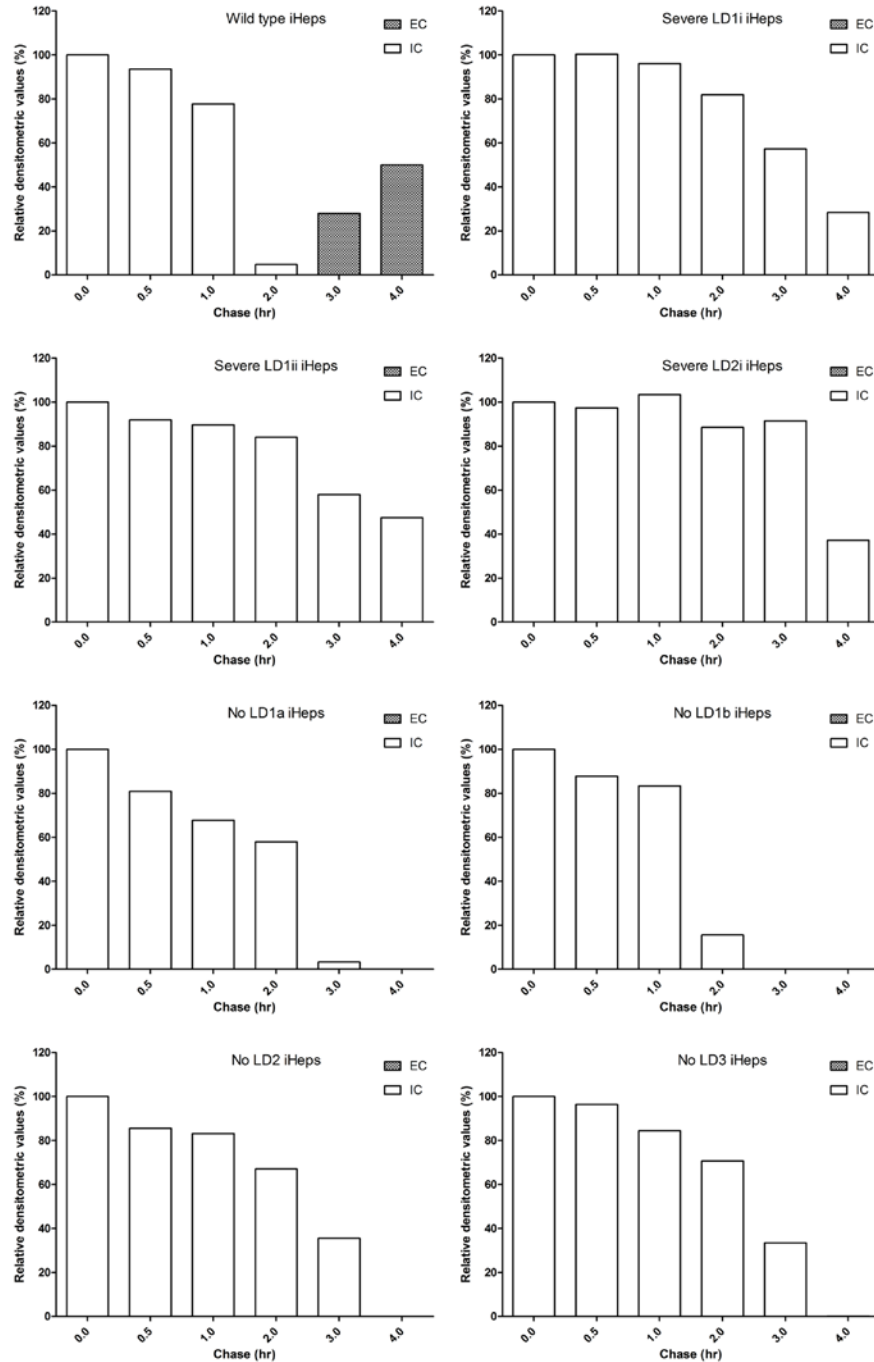


Figure 13. The disappearance of intracellular ATZ in no LD iHeps does not lead to increased secretion in the extracellular compartment

Band density values of IC and EC fractions of wild type iHeps in Figure 9A and of severe LD and no LD iHeps in Figure 12A expressed as percentage of IC signal at time 0.

4.3.3 The mutant ATZ molecule accumulates in the rER as well as in non-rER compartments of ATD iHeps

Having demonstrated that iHeps can model the fate of ATZ biochemically, we next examined the extent to which iHeps can model the disease morphologically. Early ultrastructural analysis of liver biopsies from ATD patients^{153, 184} as well as immunofluorescence studies of model cell lines transduced to express mutant ATZ¹⁸⁵ have led to the belief that misfolded ATZ accumulates in the ER. To determine the sites of ATZ accumulation in severe LD iHeps, we performed double label immunofluorescence for AT and the rough ER (rER) markers calnexin and calreticulin. AT staining co-localized with rER markers but several large areas of AT accumulation did not (Figure 14, A to D). The fact that none of the large areas of ATZ accumulation co-localized with the Golgi marker GM130 (Figure 14, E and F), together with the Endo H studies (Figure 11) indicate that ATZ predominantly localizes to pre-Golgi compartments. The co-localization of ATZ and rER markers varied within and among cells (Figure 14G). Three-dimensional reconstruction of confocal image stacks from severe LD iHeps stained for AT and calnexin shows regions of ATZ accumulation that were enveloped by calnexin and others that were not. Some areas of calnexin-enclosed AT were also observed to be continuous with calnexin-free AT accumulation (Figure 14, H and I). These results suggest that ATZ accumulates not only in the rER but also in non-rER compartments.

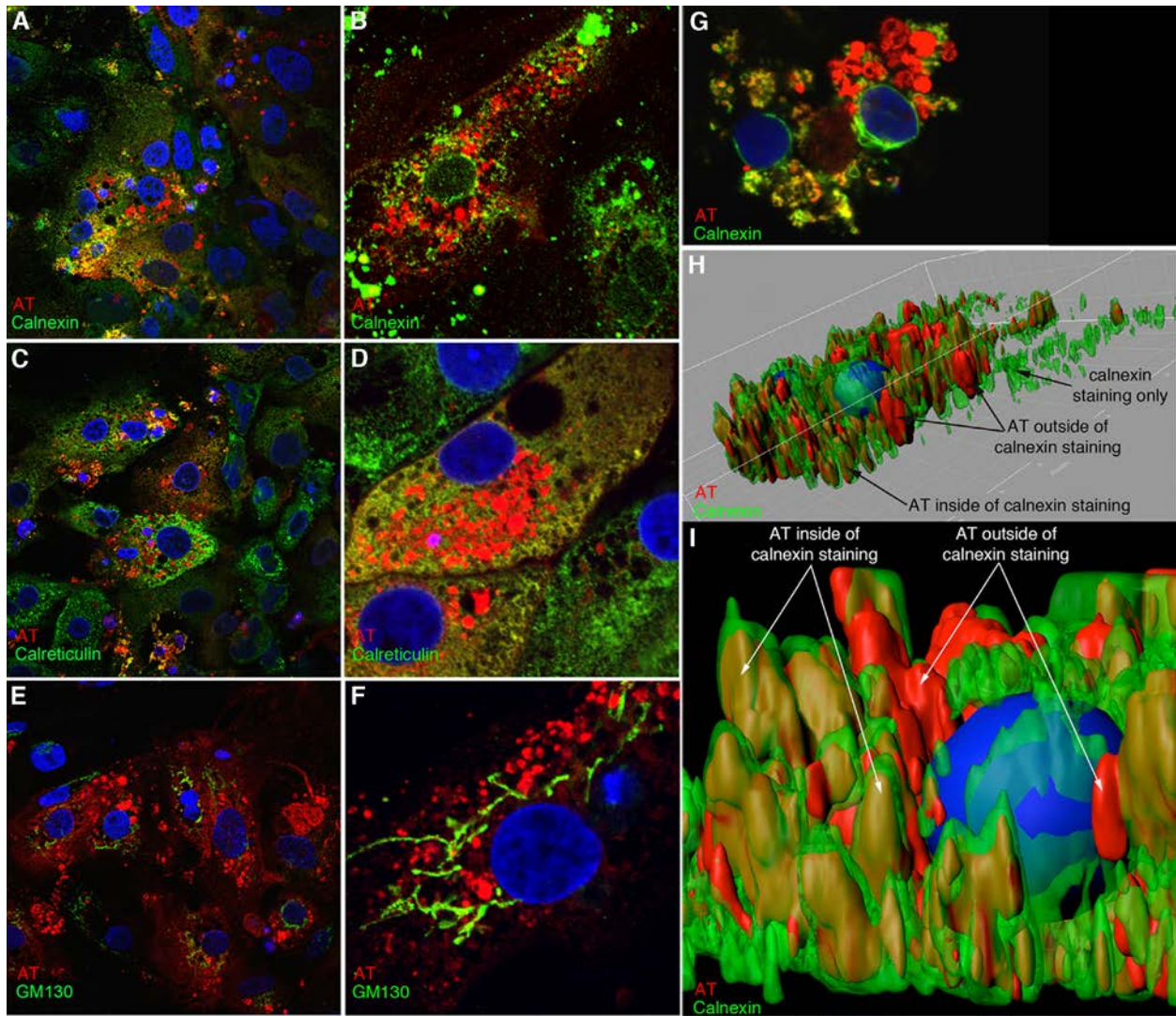


Figure 14. ATZ in severe LD iHeps accumulates in rER and in compartments that are devoid of calnexin, calreticulin, or GM130

Immunofluorescent staining of severe LD iHeps for AT and calnexin (A, B), calreticulin (C, D), or GM130 (E, F). A, C, E (600X), B, D, F (2000X). (G) Single stack image of severe LD iHeps stained for AT and calnexin. (H and I) 3D surface reconstruction of multiple stacks of images of AT/calnexin-stained severe LD iHeps with calnexin signal made partially transparent to reveal AT staining inside calnexin staining. Nuclei are stained blue.

Next we analyzed the ultrastructure of iHeps from severe LD patients and we used liver biopsy specimens from severe LD patients for comparison. In contrast to wild type iHeps which

displayed normal rER morphology, similar to those seen in wild type liver sections (Figure 15, A and B), severe LD iHeps had markedly dilated rER as well as abnormal globular inclusions, large vesicular structures enveloping proteinaceous material and partially covered with ribosomes (Figure 15, C and D). Liver sections from ATD patients with severe LD had similar morphological characteristics¹⁵³ (Figure 15, E and F). The globular inclusions are filled with granular material that, in some areas, appears electron-dense. In some cells, the globular inclusions are almost completely devoid of ribosomes but because of the single plane of the image it is not possible to exclude the presence of some ribosome-containing areas. These observations are consistent with the double immunofluorescence and three-dimensional reconstructions (Figure 14, H and I) showing accumulation of ATZ in calnexin-positive and calnexin-free structures. These globular inclusions that are calnexin-free could represent dilations of smooth ER, specialized sub-domains of the rER or a completely separate subcompartment as has been observed for other misfolded proteins¹⁸⁶. While some cells in severe LD iHeps had normal looking organelles, many cells that contained inclusions had obvious accumulation of lipid droplets, autophagosomes, abnormal mitochondrial structures and fragmented Golgi (Figures 15C and 16 to 18), remarkably similar to what was seen in liver sections of ATD patients with severe LD¹⁵³. Thus, using detailed immunofluorescent and ultramicroscopic analysis of iHeps from ATD patients, we provide evidence that iHeps recapitulate the morphological characteristics seen in the liver of ATD patients with severe LD and establish iHeps as an ideal model for analysis of the biology of the misfolded ATZ molecule at subcellular and biochemical levels, particularly because these cells are hepatocytic.

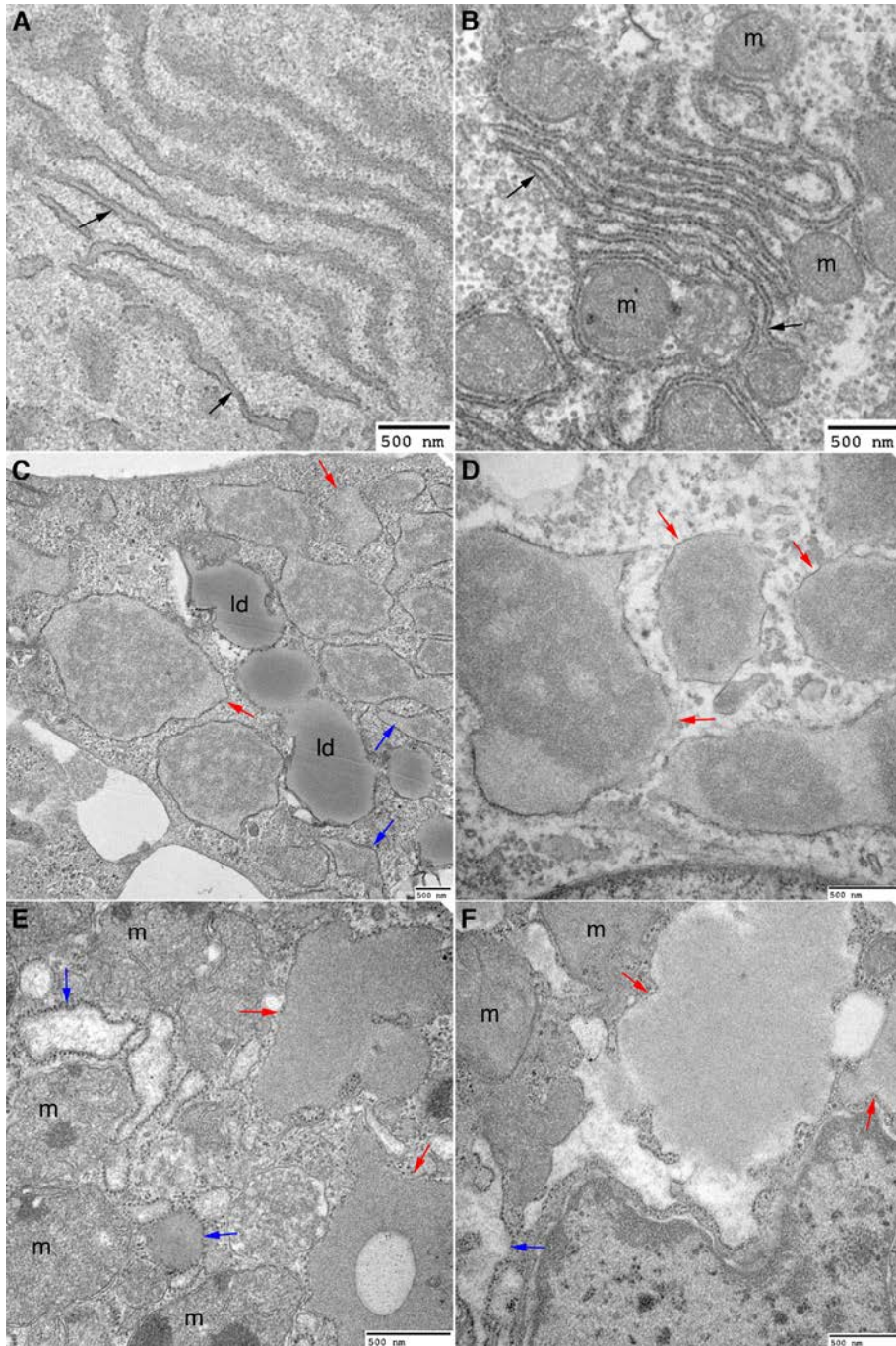


Figure 15. Severe LD iHeps and severe LD liver tissue sections exhibit dilated rER and dilated globular inclusions that are partially covered with ribosomes

Electron micrograph of wild type iHeps (A), wild type liver tissue section (B), severe LD iHeps (C, D), and severe LD liver tissue section (E, F) showing normal rER (black arrows), dilated rER (blue arrows) and dilated globular inclusions that are partially covered with ribosomes (red arrows). m: mitochondria, ld: lipid droplets.

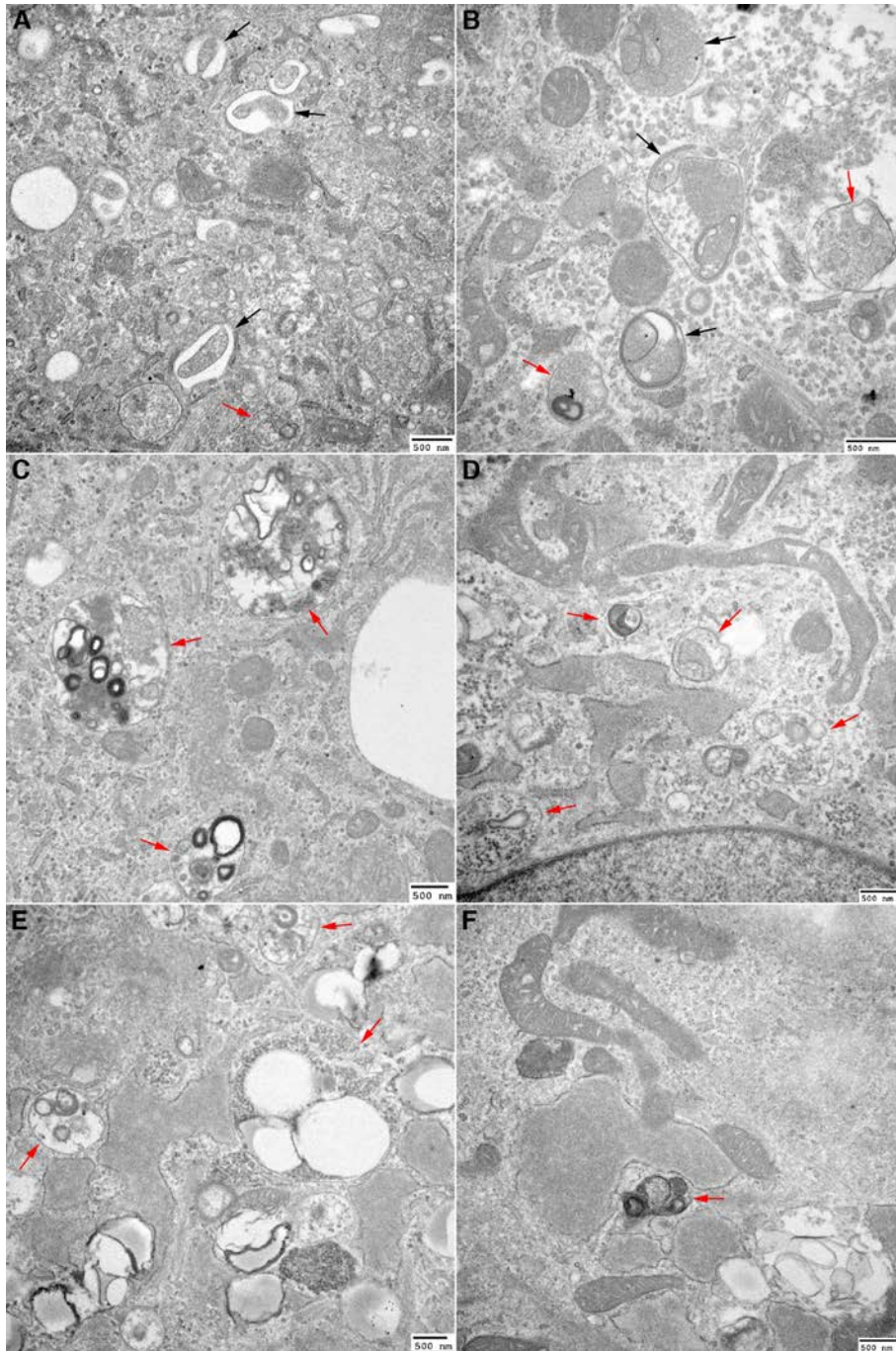


Figure 16. Electron micrographs of severe LD iHeps (A-F) showing the presence of autophagosomes (black arrows) and autophagolysosomes (red arrows)

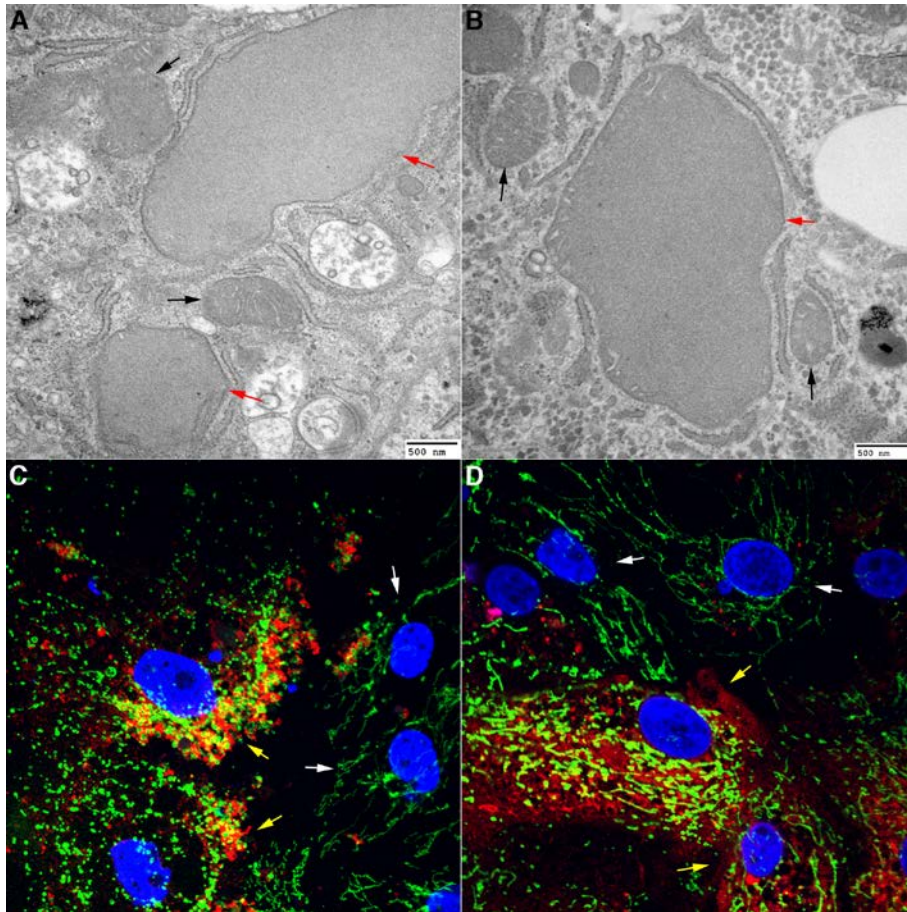


Figure 17. Mitochondrial dilation is evident in severe LD iHeps

(A and B) Electron micrograph of severe LD iHeps showing normal mitochondria (black arrows) and enlarged mitochondria (red arrows). (C and D) Immunofluorescent staining of severe LD iHeps for AT (red), TOM20 (green), and nuclei (blue) showing dilated mitochondria in cells with increased AT accumulation (yellow arrows) compared to cells with minimal AT accumulation (white arrows) (1000X).

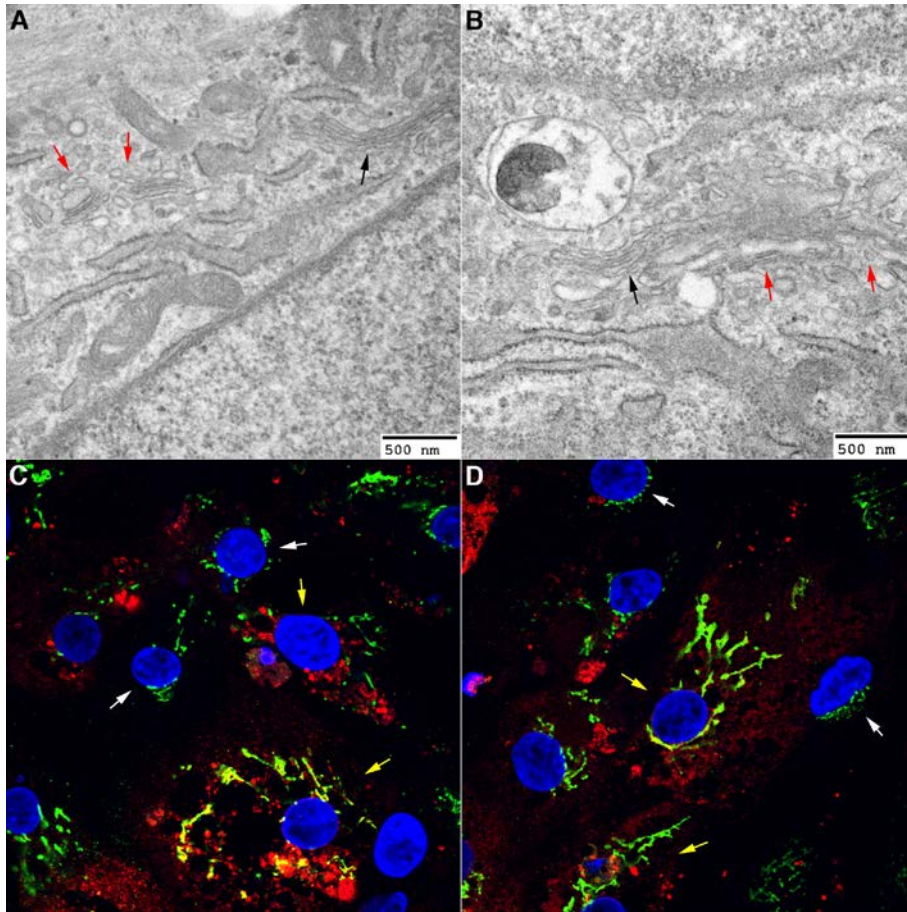


Figure 18. Golgi fragmentation is evident in severe LD iHeps

(A and B) Electron micrograph of severe LD iHeps showing normal Golgi (black arrows) and fragmented Golgi (red arrows). (C and D) Immunofluorescent staining of severe LD iHeps for AT (red), GM130 (green), and nuclei (blue) showing fragmented Golgi in cells with AT accumulation (yellow arrows) compared to cells with minimal AT accumulation (white arrows) (1000X).

4.3.4 No LD iHeps lack intracellular inclusions that are the cellular hallmark of the disease

Because liver biopsies are not routinely performed on ATD patients with no symptomatic liver disease, the ultrastructure of hepatocytes in this group of patients has not been studied. We

therefore used TEM to determine if there are ultrastructural differences between severe LD (Figure 19, A to C) and no LD iHeps (Figure 19, D to F). Although dilated rER was observed in iHeps from no LD patients, there was a remarkable absence of globular inclusions (Figure 19, D to F). Using quantitative morphometry, globular inclusions were observed in $26.59 \pm 7\%$ of iHeps from severe LD patients as compared to none of the iHeps from no LD patients. This suggests that the degradative response that leads to enhanced intracellular disposal of ATZ in no LD individuals, as shown by the pulse-chase results in Figure 12, A to C, might be sufficient to prevent this morphological hallmark of ATZ accumulation. Furthermore, this morphological difference could be used as a relatively straightforward diagnostic criterion to predict susceptibility to liver disease in individuals with ATD.

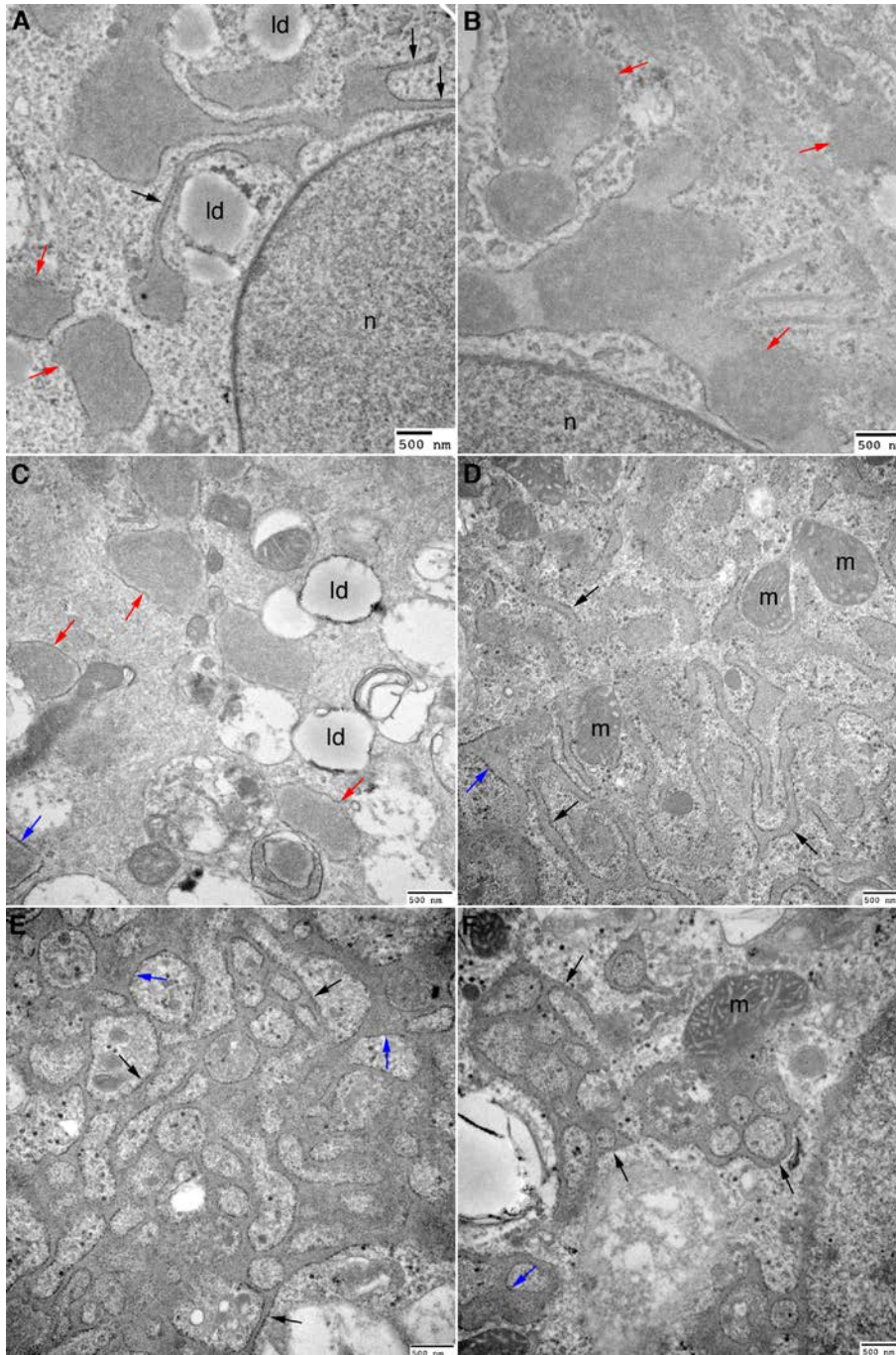


Figure 19. Severe LD iHeps and no LD iHeps exhibit dilated rER but only severe LD iHeps exhibit globular inclusions

Electron micrograph of severe LD iHeps (A-C) and no LD iHeps (D-F) showing normal rER (black arrows), dilated rER (blue arrows) and globular inclusions that are partially covered with ribosomes (red arrows). ld: lipid droplets, n: nucleus, m: mitochondria.

4.4 DISCUSSION

Previous studies have described the use of patient-derived iHeps for modeling ATD^{97, 157-159}. This study takes the technology one step further by demonstrating that patient-derived iHeps can model the biochemical and morphological manifestations of a primary genetic defect and the modifiers that correlate with the clinical phenotype in individual patients.

From a cell biological perspective, the results provide support for the concept that quality control “proteostasis” mechanisms, in this case intracellular degradation pathway(s), play a critical role in determining the severity of disease, presumably by affecting the degree of “proteotoxicity”¹⁸⁷. In terms of ATD, the current study supports a long-held hypothesis that variation in hepatic phenotype could be attributed at least in part to modifiers that target either intracellular degradation mechanisms or signaling pathways which facilitate adaptation of cells to accumulation of misfolded proteins⁷⁴. Although the studies reported here do not identify the specific genes that represent the putative modifiers, we now know that the modifiers, at least in the patients investigated here, appear to be associated with the intracellular degradation pathways or regulators of those pathways. This finding is also important because it is possible, if not probable, that variation in the liver phenotype among ATD patients is due to genetic or environmental modifiers that lead to hepatocyte dysfunction completely independent of an effect on the fate of misfolded ATZ (e.g. steatosis, iron overload). The results also indicate that iHeps will provide a valid system for identifying the mechanism by which putative modifiers affect the fate of ATZ.

It was originally thought that misfolded ATZ accumulates only within the rER of hepatocytes^{153, 184, 185}. However, results from our study also demonstrate the accumulation of ATZ in abnormal globular inclusions. These inclusions do not exhibit the normal characteristics

of rER or Golgi because they are poorly studded with ribosomes and are devoid of classical rER and Golgi markers. While the identity of these globular inclusions has not been definitively established, our results showing that only iHeps from patients with severe liver disease contained inclusions suggests that the enhanced intracellular disposal of ATZ in ATD patients “protected” from liver disease is sufficient to prevent this morphological hallmark of ATZ accumulation. More importantly, this finding presents a major advance for clinical management of the disease as it may now be used to predict which individuals are susceptible to “proteotoxic” consequences and liver disease well before liver disease progresses to end-stage, necessitating liver transplantation. By showing that patients are susceptible to liver disease because their endogenous intracellular degradation mechanisms are not as efficient as in “protected” hosts, the results provide even more optimism for the recently identified therapeutic strategies utilizing drugs such as carbamazepine and fluphenazine, which enhance autophagic degradation of ATZ⁶⁶.

5.0 CONCLUSION

The discovery that somatic cells can be reprogrammed into pluripotent stem cells, together with the development of more efficient *in vitro* differentiation techniques, has paved the way for a new source of human somatic cells for disease modeling. In recent years, a number of studies have shown that patient-derived iPSCs can recapitulate the cellular manifestations of the primary genetic defect in various genetic diseases, including ATD^{93, 94, 96-98, 100, 111, 157-159, 188-192}. However, for many genetic diseases, such as ATD-mediated liver disease, ATD-mediated lung disease, Alzheimer's disease, and hypertrophic cardiomyopathy, there is substantial clinical phenotypic variability such that patients carrying the same genetic mutation may present with severe, mild or no symptoms. The degree to which iPSCs can also model the genetic modifiers that affect disease penetrance has not been investigated.

In this study, we validate the usefulness of iPSC technology for disease modeling by demonstrating that patient-derived iHeps can model the pathogenesis and heterogeneity of ATD-mediated liver disease. Although the studies reported here do not identify the specific genes that represent the putative modifiers, we have now confirmed that these modifiers are involved with the regulation of intracellular degradation pathways. The results also indicate that iHeps will provide a valid system for identifying specific modifier genes that could be potential pharmacological targets. Since iHeps can be generated from any and all ATD patients, it also allows for the development of personalized treatment strategies. Finally, iHeps could potentially

serve as a tool for assessing predisposition to liver dysfunction in ATD patients, either by pulse-chase or by ultrastructural analysis.

6.0 FUTURE DIRECTIONS

6.1 REPROGRAMMING OF ATD PATIENT-DERIVED SOMATIC CELLS USING SENDAI VIRUS

Initial methods for generating iPSCs from human somatic cells had low efficiencies and involve the insertion of exogenous genetic material into host cells. In recent years, there have been several studies that developed new methods for reprogramming that generate footprint-free iPSCs at higher reprogramming efficiencies. Among these methods, the approach that has the greatest reprogramming efficiency uses the F-deficient Sendai viral vector (SeV). Using this method, neonatal and adult fibroblasts are reprogrammed to iPSCs at efficiencies as high as 1%¹⁹³. The Sendai virus has a genome in the form of a minus-sense single stranded RNA. Because it replicates in the cytoplasm of infected cells without the generation of DNA intermediates, it is impossible for the viral sequences to integrate into the host genome. Because entry of the virus is mediated by binding to sialic acid receptors present on the surface of many different cells, it is also a very efficient vector for introducing foreign genes in a wide spectrum of host cells. Although there are concerns that the SeV is difficult to remove from infected cells because they constitutively replicate, it has been reported that no residual virus is present by passage 10¹⁹³. Moreover, a temperature-sensitive SeV has now been developed that allows complete loss of vector copy number in cytoplasm by increasing the temperature to 38-39°C¹⁹⁴. This strategy

would therefore produce footprint-free iPSCs that would be valuable for both disease modeling and cell transplantation.

6.2 DIFFERENTIATION AND TRANSPLANTATION OF ATD PATIENT-DERIVED IPSCS TO GENERATE MATURE HEPATOCYTES

Several protocols have described the differentiation of iPSCs into iHeps that display many features of primary mature hepatocytes^{97, 116, 117, 178}. However, some of the functions of these iHeps, such as inducible cytochrome P450 enzyme expression, are underdeveloped suggesting that these cells have a phenotype that is not fully mature. So far, only two protocols have been able to generate pluripotent stem cell-derived hepatocytes that exhibit mature hepatocyte function and that can engraft and expand after transplantation in rodent models of liver repopulation^{142, 179, 180}.

In one study, three-dimensional aggregates of pluripotent stem cells called embryoid bodies (EBs) are first generated and allowed to mature for 2 days¹⁴². This allows the differentiation of stem cells towards either endodermal, mesodermal, or ectodermal derivatives. EBs are then transferred in two-dimensional cultures and treated with growth factors that induce hepatogenesis in the endodermal cells. Some of the cells that differentiate towards other non-hepatocytic lineages presumably become “supporting cells” that help the endoderm cells to differentiate into hepatocytes. Because there is a heterogeneous population of cells after the differentiation, mature hepatocytes are selected by fluorescence activated cell sorting for the mature hepatocyte marker ASGPR1. Transplantation of ASGPR1-expressing cells in rodent models for liver repopulation (Alb-uPA SCID mouse and retrorsine-treated/70% partially

hepatectomized immunosuppressed Nagase rat) showed that the cells were able to engraft in the host liver, expand in response to proliferation signals, and secrete liver-specific proteins. The rationale for this approach is that the non-hepatocyte cells presumably facilitate the differentiation and maturation of hepatocytes either by growth factor-mediated or contact-mediated signaling.

In another study, hepatocyte differentiation was performed in a three-dimensional culture system prior to tissue transplantation. When iPSc-derived hepatic endoderm, endothelial and mesenchymal cells are co-cultured, the cells spontaneously formed three-dimensional liver bud (LB) organoids capable of liver-specific functions such as protein production and human-specific drug metabolism^{179, 180}. Transplantation of the LBs in the mesentery of a drug-induced mouse repopulation model (TK-NOG mouse) or the acute liver injury model (Alb-TRECK/SCID mice) also improved survival¹⁷⁹. This study improved hepatocyte differentiation by using a three-dimensional and multicellular approach to mimic liver development.

Based on these studies, it appears that there is a significant improvement in hepatocyte differentiation in the presence of other cell types. EB-mediated and LB-mediated hepatocyte differentiations of ATD iPSCs are promising methods for obtaining mature hepatocytes. Hepatocytes that are isolated and purified using ASGPR1-selection can then be used for *in vitro* analyses or can be transplanted into FRG mouse model for repopulation¹⁹⁵ to generate an *in vivo* model for ATD.

6.3 ANALYSIS OF OTHER FORMS OF ATD-MEDIATED LIVER DISEASE

In our studies, we used iHeps from ATD patients with severe liver disease during the childhood years. It will be interesting to determine if differences in kinetic characteristics or morphology can be ascertained in iHeps representing the other forms of ATD liver disease, with onset in adolescence or adult years, or with isolated hepatocellular carcinoma. It will also be important to determine if the kinetic and morphological characteristics are stable when collected from single individuals serially over time. We suspect that these characteristics will be stable over time because of the similarities in mean rate of intracellular degradation for each group when investigated in the previously reported fibroblast cell lines⁷⁴ and iHeps in this report and because the iHeps from ATD patients with no liver disease, which had a relatively increased rate of intracellular degradation, were established from these patients at adult ages of 42-67 years. If not stable we would have expected this rate of degradation to decrease with age.

6.4 IDENTIFICATION OF MODIFIER GENES FOR ATD

Results from this study demonstrate the ability of patient-derived iHeps to model the heterogeneity of ATD-mediated liver disease. Although this study does not identify the specific genes that represent the modifiers of disease susceptibility, it provides a reliable system for identifying and validating specific modifier genes. Recent studies using genome-wide RNAi screens and genetic crosses in a *C. elegans* model for ATD have identified genetic modifiers affecting the accumulation of the alpha-1 antitrypsin Z mutant (ATZ)^{69, 70}. An important next step would be to employ gene-targeted approaches to confirm the involvement of these putative

modifier genes on the phenotype (ultrastructural characteristics and kinetics of ATZ disposal) of ATD iHeps. Genetic knockdown of modifier genes (or their endogenous inhibitors) can be done using siRNA or shRNA technology. Genomic editing using either Zinc Finger Nucleases (ZFN)¹⁰³ and piggyBac technology^{104, 105}, Clustered Regularly Interspaced Short Palindromic Repeat (CRISPR)/CRISPR-associated nuclease 9 (CRISPR/Cas9) system¹⁰⁶ or Transcription Activator-Like Effector Nucleases (TALENs)¹⁰⁷ can also be used to introduce specific mutations in modifier genes that would render the gene product inactive. Genomic editing could also be done to correct variants of modifier genes that increase susceptibility to liver disease and determine the effects on overall phenotype.

6.5 DRUG TREATMENT OF ATD IHEPS

From this study, we know that the modifiers, at least in the iHeps we studied, are involved with the regulation of intracellular degradation pathways. Moreover, results of genome-wide RNAi screens, genetic crosses, and pharmacological screens in a *C. elegans* model for ATD identified autophagy and ER-associated degradation (ERAD) pathways as critical for the degradation of intracellular ATZ⁶⁷⁻⁷⁰. The next step would be to determine if the treatment of severe LD iHeps with drugs that activate specific components of the autophagic degradation or ERAD pathways would result in decrease of intracellular ATZ load and the loss of globular inclusions. Conversely, it would also be valuable to determine whether the treatment of no LD iHeps with inhibitors of autophagic or proteosomal degradation pathways would increase ATZ load and allow the emergence of globular inclusions.

BIBLIOGRAPHY

1. Carrell, R., Jeppsson, J., Laurell, C., Brennan, S., Owen, M., Vaughan, L. and Boswell, D. Structure and variation of human alpha 1-antitrypsin. *Nature* **298**, 329-334 (1982).
2. Carrell, R.W., Jeppsson, J.O., Vaughan, L., Brennan, S.O., Owen, M.C. and Boswell, D.R. Human α 1-antitrypsin: carbohydrate attachment and sequence homology. *FEBS letters* **135** (1981).
3. Lojewski, X., Staropoli, J., Biswas-Legrand, S., Simas, A., Haliw, L., Selig, M., Coppel, S., Goss, K., Petcherski, A., Chandrachud, U., Sheridan, S., Lucente, D., Sims, K., Gusella, J., Sondhi, D., Crystal, R., Reinhardt, P., Sternecker, J., Schöler, H., Haggarty, S., Storch, A., Hermann, A. and Cotman, S. Human iPSC models of neuronal ceroid lipofuscinosis capture distinct effects of TPP1 and CLN3 mutations on the endocytic pathway. *Human molecular genetics* **23**, 2005-2022 (2014).
4. Laurell, C. and Eriksson, S. THE SERUM ALPHA-L-ANTITRYPSIN IN FAMILIES WITH HYPO-ALPHA-L-ANTITRYPSINEMIA. *Clinica chimica acta; international journal of clinical chemistry* **11**, 395-398 (1965).
5. Alper, C., Raum, D., Awdeh, Z., Petersen, B., Taylor, P. and Starzl, T. Studies of hepatic synthesis in vivo of plasma proteins, including orosomucoid, transferrin, alpha 1-antitrypsin, C8, and factor B. *Clinical immunology and immunopathology* **16**, 84-89 (1980).
6. Ito, H., Kishikawa, T., Yamakawa, Y., Toda, T., Tsunooka, H., Masaoka, A. and Ando, S. Serum acute phase reactants in pediatric patients; especially in neonates. *The Japanese journal of surgery* **13**, 506-511 (1983).
7. Travis, J. and Salvesen, G. Human plasma proteinase inhibitors. *Annual review of biochemistry* **52**, 655-709 (1983).
8. Crystal, R., Brantly, M., Hubbard, R., Curiel, D., States, D. and Holmes, M. The alpha 1-antitrypsin gene and its mutations. Clinical consequences and strategies for therapy. *Chest* **95**, 196-208 (1989).

9. Johnson, D. and Travis, J. Structural evidence for methionine at the reactive site of human alpha-1-proteinase inhibitor. *The Journal of biological chemistry* **253**, 7142-7144 (1978).
10. Beatty, K., Bieth, J. and Travis, J. Kinetics of association of serine proteinases with native and oxidized alpha-1-proteinase inhibitor and alpha-1-antichymotrypsin. *The Journal of biological chemistry* **255**, 3931-3934 (1980).
11. Olsen, G., Harris, J., Castle, J., Waldman, R. and Karmgard, H. Alpha-1-antitrypsin content in the serum, alveolar macrophages, and alveolar lavage fluid of smoking and nonsmoking normal subjects. *The Journal of clinical investigation* **55**, 427-430 (1975).
12. Fujita, J., Nakamura, H., Yamagishi, Y., Yamaji, Y., Shiotani, T. and Irino, S. Elevation of plasma truncated elastase alpha 1-proteinase inhibitor complexes in patients with inflammatory lung diseases. *Chest* **102**, 129-134 (1992).
13. Sharp, H. The current status of alpha-1-antitrypsin, a protease inhibitor, in gastrointestinal disease. *Gastroenterology* **70**, 611-621 (1976).
14. Kueppers, F. and Black, L. Alpha-1-antitrypsin and its deficiency. *The American review of respiratory disease* **110**, 176-194 (1974).
15. Nelson, D., Teckman, J., Di Bisceglie, A. and Brenner, D. Diagnosis and management of patients with α 1-antitrypsin (A1AT) deficiency. *Clinical gastroenterology and hepatology : the official clinical practice journal of the American Gastroenterological Association* **10**, 575-580 (2012).
16. Lace, B., Sveger, T., Krams, A., Cernevska, G. and Krumina, A. Age of SERPINA1 gene PI Z mutation: Swedish and Latvian population analysis. *Annals of human genetics* **72**, 300-304 (2008).
17. Long, G., Chandra, T., Woo, S., Davie, E. and Kurachi, K. Complete sequence of the cDNA for human alpha 1-antitrypsin and the gene for the S variant. *Biochemistry* **23**, 4828-4837 (1984).
18. Perlino, E., Cortese, R. and Ciliberto, G. The human alpha 1-antitrypsin gene is transcribed from two different promoters in macrophages and hepatocytes. *The EMBO journal* **6**, 2767-2771 (1987).
19. Brantly, M., Nukiwa, T. and Crystal, R. Molecular basis of alpha-1-antitrypsin deficiency. *The American journal of medicine* **84**, 13-31 (1988).

20. Rogers, J., Kalsheker, N., Wallis, S., Speer, A., Coutelle, C., Woods, D. and Humphries, S. The isolation of a clone for human alpha 1-antitrypsin and the detection of alpha 1-antitrypsin in mRNA from liver and leukocytes. *Biochemical and biophysical research communications* **116**, 375-382 (1983).
21. Perlmutter, D., Cole, F., Kilbridge, P., Rossing, T. and Colten, H. Expression of the alpha 1-proteinase inhibitor gene in human monocytes and macrophages. *Proceedings of the National Academy of Sciences of the United States of America* **82**, 795-799 (1985).
22. Mornex, J., Chytil-Weir, A., Martinet, Y., Courtney, M., LeCocq, J. and Crystal, R. Expression of the alpha-1-antitrypsin gene in mononuclear phagocytes of normal and alpha-1-antitrypsin-deficient individuals. *The Journal of clinical investigation* **77**, 1952-1961 (1986).
23. Hafeez, W., Ciliberto, G. and Perlmutter, D. Constitutive and modulated expression of the human alpha 1 antitrypsin gene. Different transcriptional initiation sites used in three different cell types. *The Journal of clinical investigation* **89**, 1214-1222 (1992).
24. Molmenti, E., Perlmutter, D. and Rubin, D. Cell-specific expression of alpha 1-antitrypsin in human intestinal epithelium. *The Journal of clinical investigation* **92**, 2022-2034 (1993).
25. Hu, C. and Perlmutter, D. Regulation of alpha1-antitrypsin gene expression in human intestinal epithelial cell line caco-2 by HNF-1alpha and HNF-4. *The American journal of physiology* **276**, 94 (1999).
26. Hu, C. and Perlmutter, D. Cell-specific involvement of HNF-1beta in alpha(1)-antitrypsin gene expression in human respiratory epithelial cells. *American journal of physiology. Lung cellular and molecular physiology* **282**, 65 (2002).
27. Courtois, G., Morgan, J., Campbell, L., Fourel, G. and Crabtree, G. Interaction of a liver-specific nuclear factor with the fibrinogen and alpha 1-antitrypsin promoters. *Science (New York, N.Y.)* **238**, 688-692 (1987).
28. De Simone, V., Ciliberto, G., Hardon, E., Paonessa, G., Palla, F., Lundberg, L. and Cortese, R. Cis- and trans-acting elements responsible for the cell-specific expression of the human alpha 1-antitrypsin gene. *The EMBO journal* **6**, 2759-2766 (1987).
29. Grayson, D., Costa, R., Xanthopoulos, K. and Darnell, J. One factor recognizes the liver-specific enhancers in alpha 1-antitrypsin and transthyretin genes. *Science (New York, N.Y.)* **239**, 786-788 (1988).

30. Kelsey, G., Povey, S., Bygrave, A. and Lovell-Badge, R. Species- and tissue-specific expression of human alpha 1-antitrypsin in transgenic mice. *Genes & development* **1**, 161-171 (1987).
31. Sifers, R., Carlson, J., Clift, S., DeMayo, F., Bullock, D. and Woo, S. Tissue specific expression of the human alpha-1-antitrypsin gene in transgenic mice. *Nucleic acids research* **15**, 1459-1475 (1987).
32. Jeppsson, J. Amino acid substitution Glu leads to Lys alpha1-antitrypsin PiZ. *FEBS letters* **65**, 195-197 (1976).
33. Chan, S. and Rees, D. Molecular basis for the alpha1-protease inhibitor deficiency. *Nature* **255**, 240-241 (1975).
34. Yoshida, A., Lieberman, J., Gaidulis, L. and Ewing, C. Molecular abnormality of human alpha1-antitrypsin variant (Pi-ZZ) associated with plasma activity deficiency. *Proceedings of the National Academy of Sciences of the United States of America* **73**, 1324-1328 (1976).
35. Lomas, D., Evans, D., Finch, J. and Carrell, R. The mechanism of Z alpha 1-antitrypsin accumulation in the liver. *Nature* **357**, 605-607 (1992).
36. Bathurst, I., Travis, J., George, P. and Carrell, R. Structural and functional characterization of the abnormal Z alpha 1-antitrypsin isolated from human liver. *FEBS letters* **177**, 179-183 (1984).
37. Burrows, J., Willis, L. and Perlmutter, D. Chemical chaperones mediate increased secretion of mutant alpha 1-antitrypsin (alpha 1-AT) Z: A potential pharmacological strategy for prevention of liver injury and emphysema in alpha 1-AT deficiency. *Proceedings of the National Academy of Sciences of the United States of America* **97**, 1796-1801 (2000).
38. Llewellyn-Jones, C., Lomas, D., Carrell, R. and Stockley, R. The effect of the Z mutation on the ability of alpha 1-antitrypsin to prevent neutrophil mediated tissue damage. *Biochimica et biophysica acta* **1227**, 155-160 (1994).
39. Mahadeva, R., Chang, W., Dafforn, T., Oakley, D., Foreman, R., Calvin, J., Wight, D. and Lomas, D. Heteropolymerization of S, I, and Z alpha1-antitrypsin and liver cirrhosis. *The Journal of clinical investigation* **103**, 999-1006 (1999).
40. Ogushi, F., Fells, G., Hubbard, R., Straus, S. and Crystal, R. Z-type alpha 1-antitrypsin is less competent than M1-type alpha 1-antitrypsin as an inhibitor of neutrophil elastase. *The Journal of clinical investigation* **80**, 1366-1374 (1987).

41. Laurell, C.-B. and Eriksson, S. The electrophoretic α 1-globulin pattern of serum in α 1-antitrypsin deficiency. 1963. *Copd* **10 Suppl 1**, 3-8 (2013).
42. Zhang, D., Wu, M., Nelson, D., Pasula, R. and Martin, W. Alpha-1-antitrypsin expression in the lung is increased by airway delivery of gene-transfected macrophages. *Gene therapy* **10**, 2148-2152 (2003).
43. Carrell, R. alpha 1-Antitrypsin: molecular pathology, leukocytes, and tissue damage. *The Journal of clinical investigation* **78**, 1427-1431 (1986).
44. Curiel, D., Holmes, M., Okayama, H., Brantly, M., Vogelmeier, C., Travis, W., Stier, L., Perks, W. and Crystal, R. Molecular basis of the liver and lung disease associated with the alpha 1-antitrypsin deficiency allele Mmalton. *The Journal of biological chemistry* **264**, 13938-13945 (1989).
45. O'Brien, M., Buist, N. and Murphey, W. Neonatal screening for alpha1-antitrypsin deficiency. *The Journal of pediatrics* **92**, 1006-1010 (1978).
46. Sveger, T. Liver disease in alpha1-antitrypsin deficiency detected by screening of 200,000 infants. *The New England journal of medicine* **294**, 1316-1321 (1976).
47. Blanco, I., de Serres, F., Fernandez-Bustillo, E., Lara, B. and Miravittles, M. Estimated numbers and prevalence of PI*S and PI*Z alleles of alpha1-antitrypsin deficiency in European countries. *The European respiratory journal* **27**, 77-84 (2006).
48. Beckman, L., Sikström, C., Mikelsaar, A., Krumina, A., Ku inskas, V. and Beckman, G. 1-Antitrypsin (PI) Alleles as Markers of Westeuropean Influence in the Baltic Sea Region. *Human heredity* **49**, 52-55 (1999).
49. Silverman, E., Miletich, J., Pierce, J., Sherman, L., Endicott, S., Broze, G. and Campbell, E. Alpha-1-antitrypsin deficiency. High prevalence in the St. Louis area determined by direct population screening. *The American review of respiratory disease* **140**, 961-966 (1989).
50. Eriksson, S. PULMONARY EMPHYSEMA AND ALPHA1-ANTITRYPSIN DEFICIENCY. *Acta medica Scandinavica* **175**, 197-205 (1964).
51. Teckman, J.H. Liver disease in alpha-1 antitrypsin deficiency: current understanding and future therapy. *Copd* **10 Suppl 1**, 35-43 (2013).
52. Crystal, R.G. Alpha 1-antitrypsin deficiency, emphysema, and liver disease. Genetic basis and strategies for therapy. *Journal of Clinical Investigation* (1990).

53. Gadek, J.E., Fells, G.A., Zimmerman, R.L., Rennard, S.I. and Crystal, R.G. Antielastases of the human alveolar structures. Implications for the protease-antiprotease theory of emphysema. *The Journal of clinical investigation* **68**, 889-898 (1981).
54. Gross, P., Pfitzer, E.A., Tolker, E., Babyak, M.A. and Kaschak, M. EXPERIMENTAL EMPHYSEMA: ITS PRODUCTION WITH PAPAINE IN NORMAL AND SILICOTIC RATS. *Archives of environmental health* **11**, 50-58 (1965).
55. Janoff, A., Sloan, B., Weinbaum, G., Damiano, V., Sandhaus, R.A., Elias, J. and Kimbel, P. Experimental emphysema induced with purified human neutrophil elastase: tissue localization of the instilled protease. *The American review of respiratory disease* **115**, 461-478 (1977).
56. Lieberman, J., Winter, B. and Sastre, A. Alpha 1-antitrypsin Pi-types in 965 COPD patients. *Chest* **89**, 370-373 (1986).
57. Lomas, D.A., Evans, D.L., Stone, S.R., Chang, W.S. and Carrell, R.W. Effect of the Z mutation on the physical and inhibitory properties of alpha 1-antitrypsin. *Biochemistry* **32**, 500-508 (1993).
58. Elliott, P.R., Bilton, D. and Lomas, D.A. Lung polymers in Z alpha1-antitrypsin deficiency-related emphysema. *American journal of respiratory cell and molecular biology* **18**, 670-674 (1998).
59. Parmar, J.S., Mahadeva, R., Reed, B.J., Farahi, N., Cadwallader, K.A., Keogan, M.T., Bilton, D., Chilvers, E.R. and Lomas, D.A. Polymers of alpha(1)-antitrypsin are chemotactic for human neutrophils: a new paradigm for the pathogenesis of emphysema. *American journal of respiratory cell and molecular biology* **26**, 723-730 (2002).
60. Mahadeva, R., Atkinson, C., Li, Z., Stewart, S., Janciauskiene, S., Kelley, D.G., Parmar, J., Pitman, R., Shapiro, S.D. and Lomas, D.A. Polymers of Z alpha1-antitrypsin co-localize with neutrophils in emphysematous alveoli and are chemotactic in vivo. *The American journal of pathology* **166**, 377-386 (2005).
61. Hidvegi, T., Schmidt, B.Z., Hale, P. and Perlmutter, D.H. Accumulation of mutant 1-antitrypsin Z in the endoplasmic reticulum activates caspases-4 and-12, NF B, and BAP31 but not the unfolded protein response. *Journal of Biological Chemistry* **280**, 39002-39015 (2005).
62. Kamimoto, T., Shoji, S., Hidvegi, T., Mizushima, N., Umebayashi, K., Perlmutter, D. and Yoshimori, T. Intracellular inclusions containing mutant alpha1-antitrypsin Z are propagated in the absence of autophagic activity. *The Journal of biological chemistry* **281**, 4467-4476 (2006).

63. Rudnick, D.A., Liao, Y., An, J.-K.K., Muglia, L.J., Perlmutter, D.H. and Teckman, J.H. Analyses of hepatocellular proliferation in a mouse model of alpha-1-antitrypsin deficiency. *Hepatology (Baltimore, Md.)* **39**, 1048-1055 (2004).
64. Teckman, J.H., An, J.K., Blumenkamp, K., Schmidt, B. and Perlmutter, D. Mitochondrial autophagy and injury in the liver in alpha 1-antitrypsin deficiency. *American journal of physiology. Gastrointestinal and liver physiology* **286**, G851-862 (2004).
65. Teckman, J.H., An, J.-K.K., Loethen, S. and Perlmutter, D.H. Fasting in alpha-1-antitrypsin deficient liver: constitutive [correction of consultative] activation of autophagy. *American journal of physiology. Gastrointestinal and liver physiology* **283**, 65 (2002).
66. Hidvegi, T., Ewing, M., Hale, P., Dippold, C., Beckett, C., Kemp, C., Maurice, N., Mukherjee, A., Goldbach, C., Watkins, S., Michalopoulos, G. and Perlmutter, D.H. An autophagy-enhancing drug promotes degradation of mutant alpha-1-antitrypsin Z and reduces hepatic fibrosis. *Science* **329**, 229-232 (2010).
67. Gosai, S., Kwak, J., Luke, C., Long, O., King, D., Kovatch, K., Johnston, P., Shun, T., Lazo, J., Perlmutter, D., Silverman, G. and Pak, S. Automated high-content live animal drug screening using *C. elegans* expressing the aggregation prone serpin α 1-antitrypsin Z. *PloS one* **5** (2010).
68. Li, J., Pak, S.C., O'Reilly, L.P., Benson, J.A., Wang, Y., Hidvegi, T., Hale, P., Dippold, C., Ewing, M., Silverman, G.A. and Perlmutter, D.H. Fluphenazine reduces proteotoxicity in *C. elegans* and mammalian models of alpha-1-antitrypsin deficiency. *PloS one* **9**, e87260 (2014).
69. Long, O.S., Benson, J.A., Kwak, J.H., Luke, C.J., Gosai, S.J., O'Reilly, L.P., Wang, Y., Li, J., Vetica, A.C., Miedel, M.T., Stolz, D.B., Watkins, S.C., Züchner, S., Perlmutter, D.H., Silverman, G.A. and Pak, S.C. A *C. elegans* model of human α 1-antitrypsin deficiency links components of the RNAi pathway to misfolded protein turnover. *Human molecular genetics* **23**, 5109-5122 (2014).
70. O'Reilly, L.P., Long, O.S., Cobanoglu, M.C., Benson, J.A., Luke, C.J., Miedel, M.T., Hale, P., Perlmutter, D.H., Bahar, I., Silverman, G.A. and Pak, S.C. A genome-wide RNAi screen identifies potential drug targets in a *C. elegans* model of α 1-antitrypsin deficiency. *Human molecular genetics* **23**, 5123-5132 (2014).
71. Teckman, J.H. and Perlmutter, D.H. Retention of mutant alpha(1)-antitrypsin Z in endoplasmic reticulum is associated with an autophagic response. *American journal of physiology. Gastrointestinal and liver physiology* **279**, 74 (2000).

72. Teckman, J.H., Burrows, J., Hidvegi, T., Schmidt, B., Hale, P.D. and Perlmutter, D.H. The proteasome participates in degradation of mutant alpha 1-antitrypsin Z in the endoplasmic reticulum of hepatoma-derived hepatocytes. *J Biol Chem* **276**, 44865-44872 (2001).
73. Qu, D., Teckman, J.H., Omura, S. and Perlmutter, D.H. Degradation of a mutant secretory protein, 1-antitrypsin Z, in the endoplasmic reticulum requires proteasome activity. *Journal of Biological Chemistry* **271**, 22791-22795 (1996).
74. Wu, Y., Whitman, I., Molmenti, E., Moore, K., Hippenmeyer, P. and Perlmutter, D. A lag in intracellular degradation of mutant alpha 1-antitrypsin correlates with the liver disease phenotype in homozygous PiZZ alpha 1-antitrypsin deficiency. *Proceedings of the National Academy of Sciences of the United States of America* **91**, 9014-9018 (1994).
75. Perlmutter, D.H. Alpha-1-antitrypsin deficiency: diagnosis and treatment. *Clinics in liver disease* **8**, 839 (2004).
76. Ferrarotti, I., Scabini, R., Campo, I., Ottaviani, S., Zorzetto, M., Gorrini, M. and Luisetti, M. Laboratory diagnosis of alpha1-antitrypsin deficiency. *Translational research : the journal of laboratory and clinical medicine* **150**, 267-274 (2007).
77. Carlson, J.A., Rogers, B.B., Sifers, R.N., Finegold, M.J., Clift, S.M., DeMayo, F.J., Bullock, D.W. and Woo, S.L. Accumulation of PiZ alpha 1-antitrypsin causes liver damage in transgenic mice. *The Journal of clinical investigation* **83**, 1183-1190 (1989).
78. Thomson, J.A., Itskovitz-Eldor, J., Shapiro, S.S., Waknitz, M.A., Swiergiel, J.J., Marshall, V.S. and Jones, J.M. Embryonic stem cell lines derived from human blastocysts. *Science (New York, N.Y.)* **282**, 1145-1147 (1998).
79. Reubinoff, B.E., Pera, M.F., Fong, C.Y., Trounson, A. and Bongso, A. Embryonic stem cell lines from human blastocysts: somatic differentiation in vitro. *Nature biotechnology* **18**, 399-404 (2000).
80. de Wert, G. and Mummery, C. Human embryonic stem cells: research, ethics and policy. *Human reproduction (Oxford, England)* **18**, 672-682 (2003).
81. Takahashi, K., Tanabe, K., Ohnuki, M., Narita, M., Ichisaka, T., Tomoda, K. and Yamanaka, S. Induction of pluripotent stem cells from adult human fibroblasts by defined factors. *Cell* **131**, 861-872 (2007).
82. Yu, J., Vodyanik, M.A., Smuga-Otto, K., Antosiewicz-Bourget, J., Frane, J.L., Tian, S., Nie, J., Jonsdottir, G.A., Ruotti, V., Stewart, R., Slukvin, II and Thomson, J.A. Induced

- pluripotent stem cell lines derived from human somatic cells. *Science* **318**, 1917-1920 (2007).
83. Takahashi, K. and Yamanaka, S. Induction of pluripotent stem cells from mouse embryonic and adult fibroblast cultures by defined factors. *Cell* **126**, 663-676 (2006).
 84. Yu, J. and Thomson, J.A. Pluripotent stem cell lines. *Genes & development* **22**, 1987-1997 (2008).
 85. Hacein-Bey-Abina, S., Von Kalle, C., Schmidt, M., McCormack, M.P., Wulffraat, N., Leboulch, P., Lim, A., Osborne, C.S., Pawliuk, R., Morillon, E., Sorensen, R., Forster, A., Fraser, P., Cohen, J.I., de Saint Basile, G., Alexander, I., Wintergerst, U., Frebourg, T., Aurias, A., Stoppa-Lyonnet, D., Romana, S., Radford-Weiss, I., Gross, F., Valensi, F., Delabesse, E., Macintyre, E., Sigaux, F., Soulier, J., Leiva, L.E., Wissler, M., Prinz, C., Rabbitts, T.H., Le Deist, F., Fischer, A. and Cavazzana-Calvo, M. LMO2-associated clonal T cell proliferation in two patients after gene therapy for SCID-X1. *Science (New York, N.Y.)* **302**, 415-419 (2003).
 86. Lee, A.S., Tang, C., Rao, M.S., Weissman, I.L. and Wu, J.C. Tumorigenicity as a clinical hurdle for pluripotent stem cell therapies. *Nature medicine* (2013).
 87. Somers, G.I., Lindsay, N., Lowdon, B.M., Jones, A.E., Freathy, C., Ho, S., Woodrooffe, A.J., Bayliss, M.K. and Manchee, G.R. A comparison of the expression and metabolizing activities of phase I and II enzymes in freshly isolated human lung parenchymal cells and cryopreserved human hepatocytes. *Drug metabolism and disposition: the biological fate of chemicals* **35**, 1797-1805 (2007).
 88. Yu, J., Hu, K., Smuga-Otto, K., Tian, S., Stewart, R., Slukvin, I.I. and Thomson, J.A. Human induced pluripotent stem cells free of vector and transgene sequences. *Science* **324**, 797-801 (2009).
 89. Hu, K., Yu, J., Suknuntha, K., Tian, S., Montgomery, K., Choi, K.-D.D., Stewart, R., Thomson, J.A. and Slukvin, I.I. Efficient generation of transgene-free induced pluripotent stem cells from normal and neoplastic bone marrow and cord blood mononuclear cells. *Blood* **117**, 19 (2011).
 90. Okita, K., Matsumura, Y., Sato, Y., Okada, A., Morizane, A., Okamoto, S., Hong, H., Nakagawa, M., Tanabe, K., Tezuka, K.-i., Shibata, T., Kunisada, T., Takahashi, M., Takahashi, J., Saji, H. and Yamanaka, S. A more efficient method to generate integration-free human iPS cells. *Nature methods* **8**, 409-412 (2011).
 91. Warren, L., Manos, P.D., Ahfeldt, T., Loh, Y.-H.H., Li, H., Lau, F., Ebina, W., Mandal, P.K., Smith, Z.D., Meissner, A., Daley, G.Q., Brack, A.S., Collins, J.J., Cowan, C., Schlaeger, T.M. and Rossi, D.J. Highly efficient reprogramming to pluripotency and

- directed differentiation of human cells with synthetic modified mRNA. *Cell stem cell* **7**, 618-630 (2010).
92. Kim, D., Kim, C.-H.H., Moon, J.-I.I., Chung, Y.-G.G., Chang, M.-Y.Y., Han, B.-S.S., Ko, S., Yang, E., Cha, K.Y., Lanza, R. and Kim, K.-S.S. Generation of human induced pluripotent stem cells by direct delivery of reprogramming proteins. *Cell stem cell* **4**, 472-476 (2009).
 93. Dimos, J.T., Rodolfa, K.T., Niakan, K.K., Weisenthal, L.M., Mitsumoto, H., Chung, W., Croft, G.F., Saphier, G., Leibel, R., Goland, R., Wichterle, H., Henderson, C.E. and Eggan, K. Induced pluripotent stem cells generated from patients with ALS can be differentiated into motor neurons. *Science* **321**, 1218-1221 (2008).
 94. Park, I.H., Arora, N., Huo, H., Maherali, N., Ahfeldt, T., Shimamura, A., Lensch, M.W., Cowan, C., Hochedlinger, K. and Daley, G.Q. Disease-specific induced pluripotent stem cells. *Cell* **134**, 877-886 (2008).
 95. Ebert, A.D., Yu, J., Rose, F.F., Jr., Mattis, V.B., Lorson, C.L., Thomson, J.A. and Svendsen, C.N. Induced pluripotent stem cells from a spinal muscular atrophy patient. *Nature* **457**, 277-280 (2009).
 96. Soldner, F., Hockemeyer, D., Beard, C., Gao, Q., Bell, G.W., Cook, E.G., Hargus, G., Blak, A., Cooper, O., Mitalipova, M., Isacson, O. and Jaenisch, R. Parkinson's disease patient-derived induced pluripotent stem cells free of viral reprogramming factors. *Cell* **136**, 964-977 (2009).
 97. Rashid, S.T., Corbineau, S., Hannan, N., Marciniak, S.J., Miranda, E., Alexander, G., Huang-Doran, I., Griffin, J., Ahrlund-Richter, L., Skepper, J., Semple, R., Weber, A., Lomas, D.A. and Vallier, L. Modeling inherited metabolic disorders of the liver using human induced pluripotent stem cells. *The Journal of clinical investigation* **120**, 3127-3136 (2010).
 98. Cayo, M.A., Cai, J., DeLaForest, A., Noto, F.K., Nagaoka, M., Clark, B.S., Collery, R.F., Si-Tayeb, K. and Duncan, S.A. JD induced pluripotent stem cell-derived hepatocytes faithfully recapitulate the pathophysiology of familial hypercholesterolemia. *Hepatology* **56**, 2163-2171 (2012).
 99. Zhang, S., Chen, S., Li, W., Guo, X., Zhao, P., Xu, J., Chen, Y., Pan, Q., Liu, X., Zychlinski, D., Lu, H., Tortorella, M.D., Schambach, A., Wang, Y., Pei, D. and Esteban, M.A. Rescue of ATP7B function in hepatocyte-like cells from Wilson's disease induced pluripotent stem cells using gene therapy or the chaperone drug curcumin. *Human molecular genetics* **20**, 3176-3187 (2011).

100. Leung, A., Nah, S.K., Reid, W., Ebata, A., Koch, C.M., Monti, S., Genereux, J.C., Wiseman, R.L., Wolozin, B., Connors, L.H., Berk, J.L., Seldin, D.C., Mostoslavsky, G., Kotton, D.N. and Murphy, G.J. Induced pluripotent stem cell modeling of multisystemic, hereditary transthyretin amyloidosis. *Stem cell reports* **1**, 451-463 (2012).
101. Caspi, O., Huber, I., Gepstein, A., Arbel, G., Maizels, L., Boulos, M. and Gepstein, L. Modeling of arrhythmogenic right ventricular cardiomyopathy with human induced pluripotent stem cells. *Circulation. Cardiovascular genetics* **6**, 557-568 (2013).
102. Fatima, A., Kaifeng, S., Dittmann, S., Xu, G., Gupta, M.K., Linke, M., Zechner, U., Nguemo, F., Milting, H., Farr, M., Hescheler, J. and Sarić, T. The disease-specific phenotype in cardiomyocytes derived from induced pluripotent stem cells of two long QT syndrome type 3 patients. *PloS one* **8** (2012).
103. Urnov, F.D., Miller, J.C., Lee, Y.-L.L., Beausejour, C.M., Rock, J.M., Augustus, S., Jamieson, A.C., Porteus, M.H., Gregory, P.D. and Holmes, M.C. Highly efficient endogenous human gene correction using designed zinc-finger nucleases. *Nature* **435**, 646-651 (2005).
104. Wang, W., Lin, C., Lu, D., Ning, Z., Cox, T., Melvin, D., Wang, X., Bradley, A. and Liu, P. Chromosomal transposition of PiggyBac in mouse embryonic stem cells. *Proceedings of the National Academy of Sciences of the United States of America* **105**, 9290-9295 (2008).
105. Yusa, K., Zhou, L., Li, M.A., Bradley, A. and Craig, N.L. A hyperactive piggyBac transposase for mammalian applications. *Proceedings of the National Academy of Sciences of the United States of America* **108**, 1531-1536 (2011).
106. Jinek, M., East, A., Cheng, A., Lin, S., Ma, E. and Doudna, J. RNA-programmed genome editing in human cells. *eLife* **2** (2012).
107. Cermak, T., Doyle, E.L., Christian, M., Wang, L., Zhang, Y., Schmidt, C., Baller, J.A., Somia, N.V., Bogdanove, A.J. and Voytas, D.F. Efficient design and assembly of custom TALEN and other TAL effector-based constructs for DNA targeting. *Nucleic acids research* **39** (2011).
108. Reinhardt, P., Schmid, B., Burbulla, L.F., Schöndorf, D.C., Wagner, L., Glatza, M., Höing, S., Hargus, G., Heck, S.A., Dhingra, A., Wu, G., Müller, S., Brockmann, K., Kluba, T., Maisel, M., Krüger, R., Berg, D., Tsytsyura, Y., Thiel, C.S., Psathaki, O.-E.E., Klingauf, J., Kuhlmann, T., Klewin, M., Müller, H., Gasser, T., Schöler, H.R. and Sternecker, J. Genetic correction of a LRRK2 mutation in human iPSCs links parkinsonian neurodegeneration to ERK-dependent changes in gene expression. *Cell stem cell* **12**, 354-367 (2013).

109. Soldner, F., Laganière, J., Cheng, A.W., Hockemeyer, D., Gao, Q., Alagappan, R., Khurana, V., Golbe, L.I., Myers, R.H., Lindquist, S., Zhang, L., Guschin, D., Fong, L.K., Vu, B.J., Meng, X., Urnov, F.D., Rebar, E.J., Gregory, P.D., Zhang, H.S. and Jaenisch, R. Generation of isogenic pluripotent stem cells differing exclusively at two early onset Parkinson point mutations. *Cell* **146**, 318-331 (2011).
110. Sebastiano, V., Maeder, M.L., Angstman, J.F., Haddad, B., Khayter, C., Yeo, D.T., Goodwin, M.J., Hawkins, J.S., Ramirez, C.L., Batista, L.F., Artandi, S.E., Wernig, M. and Joung, J.K. In situ genetic correction of the sickle cell anemia mutation in human induced pluripotent stem cells using engineered zinc finger nucleases. *Stem cells (Dayton, Ohio)* **29**, 1717-1726 (2011).
111. Sun, N. and Zhao, H. Seamless correction of the sickle cell disease mutation of the HBB gene in human induced pluripotent stem cells using TALENs. *Biotechnology and bioengineering* **111**, 1048-1053 (2014).
112. Zou, J., Mali, P., Huang, X., Dowey, S.N. and Cheng, L. Site-specific gene correction of a point mutation in human iPS cells derived from an adult patient with sickle cell disease. *Blood* **118**, 4599-4608 (2011).
113. Liu, G.-H.H., Qu, J., Suzuki, K., Nivet, E., Li, M., Montserrat, N., Yi, F., Xu, X., Ruiz, S., Zhang, W., Wagner, U., Kim, A., Ren, B., Li, Y., Goebel, A., Kim, J., Soligalla, R.D., Dubova, I., Thompson, J., Yates, J., Esteban, C.R., Sancho-Martinez, I. and Izpisua Belmonte, J.C. Progressive degeneration of human neural stem cells caused by pathogenic LRRK2. *Nature* **491**, 603-607 (2012).
114. Patani, R., Lewis, P.A., Trabzuni, D., Puddifoot, C.A., Wyllie, D.J., Walker, R., Smith, C., Hardingham, G.E., Weale, M., Hardy, J., Chandran, S. and Ryten, M. Investigating the utility of human embryonic stem cell-derived neurons to model ageing and neurodegenerative disease using whole-genome gene expression and splicing analysis. *Journal of neurochemistry* **122**, 738-751 (2012).
115. Guo, L., Abrams, R.M., Babiarez, J.E., Cohen, J.D., Kameoka, S., Sanders, M.J., Chiao, E. and Kolaja, K.L. Estimating the risk of drug-induced proarrhythmia using human induced pluripotent stem cell-derived cardiomyocytes. *Toxicological sciences : an official journal of the Society of Toxicology* **123**, 281-289 (2011).
116. Si-Tayeb, K., Noto, F.K., Nagaoka, M., Li, J., Battle, M.A., Duris, C., North, P.E., Dalton, S. and Duncan, S.A. Highly efficient generation of human hepatocyte-like cells from induced pluripotent stem cells. *Hepatology* **51**, 297-305 (2010).
117. Song, Z., Cai, J., Liu, Y., Zhao, D., Yong, J., Duo, S., Song, X., Guo, Y., Zhao, Y., Qin, H., Yin, X., Wu, C., Che, J., Lu, S., Ding, M. and Deng, H. Efficient generation of

- hepatocyte-like cells from human induced pluripotent stem cells. *Cell research* **19**, 1233-1242 (2009).
118. Ambrosino, G., Varotto, S., Strom, S.C., Guariso, G., Franchin, E., Miotto, D., Caenazzo, L., Basso, S., Carraro, P., Valente, M.L., D'Amico, D., Zancan, L. and D'Antiga, L. Isolated hepatocyte transplantation for Crigler-Najjar syndrome type 1. *Cell transplantation* **14**, 151-157 (2004).
 119. Horslen, S.P., McCowan, T.C., Goertzen, T.C., Warkentin, P.I., Cai, H.B., Strom, S.C. and Fox, I.J. Isolated hepatocyte transplantation in an infant with a severe urea cycle disorder. *Pediatrics* **111**, 1262-1267 (2003).
 120. Meyburg, J., Das, A.M., Hoerster, F., Lindner, M., Kriegbaum, H., Engelmann, G., Schmidt, J., Ott, M., Pettenazzo, A., Luecke, T., Bertram, H., Hoffmann, G.F. and Burlina, A. One liver for four children: first clinical series of liver cell transplantation for severe neonatal urea cycle defects. *Transplantation* **87**, 636-641 (2009).
 121. Puppi, J., Tan, N., Mitry, R.R., Hughes, R.D., Lehec, S., Mieli-Vergani, G., Karani, J., Champion, M.P., Heaton, N., Mohamed, R. and Dhawan, A. Hepatocyte transplantation followed by auxiliary liver transplantation--a novel treatment for ornithine transcarbamylase deficiency. *American journal of transplantation : official journal of the American Society of Transplantation and the American Society of Transplant Surgeons* **8**, 452-457 (2008).
 122. Burlina, A.B. Hepatocyte transplantation for inborn errors of metabolism. *Journal of inherited metabolic disease* (2004).
 123. Logan, G.J., de Alencastro, G., Alexander, I.E. and Yeoh, G.C. Exploiting the unique regenerative capacity of the liver to underpin cell and gene therapy strategies for genetic and acquired liver disease. *The international journal of biochemistry & cell biology* **56C**, 141-152 (2014).
 124. Wilkinson, G.R. Drug metabolism and variability among patients in drug response. *New England Journal of Medicine* **352**, 2211-2221 (2005).
 125. Cascio, S.M. Novel strategies for immortalization of human hepatocytes. *Artificial organs* **25**, 529-538 (2001).
 126. Runge, D., Runge, D., Jäger, D., Lubecki, K., Beer Stolz, D., Karathanasis, S., Kietzmann, T., Strom, S., Jungermann, K., Fleig, W. and Michalopoulos, G. Serum-free, long-term cultures of human hepatocytes: maintenance of cell morphology, transcription factors, and liver-specific functions. *Biochemical and biophysical research communications* **269**, 46-53 (2000).

127. Adams, R.M., Wang, M., Crane, A.M., Brown, B., Darlington, G.J. and Ledley, F.D. Effective cryopreservation and long-term storage of primary human hepatocytes with recovery of viability, differentiation, and replicative potential. *Cell transplantation* **4**, 579-586 (1994).
128. Alexandre, E., Viollon-Abadie, C., David, P., Gandillet, A., Coassolo, P., Heyd, B., Manton, G., Wolf, P., Bachellier, P., Jaeck, D. and Richert, L. Cryopreservation of adult human hepatocytes obtained from resected liver biopsies. *Cryobiology* **44**, 103-113 (2002).
129. Diener, B., Traiser, M., Arand, M., Leissner, J., Witsch, U., Hohenfellner, R., Fändrich, F., Vogel, I., Utesch, D. and Oesch, F. Xenobiotic metabolizing enzyme activities in isolated and cryopreserved human liver parenchymal cells. *Toxicology in vitro : an international journal published in association with BIBRA* **8**, 1161-1166 (1994).
130. Dou, M., de Sousa, G., Lacarelle, B., Placidi, M., Lechene de la Porte, P., Domingo, M., Lafont, H. and Rahmani, R. Thawed human hepatocytes in primary culture. *Cryobiology* **29**, 454-469 (1992).
131. Hengstler, J.G., Utesch, D., Steinberg, P., Platt, K.L., Diener, B., Ringel, M., Swales, N., Fischer, T., Biefang, K., Gerl, M., Böttger, T. and Oesch, F. Cryopreserved primary hepatocytes as a constantly available in vitro model for the evaluation of human and animal drug metabolism and enzyme induction. *Drug metabolism reviews* **32**, 81-118 (2000).
132. Li, A.P., Lu, C., Brent, J.A., Pham, C., Fackett, A., Ruegg, C.E. and Silber, P.M. Cryopreserved human hepatocytes: characterization of drug-metabolizing enzyme activities and applications in higher throughput screening assays for hepatotoxicity, metabolic stability, and drug-drug interaction potential. *Chemico-biological interactions* **121**, 17-35 (1999).
133. Loretz, L.J., Li, A.P., Flye, M.W. and Wilson, A.G. Optimization of cryopreservation procedures for rat and human hepatocytes. *Xenobiotica; the fate of foreign compounds in biological systems* **19**, 489-498 (1989).
134. Ostrowska, A., Bode, D.C., Pruss, J., Bilir, B., Smith, G.D. and Zeisloft, S. Investigation of functional and morphological integrity of freshly isolated and cryopreserved human hepatocytes. *Cell and tissue banking* **1**, 55-68 (1999).
135. Rijntjes, P.J., Moshage, H.J., Van Gemert, P.J., De Waal, R. and Yap, S.H. Cryopreservation of adult human hepatocytes. The influence of deep freezing storage on the viability, cell seeding, survival, fine structures and albumin synthesis in primary cultures. *Journal of hepatology* **3**, 7-18 (1985).

136. Steinberg, P., Fischer, T., Kiulies, S., Biefang, K., Platt, K.L., Oesch, F., Böttger, T., Bulitta, C., Kempf, P. and Hengstler, J. Drug metabolizing capacity of cryopreserved human, rat, and mouse liver parenchymal cells in suspension. *Drug metabolism and disposition: the biological fate of chemicals* **27**, 1415-1422 (1999).
137. Cai, J., Zhao, Y., Liu, Y., Ye, F., Song, Z., Qin, H., Meng, S., Chen, Y., Zhou, R., Song, X., Guo, Y., Ding, M. and Deng, H. Directed differentiation of human embryonic stem cells into functional hepatic cells. *Hepatology (Baltimore, Md.)* **45**, 1229-1239 (2007).
138. Duan, Y., Catana, A., Meng, Y., Yamamoto, N., He, S., Gupta, S., Gambhir, S.S. and Zern, M.A. Differentiation and enrichment of hepatocyte-like cells from human embryonic stem cells in vitro and in vivo. *Stem cells (Dayton, Ohio)* **25**, 3058-3068 (2007).
139. Hay, D.C., Fletcher, J., Payne, C., Terrace, J.D., Gallagher, R.C., Snoeys, J., Black, J.R., Wojtacha, D., Samuel, K., Hannoun, Z., Pryde, A., Filippi, C., Currie, I.S., Forbes, S.J., Ross, J.A., Newsome, P.N. and Iredale, J.P. Highly efficient differentiation of hESCs to functional hepatic endoderm requires ActivinA and Wnt3a signaling. *Proceedings of the National Academy of Sciences of the United States of America* **105**, 12301-12306 (2008).
140. Agarwal, S., Holton, K.L. and Lanza, R. Efficient differentiation of functional hepatocytes from human embryonic stem cells. *Stem cells (Dayton, Ohio)* **26**, 1117-1127 (2008).
141. Haridass, D., Yuan, Q., Becker, P.D., Cantz, T., Iken, M., Rothe, M., Narain, N., Bock, M., Nörder, M., Legrand, N., Wedemeyer, H., Weijer, K., Spits, H., Manns, M.P., Cai, J., Deng, H., Di Santo, J.P., Guzman, C.A. and Ott, M. Repopulation efficiencies of adult hepatocytes, fetal liver progenitor cells, and embryonic stem cell-derived hepatic cells in albumin-promoter-enhancer urokinase-type plasminogen activator mice. *The American journal of pathology* **175**, 1483-1492 (2009).
142. Basma, H., Soto-Gutierrez, A., Yannam, G.R., Liu, L., Ito, R., Yamamoto, T., Ellis, E., Carson, S.D., Sato, S., Chen, Y., Muirhead, D., Navarro-Alvarez, N., Wong, R.J., Roy-Chowdhury, J., Platt, J.L., Mercer, D.F., Miller, J.D., Strom, S.C., Kobayashi, N. and Fox, I.J. Differentiation and transplantation of human embryonic stem cell-derived hepatocytes. *Gastroenterology* **136**, 990-999 (2009).
143. Shiraki, N., Umeda, K., Sakashita, N., Takeya, M., Kume, K. and Kume, S. Differentiation of mouse and human embryonic stem cells into hepatic lineages. *Genes to cells : devoted to molecular & cellular mechanisms* **13**, 731-746 (2008).
144. Touboul, T., Hannan, N.R., Corbineau, S., Martinez, A., Martinet, C., Branchereau, S., Mainot, S., Strick-Marchand, H., Pedersen, R., Di Santo, J., Weber, A. and Vallier, L.

- Generation of functional hepatocytes from human embryonic stem cells under chemically defined conditions that recapitulate liver development. *Hepatology* **51**, 1754-1765 (2010).
145. Zhao, D., Chen, S., Cai, J., Guo, Y., Song, Z., Che, J., Liu, C., Wu, C., Ding, M. and Deng, H. Derivation and characterization of hepatic progenitor cells from human embryonic stem cells. *PLoS one* **4**, e6468 (2009).
 146. Sasaki, K., Ichikawa, H., Takei, S., No, H.S., Tomotsune, D., Kano, Y., Yokoyama, T., Sirasawa, S., Mogi, A., Yoshie, S., Sasaki, S., Yamada, S., Matsumoto, K., Mizuguchi, M., Yue, F. and Tanaka, Y. Hepatocyte differentiation from human ES cells using the simple embryoid body formation method and the staged-additional cocktail. *TheScientificWorldJournal* **9**, 884-890 (2009).
 147. Rambhatla, L., Chiu, C.P., Kundu, P., Peng, Y. and Carpenter, M.K. Generation of hepatocyte-like cells from human embryonic stem cells. *Cell transplantation* **12**, 1-11 (2003).
 148. Pei, H., Yang, Y., Xi, J., Bai, Z., Yue, W., Nan, X., Bai, C., Wang, Y. and Pei, X. Lineage restriction and differentiation of human embryonic stem cells into hepatic progenitors and zone 1 hepatocytes. *Tissue engineering. Part C, Methods* **15**, 95-104 (2009).
 149. Cascio, S. and Zaret, K.S. Hepatocyte differentiation initiates during endodermal-mesenchymal interactions prior to liver formation. *Development* **113**, 217-225 (1991).
 150. Gualdi, R., Bossard, P., Zheng, M., Hamada, Y., Coleman, J.R. and Zaret, K.S. Hepatic specification of the gut endoderm in vitro: cell signaling and transcriptional control. *Genes & development* **10**, 1670-1682 (1996).
 151. Si-Tayeb, K., Lemaigre, F.P. and Duncan, S.A. Organogenesis and development of the liver. *Dev Cell* **18**, 175-189 (2010).
 152. Zaret, K.S. Liver specification and early morphogenesis. *Mechanisms of development* **92**, 83-88 (2000).
 153. Yunis, E., Agostini, R. and Glew, R. Fine structural observations of the liver in alpha-1-antitrypsin deficiency. *The American journal of pathology* **82**, 265-286 (1976).
 154. Hidvegi, T., Mirnics, K., Hale, P., Ewing, M., Beckett, C. and Perlmutter, D.H. Regulator of G Signaling 16 is a marker for the distinct endoplasmic reticulum stress state associated with aggregated mutant alpha1-antitrypsin Z in the classical form of alpha1-antitrypsin deficiency. *The Journal of biological chemistry* **282**, 27769-27780 (2007).

155. Teckman, J., Qu, D. and Perlmutter, D. Molecular pathogenesis of liver disease in alpha1-antitrypsin deficiency. *Hepatology (Baltimore, Md.)* **24**, 1504-1516 (1996).
156. Wang, Y. and Perlmutter, D. Targeting intracellular degradation pathways for treatment of liver disease caused by α 1-antitrypsin deficiency. *Pediatric research* **75**, 133-139 (2014).
157. Choi, S.M., Kim, Y., Shim, J.S., Park, J.T., Wang, R.-H.H., Leach, S.D., Liu, J.O., Deng, C., Ye, Z. and Jang, Y.-Y.Y. Efficient drug screening and gene correction for treating liver disease using patient-specific stem cells. *Hepatology (Baltimore, Md.)* **57**, 2458-2468 (2013).
158. Eggenschwiler, R., Loya, K., Wu, G., Sharma, A.D., Sgodda, M., Zychlinski, D., Herr, C., Steinemann, D., Teckman, J., Bals, R., Ott, M., Schambach, A., Schöler, H.R. and Cantz, T. Sustained knockdown of a disease-causing gene in patient-specific induced pluripotent stem cells using lentiviral vector-based gene therapy. *Stem cells translational medicine* **2**, 641-654 (2013).
159. Yusa, K., Rashid, S.T., Strick-Marchand, H., Varela, I., Liu, P.-Q.Q., Paschon, D.E., Miranda, E., Ordóñez, A., Hannan, N.R., Rouhani, F.J., Darche, S., Alexander, G., Marciniak, S.J., Fusaki, N., Hasegawa, M., Holmes, M.C., Di Santo, J.P., Lomas, D.A., Bradley, A. and Vallier, L. Targeted gene correction of α 1-antitrypsin deficiency in induced pluripotent stem cells. *Nature* **478**, 391-394 (2011).
160. Kostrubsky, V.E., Ramachandran, V., Venkataramanan, R., Dorko, K., Esplen, J.E., Zhang, S., Sinclair, J.F., Wrighton, S.A. and Strom, S.C. The use of human hepatocyte cultures to study the induction of cytochrome P-450. *Drug metabolism and disposition: the biological fate of chemicals* **27**, 887-894 (1999).
161. Strom, S.C., Pisarov, L.A., Dorko, K., Thompson, M.T., Schuetz, J.D. and Schuetz, E.G. Use of human hepatocytes to study P450 gene induction. *Methods in enzymology* **272**, 388-401 (1995).
162. Somers, A., Jean, J.-C., Sommer, C., Omari, A., Ford, C., Mills, J., Ying, L., Sommer, A., Jean, J., Smith, B., Lafyatis, R., Demierre, M.-F., Weiss, D., French, D., Gadue, P., Murphy, G., Mostoslavsky, G. and Kotton, D. Generation of transgene-free lung disease-specific human induced pluripotent stem cells using a single excisable lentiviral stem cell cassette. *Stem cells (Dayton, Ohio)* **28**, 1728-1740 (2010).
163. O'Connor, M.D., Kardel, M.D., Iosfina, I. and Youssef, D. Alkaline Phosphatase-Positive Colony Formation Is a Sensitive, Specific, and Quantitative Indicator of Undifferentiated Human Embryonic Stem Cells. *Stem ...* (2008).

164. Chan, E.M., Ratanasirintrawoot, S., Park, I.H., Manos, P.D., Loh, Y.H., Huo, H., Miller, J.D., Hartung, O., Rho, J., Ince, T.A., Daley, G.Q. and Schlaeger, T.M. Live cell imaging distinguishes bona fide human iPS cells from partially reprogrammed cells. *Nature biotechnology* **27**, 1033-1037 (2009).
165. Schopperle, W.M. and DeWolf, W.C. The TRA-1-60 and TRA-1-81 human pluripotent stem cell markers are expressed on podocalyxin in embryonal carcinoma. *Stem cells (Dayton, Ohio)* **25**, 723-730 (2007).
166. Gopalakrishna-Pillai, S. and Iverson, L.E. A DNMT3B alternatively spliced exon and encoded peptide are novel biomarkers of human pluripotent stem cells. *PLoS one* **6** (2010).
167. Son, M.-Y.Y., Choi, H., Han, Y.-M.M. and Cho, Y.S. Unveiling the critical role of REX1 in the regulation of human stem cell pluripotency. *Stem cells (Dayton, Ohio)* **31**, 2374-2387 (2013).
168. Bhatia, S., Pilquill, C., Roth-Albin, I. and Draper, J.S. Demarcation of stable subpopulations within the pluripotent hESC compartment. *PLoS one* **8** (2012).
169. Narsinh, K.H., Sun, N., Sanchez-Freire, V., Lee, A.S., Almeida, P., Hu, S., Jan, T., Wilson, K.D., Leong, D., Rosenberg, J., Yao, M., Robbins, R.C. and Wu, J.C. Single cell transcriptional profiling reveals heterogeneity of human induced pluripotent stem cells. *The Journal of clinical investigation* **121**, 1217-1221 (2011).
170. Zhang, W.Y., de Almeida, P.E. and Wu, J.C. in *StemBook* Cambridge (MA); 2008).
171. Daley, G.Q., Lensch, M.W., Jaenisch, R., Meissner, A., Plath, K. and Yamanaka, S. Broader implications of defining standards for the pluripotency of iPSCs. *Cell stem cell* **4**, 200 (2009).
172. Hanna, J.H., Saha, K. and Jaenisch, R. Pluripotency and cellular reprogramming: facts, hypotheses, unresolved issues. *Cell* **143**, 508-525 (2010).
173. Schneider, C., Rasband, W. and Eliceiri, K. NIH Image to ImageJ: 25 years of image analysis. *Nature methods* **9**, 671-675 (2012).
174. Gualdi, R., Bossard, P., Zheng, M., Hamada, Y., Coleman, J.R. and Zaret, K.S. Hepatic specification of the gut endoderm in vitro: cell signaling and transcriptional control. *Genes & development* **10**, 1670-1682 (1996).
175. Lee, C.S., Friedman, J.R., Fulmer, J.T. and Kaestner, K.H. The initiation of liver development is dependent on Foxa transcription factors. *Nature* **435**, 944-947 (2005).

176. D'Amour, K.A., Agulnick, A.D., Eliazer, S., Kelly, O.G., Kroon, E. and Baetge, E.E. Efficient differentiation of human embryonic stem cells to definitive endoderm. *Nature biotechnology* **23**, 1534-1541 (2005).
177. DeLaForest, A., Nagaoka, M., Si-Tayeb, K., Noto, F.K., Konopka, G., Battle, M.A. and Duncan, S.A. HNF4A is essential for specification of hepatic progenitors from human pluripotent stem cells. *Development (Cambridge, England)* **138**, 4143-4153 (2011).
178. Ma, X., Duan, Y., Tschudy-Seney, B., Roll, G., Behbahan, I.S., Ahuja, T.P., Tolstikov, V., Wang, C., McGee, J., Khoobyari, S., Nolta, J.A., Willenbring, H. and Zern, M.A. Highly efficient differentiation of functional hepatocytes from human induced pluripotent stem cells. *Stem cells translational medicine* **2**, 409-419 (2013).
179. Takebe, T., Sekine, K., Enomura, M., Koike, H., Kimura, M., Ogaeri, T., Zhang, R.-R.R., Ueno, Y., Zheng, Y.-W.W., Koike, N., Aoyama, S., Adachi, Y. and Taniguchi, H. Vascularized and functional human liver from an iPSC-derived organ bud transplant. *Nature* **499**, 481-484 (2013).
180. Takebe, T., Zhang, R.-R.R., Koike, H., Kimura, M., Yoshizawa, E., Enomura, M., Koike, N., Sekine, K. and Taniguchi, H. Generation of a vascularized and functional human liver from an iPSC-derived organ bud transplant. *Nature protocols* **9**, 396-409 (2014).
181. Perlmutter, D.H. and Silverman, G.A. Hepatic fibrosis and carcinogenesis in alpha1-antitrypsin deficiency: a prototype for chronic tissue damage in gain-of-function disorders. *Cold Spring Harbor perspectives in biology* **3** (2011).
182. Nakagawa, M., Koyanagi, M., Tanabe, K., Takahashi, K., Ichisaka, T., Aoi, T., Okita, K., Mochiduki, Y., Takizawa, N. and Yamanaka, S. Generation of induced pluripotent stem cells without Myc from mouse and human fibroblasts. *Nature biotechnology* **26**, 101-106 (2008).
183. Perlmutter, D.H., Kay, R.M., Cole, F.S., Rossing, T.H., Van Thiel, D. and Colten, H.R. The cellular defect in alpha 1-proteinase inhibitor (alpha 1-PI) deficiency is expressed in human monocytes and in *Xenopus* oocytes injected with human liver mRNA. *Proceedings of the National Academy of Sciences of the United States of America* **82**, 6918-6921 (1985).
184. Hultcrantz, R. and Mengarelli, S. Ultrastructural liver pathology in patients with minimal liver disease and alpha 1-antitrypsin deficiency: a comparison between heterozygous and homozygous patients. *Hepatology (Baltimore, Md.)* **4**, 937-945 (1983).
185. Miranda, E., Pérez, J., Ekeowa, U.I., Hadzic, N., Kalsheker, N., Gooptu, B., Portmann, B., Belorgey, D., Hill, M., Chambers, S., Teckman, J., Alexander, G.J., Marciniak, S.J. and Lomas, D.A. A novel monoclonal antibody to characterize pathogenic polymers in

- liver disease associated with alpha1-antitrypsin deficiency. *Hepatology (Baltimore, Md.)* **52**, 1078-1088 (2010).
186. Wolff, S., Weissman, J. and Dillin, A. Differential scales of protein quality control. *Cell* **157**, 52-64 (2014).
187. Balch, W., Morimoto, R., Dillin, A. and Kelly, J. Adapting proteostasis for disease intervention. *Science (New York, N.Y.)* **319**, 916-919 (2008).
188. Lojewski, X., Staropoli, J.F., Biswas-Legrand, S., Simas, A.M., Haliw, L., Selig, M.K., Coppel, S.H., Goss, K.A., Petcherski, A., Chandrachud, U., Sheridan, S.D., Lucente, D., Sims, K.B., Gusella, J.F., Sondhi, D., Crystal, R.G., Reinhardt, P., Sternecker, J., Scholer, H., Haggarty, S.J., Storch, A., Hermann, A. and Cotman, S.L. Human iPSC models of neuronal ceroid lipofuscinosis capture distinct effects of TPP1 and CLN3 mutations on the endocytic pathway. *Human molecular genetics* **23**, 2005-2022 (2014).
189. Lee, J., Kim, Y., Yi, H., Diecke, S., Kim, J., Jung, H., Rim, Y.A., Jung, S.M., Kim, M., Kim, Y.G., Park, S.H., Kim, H.Y. and Ju, J.H. Generation of disease-specific induced pluripotent stem cells from patients with rheumatoid arthritis and osteoarthritis. *Arthritis research & therapy* **16**, R41 (2014).
190. Yi, F., Qu, J., Li, M., Suzuki, K., Kim, N.Y., Liu, G.-H.H. and Belmonte, J.C. Establishment of hepatic and neural differentiation platforms of Wilson's disease specific induced pluripotent stem cells. *Protein & cell* **3**, 855-863 (2012).
191. Devine, M.J., Ryten, M., Vodicka, P., Thomson, A.J., Burdon, T., Houlden, H., Cavaleri, F., Nagano, M., Drummond, N.J., Taanman, J.W., Schapira, A.H., Gwinn, K., Hardy, J., Lewis, P.A. and Kunath, T. Parkinson's disease induced pluripotent stem cells with triplication of the alpha-synuclein locus. *Nature communications* **2**, 440 (2011).
192. Lee, G., Papapetrou, E.P., Kim, H., Chambers, S.M., Tomishima, M.J., Fasano, C.A., Ganat, Y.M., Menon, J., Shimizu, F., Viale, A., Tabar, V., Sadelain, M. and Studer, L. Modelling pathogenesis and treatment of familial dysautonomia using patient-specific iPSCs. *Nature* **461**, 402-406 (2009).
193. Fusaki, N., Ban, H., Nishiyama, A., Saeki, K. and Hasegawa, M. Efficient induction of transgene-free human pluripotent stem cells using a vector based on Sendai virus, an RNA virus that does not integrate into the host genome. *Proceedings of the Japan Academy. Series B, Physical and biological sciences* **85**, 348-362 (2008).
194. Ban, H., Nishishita, N., Fusaki, N., Tabata, T., Saeki, K., Shikamura, M., Takada, N., Inoue, M., Hasegawa, M., Kawamata, S. and Nishikawa, S.-I. Efficient generation of transgene-free human induced pluripotent stem cells (iPSCs) by temperature-sensitive

Sendai virus vectors. *Proceedings of the National Academy of Sciences of the United States of America* **108**, 14234-14239 (2011).

195. Azuma, H., Paulk, N., Ranade, A., Dorrell, C., Al-Dhalimy, M., Ellis, E., Strom, S., Kay, M.A., Finegold, M. and Grompe, M. Robust expansion of human hepatocytes in *Fah^{-/-}/Rag2^{-/-}/Il2rg^{-/-}* mice. *Nature biotechnology* **25**, 903-910 (2007).